Imperial College London
Department of Physics

# Towards Thermodynamics of Quantum Systems away from Equilibrium

Tanapat Deesuwan

November 14, 2016

Supervised by Dr Janet Anders and Prof Terry Rudolph

Submitted in part fulfilment of the requirements for the degree of
Doctor of Philosophy in Physics of Imperial College London

# Declaration of originality

I hereby declare the originality of my study reported in this thesis with all the reference materials being appropriately cited.

**Tanapat Deesuwan**

# Copyright declaration

The copyright of this thesis rests with the author and is made available under a Creative Commons Attribution Non-Commercial No Derivatives licence. Researchers are free to copy, distribute or transmit the thesis on the condition that they attribute it, that they do not use it for commercial purposes and that they do not alter, transform or build upon it. For any reuse or redistribution, researchers must make clear to others the licence terms of this work.

# Abstract

A probability distribution encodes all the statistics of its corresponding random variable, hence it encodes all one can learn about the system via the random variable. In the theoretical part of this thesis, we discuss several equivalent representations of probability distributions in physics which establishes their roles as complete information measures in their own contexts. In particular, we show how Rényi entropies (as well as relative Rényi entropies) completely characterise the uncertainty of a system, hence implies the insufficiency of Shannon entropy (as well as relative entropy) in capturing the information in the presence of strong fluctuation. We also generalise Jarzynski equality in terms of relative Rényi entropies and show the equivalence between the generalised equality and the work distribution. As a consequence, an equivalence between a monotonic property of relative Rényi entropies and a kind of second law relations is revealed. In the experimental part, we study the non-equilibrium dynamics of an optically levitated nanosphere system in Knudsen regime and discover that, even though the system is not in equilibrium, the dynamics can still be treated as a Brownian motion with an effective temperature and an effective coefficient. Due to the Gaussian statistics of the levitated sphere, we show how some relevant non-equilibrium properties of the system, including several local temperatures, can be analysed from its power spectrum.

# Acknowledgement

First of all, I would like to express my gratitude to my first supervisor, Dr Janet Anders who has been helping me a lot to get into the research. Without her help, kindness, empathy, and encouragement, this work would have been impossible. Thanks to my secondary supervisor, Prof Terry Rudolph who always listens to my problem and is always willing to help. Another highly respectful gratitude is also for Prof Kim Myungshik for his great help and understanding.

It would have been impossible for me to study in UK in the first place unless being granted a scholarship from The Royal Thai Government. Thanks also to EPSRC and Centre for Doctoral Training in Controlled Quantum Dynamics at Imperial College London for opportunities and supports. I am indebted to many people at Imperial College London, University College London and University of Exeter for their support and discussion, in particular, Prof Peter Barker and Dr James Millen for their collaboration. I also would like to thanks to people in the Controlled Quantum Dynamics group at Imperial College London, Dr Dan Browne's group at University College London, and the Quantum Optics and Quantum Information Science group at University of Exeter who are always generous and helpful.

Life would be much more depressing unless I had known many good friends. I would like to thank everyone of them for their warmest friendship. These relationships are very important for me when I am far away from home.

Finally, I would like to thank my parents and sister for their greatest love, understanding, and support.

**Tanapat Deesuwan**

To my beloved grandmother.
I hope this would make you proud from up there.

# Contents

**1. Introduction** **11**

**2. Equivalent representations of a probability distribution** **15**
2.1. Laplace transform . . . . . 16
2.1.1. Inverse Laplace transform . . . . . 17
2.1.2. Discrete Laplace transform . . . . . 17
2.1.3. Laplace transform of a probability distribution . . . . 18
2.2. Moment-generating function . . . . . 19
2.3. Cumulant-generating function . . . . . 19
2.3.1. Relation to moments . . . . . 20
2.3.2. Cumulants of Gaussian distribution . . . . . 20
2.4. The effective values . . . . . 21
2.4.1. The effective values as generalised expectation values . 22
2.4.2. The effective values and the fluctuation . . . . . 23
2.4.3. Some properties of the effective values . . . . . 24
2.5. Some applications in physics . . . . . 26
2.5.1. Partition function . . . . . 26
2.5.2. Rényi entropy . . . . . 28
2.5.3. Relative Rényi entropy . . . . . 36
2.5.4. Tsallis entropy and relative Tsallis entropy . . . . . 46
2.6. Chapter summary . . . . . 49

**3. $\alpha$-Jarzynski equality: a Generalisation of Jarzynski equality** **50**
3.1. Crooks fluctuation theorem . . . . . 51
3.2. The original Jarzynski equality . . . . . 55
3.2.1. A free energy-work inequality . . . . . 57
3.2.2. A fluctuation-dissipation relation . . . . . 58

3.3. $\alpha$-Jarzynski equality . . . . . 59
3.3.1. $\alpha$-Jarzynski equality as a generalisation of Jarzynski equality and a meaning of relative Tsallis entropy of order 0 . . . . . 61
3.3.2. $\alpha$-Jarzynski equality as equivalent representations of forward and backward work distributions . . . . . 64
3.3.3. $\alpha$-Jarzynski equality in terms of $\alpha$-free energy difference 66
3.3.4. $\alpha$-monotonicity as a kind of generalised second law relations . . . . . 68
3.3.5. Support expansion and fluctuation-dissipation relations 72
3.4. Chapter summary . . . . . 74

**4. A non-equilibrium thermodynamic analysis of an optically levitated nanosphere 76**
4.1. Overview and motivation . . . . . 76
4.2. Experimental setup . . . . . 78
4.3. Theoretical background . . . . . 80
4.3.1. Optically levitated nanosphere . . . . . 80
4.3.2. Power Spectrum . . . . . 83
4.4. The heating effect . . . . . 85
4.4.1. The non-interacting baths model . . . . . 86
4.4.2. Diffusive collision . . . . . 89
4.4.3. Slow bead approximation and the finding of the emerging gas temperature . . . . . 94
4.5. Accommodation coefficient and the surface temperature estimation . . . . . 95
4.6. Results and analysis . . . . . 96
4.7. Chapter summary . . . . . 104
4.8. Remark on Jarzynski equality verification . . . . . 106

**5. Summary and outlook 108**

**A. Appendix 111**
A.1. Multivariate Laplace transform . . . . . 111
A.2. Multivariate moment-generating function . . . . . 111
A.3. Characteristic function . . . . . 111
A.4. Computing moments . . . . . 112

A.5. Some properties of characteristic function and moment-generating function . . . 113
A.5.1. Existence . . . 113
A.5.2. Sum of independent random variables . . . 113
A.5.3. Monotonicity . . . 114
A.6. Some properties of the cumulant-generating function and cumulant . . . 114
A.6.1. Existence . . . 114
A.6.2. Sum of independent random variables . . . 115
A.7. Non-addivitity property of Tsallis entropy and relative Tsallis entropy . . . 115

**Bibliography** **123**

# List of Figures

4.1. Picture of the actual setup . . . . . 79
4.3. Two-dimensional Brownian motion and its variation with trap laser intensity . . . . . 97
4.4. Analysis of heating as a function of pressure, spatial direction and sphere size . . . . . 99
4.5. Minimum attainable pressure . . . . . 104
4.2. Experimental schematic and photograph of levitation experiment . . . . . 107

# 1. Introduction

Throughout history, curiosity has driven physicists to propose many theories with the hope of understanding nature better. The theories have been constructed bit by bit, starting from the coarser ones which simplify the situations of interest to great extent, although sometimes over simplifying it too much, to finer theories where factors previously ignored are taken into account. Take the development of mechanics for example. An early major success was the formulation of classical mechanics in the $17^{\text{th}}$ century. The theory describes dynamics of a physical body only by deterministic factors, without elements of uncertainty, and is greatly successful when applied to study interactions between the bulks of two physical bodies. However, classical mechanics becomes unsuitable when applied to many-body systems, such as gas in a container, because it is practically impossible to precisely determine the dynamics of every presented molecules as is required by the theory. It was not until the birth of statistical mechanics in the $19^{\text{th}}$ century that such system can be studied in detail by the application of statistical methods, which allow one to extract some features of the system from non-deterministic factors. Since then, statistical methods have become an unexpendable tool that is used extensively in physics. Statistical mechanics reveals that there are a lot of information hidden in the fluctuation of the observables of interest, which are normally treated as noise in the context of classical mechanics. The power of statistical techniques is due to the fact that it allows these meaningful information to be extracted from the fluctuations. With statistical treatment, the description offered by classical mechanics becomes only the first approximation when the fluctuations are not taken into account.

In its earlier development, statistical mechanics was mostly applied to study many-body systems which are at or very near to thermal equilibrium. As a result, we now have a very good understanding of most of the phenomena taking place at thermal equilibrium. The thermal equilibrium

states are special because their collective properties are well-defined. There is only small fluctuations in the properties of the system so only the first and the second moments of the corresponding probability distribution are effectively sufficient to describe their behaviours in most cases. In other words, thermal equilibrium phenomena mostly follow Gaussian approximation. Equilibrium thermodynamics proves to be a very successful theory, being a key principle underlying the construction of machines since the industrial revolution until today.

Although equilibrium thermodynamics is a very successful theory, it is quite limited. This is because many realistic physical phenomena do not take place at thermal equilibrium, which is the reason non-equilibrium thermodynamics is a very active field of research. Not only the understanding of the physics of non-equilibrium is interesting in itself, the applications, particularly in developing nano and quantum technology, are also important, due to the relatively large fluctuating nature of small sized systems.

In this thesis, we present our study of some aspects of non-equilibrium thermodynamics in both classical and quantum settings. The main questions/topics we investigate are

1. How to completely capture the information encoded in random variables, especially when they are corresponding to a system which is far away from equilibrium where a large degree of fluctuation is involved. This includes the fluctuation induced by the intrinsic indeterministic nature of measurement in quantum mechanics. [Chapter 2]

2. Suppose a system is connected to a single large heat bath, how to completely capture the information encoded in the distribution of work that is done on the system according to a certain protocol? In addition, what can one learn about the thermodynamics of the system from that? [Chapter 3]

3. Is it possible to test our results on the work distribution in an optically levitated nanosphere setup? If that is so, how?, or if that is not so, why? And, what else the setup maybe used to learn about non-equilibrium thermodynamics? [Chapter 4]

For clarification, what we mean by a large heat bath in Question 2 above is that the temperature of the bath does not change even after it interacts

with the system. The reason we are particularly interested in the system that is connected to a single large heat bath is because such a situation is quite common in reality. For example, one can think of a very simple situation where the system of interest is placed in a relatively big room. In this case, the air in the room can generally be treated as a single large heat bath. Another point that should be clarified is the reasons why we are particularly interested in the optically levitated nanosphere in Question 3. The answer is, because of its simplicity in setting up and control, and above all, its potential to transition between classical and quantum regimes. The last point suggests that this system may enable one to study non-equilibrium thermodynamics both in classical and quantum settings, as well as at the transition between the two regimes.

The structure of this thesis is the following. In Chapter 2, we discuss the mathematics of probability distributions and its equivalent representations, namely the moment-generating functions, the characteristic functions, and the cumulant-generating functions. We also introduce a new concept called the "effective values", which is basically a kind of generalised mean that form another equivalent representation of a probability distribution. Then we go on to show that various existing concepts in physics, namely, partition function, Rényi entropy, relative Rényi entropy, Tsallis entropy, and relative Tsallis entropy can all be viewed as variations of these "probability distribution-equivalent" concepts. In particular, we show that Rényi entropy is an example of an effective value, and explain why the Shannon entropy alone is not sufficient in non-equilibrium situations where fluctuation becomes significant and the need for Rényi entropies arises naturally. Next, in Chapter 3, we propose a generalisation of the renowned Jarzynski equality. This generalised equality, written in terms of a relative Rényi entropy, does not only capture the complete statistics of the work done on a system that is connected to a single large heat bath, but also leads to a generalisation of the second law relation in terms of a parameterised inequality between work and free energy difference, as well as a generalisation of a fluctuation-dissipation relation. These reflect the fundamental role of fluctuation in thermodynamics, especially when the system of interest is far from equilibrium. In Chapter 4, we discuss our study of the dynamics of an optically levitated nanosphere in vacuum. The original aim leading to this study is an attempt to experimentally verify Jarzynski equality, both

in classical and quantum regimes. However, in order to accomplish that, one needs to understand the dynamics of this setting well first. The system is found to display a highly non-equilibrium characteristics and some of the ideas and mathematical concepts discussed in Chapter 2 and Chapter 3 are used to construct a theoretical model to describe its behaviour. The model appears to fit well with the actual data from the experiment, enabling us to extract several thermodynamic properties, such as a local temperature from the data. This leads to our proposal that the optically levitated nanosphere setup can be applied as an alternative means to determine non-equilibrium properties in a dilute gas, for example, local temperatures of different degrees of freedom, with a nanoscale resolution. Finally, in Chapter 5, we provide a summary and an outlook for future works.

# 2. Equivalent representations of a probability distribution

In physics, there are many settings where the nature of the system of interest is non-deterministic. This can be due either to mere ignorance of the observer as in classical physics or more subtle reasons as in quantum theory, or both. In such situations, the values of the observables of interest obtained from individual measurements cannot be predicted with certainty. This is the reason why statistical methods are required for studying them. From the statistical perspective, an observable of interest of a non-deterministic system can be treated as a random variable $X$ and its value distribution can be described by a function called *probability distribution* $P(X)$.

A probability distribution completely characterises its corresponding random variable. From it, one can extract a lot of features of the variable via various mean values. Note that what we call the mean values here is not restricted to only the arithmetic mean of the random variable, but includes other quantities, for example other moments and correlations, each of which can be expressed as an average of a function of the random variable with respect to the probability distribution.

The probability distribution is not the only fundamental function that completely characterises a random variable. In statistics, there are other functions with such property, for example, the moment-generating function and the cumulant-generating function. All of these functions are related to the probability distribution by some kinds of invertible transform. The existence of these functions is one of the key concepts underlying most of the theoretical results in this thesis.

We will start this chapter by first reviewing continuous Laplace transform and discussing its discrete version. Then we will examine the *moment-generating function* which is the Laplace transform of a probability distribution, and the *cumulant-generating function* which is the logarithm of the

moment-generating function.Also, we will introduce the concept of the *effective value*, a special kind of mean value of the observable of interest which is proportional to the cumulant-generating function, and show how it is a generalisation of the arithmetic mean, taking into account the fluctuation around it. Finally, we will discuss several concepts in physics, in particular, Rényi entropy, Tsallis entropy, and the related concepts, which can be viewed as equivalent representations of their corresponding distributions. This gives new perspective to these quantities and provides an explanation of why these quantities are essential in the first place.

## 2.1. Laplace transform

The Laplace transform, denoted by $\mathcal{L}$, is a linear bijective map taking a real function $b(y)$ to a complex function $B(\xi)$.

$$B(\xi) = \mathcal{L}\left\{b\left(y\right)\right\}\left(\xi\right) = \int_0^\infty b(y)\, e^{-\xi y} dy. \tag{2.1}$$

The complex variable $\xi$ is called the Laplace conjugate of the real variable $y$ [1]. The Laplace transform provides an alternative way to represent functions which, in certain situations, allows equations involving the functions to be solved or analysed more effectively. This is particularly the case when dealing with differential or integral equations and in statistical analysis.

There are actually two types of Laplace transforms, namely the *unilateral* and the *bilateral* transforms. The former type, as shown in (2.1), is the standard form that is usually referred to as just the Laplace transform, without any more specification. The bilateral transform, on the other hand, is normally referred to with its full name. The only difference between the two are the lower limits of integration, which is from $-\infty$ in the bilateral case instead of 0 as in the unilateral case. Normally, there is no difference in the notations used to represent the two types of the transform. However, for the sake of clarity, we will put a bar over the bilateral transformation.

$$\overline{B}(\xi) = \overline{\mathcal{L}}\left\{b\left(y\right)\right\}\left(\xi\right) = \int_{-\infty}^\infty b(y)\, e^{-\xi y} dy. \tag{2.2}$$

Of course, the *Fourier transform* ($\mathcal{F}$) is a special case of the bilateral Laplace

transform when the variable $\xi$ is purely imaginary (i.e. $\xi = i\eta$).

$$\overline{\mathcal{L}}\left\{b\left(y\right)\right\}\left(i\eta\right) = \int_{-\infty}^{\infty} b(y)\, e^{-i\eta y} dy = \mathcal{F}\left\{b\left(y\right)\right\}\left(\eta\right). \tag{2.3}$$

### 2.1.1. Inverse Laplace transform

The form of the inverse transform is the same for both the unilateral and bilateral case [2]. Suppose $\tilde{B}(\xi)$ is a Laplace transform of $b(y)$, its inverse can be computed by

$$\tilde{b}\left(y\right) = \frac{1}{2\pi i} \int_{c-i\infty}^{c+i\infty} \tilde{B}\left(\xi\right)\, e^{\xi y} d\xi, \tag{2.4}$$

where the constant $c$ is an arbitrary real number which must be chosen such that the line integral is convergent. The relationship between the functions $\tilde{b}(y)$ and $b(y)$ depends on whether $\tilde{B}(\xi)$ is a unilateral or bilateral transform of $b(y)$. If it is bilateral, one will recover the original function, i.e.

$$\tilde{B}(\xi) = \overline{\mathcal{L}}\left\{b(y)\right\}\left(\xi\right) \;\longrightarrow\; \tilde{b}(y) = b(y), \tag{2.5}$$

whereas in the unilateral case, one will generally lose the negative real part of the function, i.e.

$$\tilde{B}(\xi) = \mathcal{L}\left\{b(y)\right\}\left(\xi\right) \;\longrightarrow\; \tilde{b}(y) = b(y)\theta(y), \tag{2.6}$$

where $\theta(y)$ is the Heaviside step function. Since we are interested in a completely equivalent representation of a function, we will only consider the bilateral transform from now on.

### 2.1.2. Discrete Laplace transform

Consider a situation where the value of the initial function $b(y)$ is discrete. Assuming that $y$ has a continuous real value, one can write this function using Dirac delta function as

$$b\left(y\right) = \sum_{n} b_n\, \delta\left(y - y_n\right),$$

where $b_n$ is the value of the function for the corresponding input $y_n$. Putting this function in the bilateral transformation formula (2.2), one obtains

$$\begin{aligned}\overline{B}(\xi) &= \int_{-\infty}^{\infty} \sum_n b_n \delta(y - y_n)\, e^{-\xi y} dy \\ &= \sum_n b_n\, e^{-\xi y_n}. \end{aligned} \tag{2.7}$$

Now we have a *discrete* version of the Laplace transform. The inverse of the discrete Laplace transform can be carried out in the same way as in the continuous case using Eq.(2.4). Note that we can also use the unilateral formula to derive the above result if we choose to take into account only the non-negative value of $y_n$. The discrete Laplace transform is called *Z-transform* if the values of the discrete inputs are equally spaced. For example, let $y_n = na$, where $a$ is a real constant and $n$ is the running index, one can rewrite Eq.(2.7) as Z-transform as

$$\overline{B}(\xi) = \sum_n b_n\, e^{-\xi n a} = \sum_n b_n z^n, \tag{2.8}$$

where $z = e^{-\xi a}$ is a complex constant.

### 2.1.3. Laplace transform of a probability distribution

Now, we will consider a special case of the transform where the initial function to be transformed is a probability distribution $P(X)$ of an observable of interest $X$. Note that, in the following discussion, the upper case $X$ denotes the observable of interest in general whereas the lower case $x_i$ with the index $i$ means its particular instance. By substituting $P(X)$ for $b(y)$ and $\xi'$ for $-\xi$ in (2.2), we obtain

$$\overline{\mathcal{L}}\{P(X)\}\left(-\xi'\right) = \langle e^{\xi' X}\rangle = \langle e^{(\alpha + i\eta)X}\rangle, \tag{2.9}$$

where the angle brackets denote the average with respect to the probability distribution $P(X)$. In the last equation, we decompose the complex variable $\xi'$ into its real and imaginary parts, i.e. $\xi' = \alpha + i\eta$, where $\alpha$ and $\eta$ are real variables. Again, the inverse transform, which returns the probability distribution, can be performed using Eq.(2.4). Note that we use the bilateral Laplace transform to ensure that the transform covers the whole domain

for which the probability distribution is defined. It includes the unilateral and the discrete transforms as its special cases in which the probability distribution is non-vanishing only for the non-negative and discrete values of $X$, respectively.

Next, let us examine an interesting situation when the values of $\xi'$ are purely real.

## 2.2. Moment-generating function

Consider the Laplace transform of a probability distribution $P(X)$ of the random variable $X$ when the Laplace conjugate variable is real, i.e. $\xi' = \alpha$. This transform is equivalent to the moment-generating function in statistics, denoted by $M_X(\alpha)$, which is a real function of the real variable $\alpha$ [3]. From Eq.(2.9), we get

$$M_X(\alpha) \equiv \overline{\mathcal{L}}\{P(X)\}(-\alpha) = \langle e^{\alpha X} \rangle, \tag{2.10}$$

Since a moment-generating function is a Laplace transform of a probability distribution, it is an equivalent representation of the probability distribution.

## 2.3. Cumulant-generating function

A cumulant-generating function $C_X(\alpha)$ is defined as the logarithm of the moment-generating function i.e.

$$C_X(\alpha) = \ln[M_X(\alpha)]. \tag{2.11}$$

Hence, it is another equivalent representation of a probability distribution. As the moment-generating function is a real-valued function, so is the cumulant-generating function. It can also be expressed as a Taylor series of $\alpha$ as follows

$$C_X(\alpha) = \sum_{n=1}^{\infty} \frac{\kappa_n(X)}{n!} \alpha^n. \tag{2.12}$$

The coefficient $\kappa_n(X)$ is called the *cumulant* of order $n$ of the random variable $X$. The cumulants are an alternative to the moments and can also characterise a probability distribution. The cumulant-generating function generates cumulants in a similar fashion to how the moment-generating function generates moments (cf. Eq.(A.6)), i.e.

$$\kappa_n(X) = \frac{d^n}{d\alpha^n} C_X(\alpha)\bigg|_{\alpha=0}. \tag{2.13}$$

In the multivariate case, the cross-cumulants can be found by a similar method.

### 2.3.1. Relation to moments

Different cumulants can be written in the forms of different polynomials of moments. However, it is noteworthy that the first two cumulants

$$\kappa_1(X) = \langle X \rangle \tag{2.14}$$

$$\kappa_2(X) = \langle X^2 \rangle - \langle X \rangle^2 \tag{2.15}$$

are always equal to the mean and the variance of $X$, respectively.

### 2.3.2. Cumulants of Gaussian distribution

In the context of a cumulant-generating function, a Gaussian distribution is unique [4] because it is the only kind of probability distribution in which the number of non-zero terms in the Taylor expansion of its cumulant-generating function is finite, composed of only the first two terms. Suppose a random variable $X'$ has a Gaussian distribution $p(X' = x') = \frac{1}{\sigma\sqrt{2\pi}} e^{-\frac{(x'-\mu)^2}{2\sigma^2}}$, where $\mu$ and $\sigma$ are the mean and the variance of $X'$ respectively, then its cumulant-generating function is

$$C_{X'}(\alpha) = \mu\alpha + \frac{\sigma}{2}\alpha^2. \tag{2.16}$$

This implies that all of its cumulants of order higher than 2 must be zero. It is also proved in Ref. [4] that the number of non-zero terms for all other distributions, apart from the Gaussian, is infinite. Thus, there is no distribution with three or more finite number of non-zero cumulants. It is

shown that this special feature continues to hold also for a multivariate Gaussian distribution [5] where the second order terms are proportional to the covariances.

## 2.4. The effective values

From the discussion so far, we see that the probability distribution, moment-generating function, characteristic function, and cumulant-generating function are different representations of the same underlying statistics of the random variable of interest. This is manifest from the fact that they are particular invertible transforms of one another. Here, we *propose* the notion of *the effective values* of a random variable, the whole set of which forms another equivalent representation of the corresponding statistics of the variable. However, unlike the other representations which are dimensionless, the effective values have the same dimension as the random variable itself. They can therefore act as physical quantities, similar to how the moments and cumulants of the random variable do.

To define and give an interpretation of the effective values, let us start by considering Eq.(2.10) and Eq.(2.11). We will have

$$e^{C_X[\alpha-1]} = \langle e^{(\alpha-1)\cdot X} \rangle, \tag{2.17}$$

where $C_X\left[\alpha-1\right]$ is the cumulant-generating function of the random variable $X$ evaluated at the conjugate variable $\alpha-1$. Note the use of square brackets here instead of round brackets as was previously done in section 2.3. The only reason we choose to do this here is to emphasise the difference between the terms $\alpha-1$ between the two sides of the equation, i.e. while the one on the left-hand side of the equation is the argument of the cumulant-generating function, the one on the right-hand side of the equation is a multiplication factor. In order to match them, one can simply change the one on the left-hand side to be a multiplication factor as well by assigning a new notation, denoted $X_\alpha$, such that

$$(\alpha-1)\cdot X_\alpha \equiv C_X\left[\alpha-1\right]. \tag{2.18}$$

Then we will have

$$e^{(\alpha-1)\cdot X_\alpha} = e^{C_X[\alpha-1]} = \langle e^{(\alpha-1)\cdot X}\rangle, \tag{2.19}$$

or equivalently,

$$X_\alpha = \sum_{n=1}^{\infty} \frac{\kappa_n(X)}{n!}\,(\alpha-1)^{n-1} = \frac{1}{\alpha-1}\ln\langle e^{(\alpha-1)\cdot X}\rangle, \tag{2.20}$$

where we have rewritten the cumulant-generating function in terms of a series using Eq.(2.12). We will call $X_\alpha$ the *effective value* of order $\alpha$ of the single random variable $X$. To avoid possible confusion in notations, Greek letters will be used as subscripts instead of Latin letters to denote the effective values. It is clear from Eq.(2.14) and Eq.(2.20) that

$$X_1 = \kappa_1(X) = \langle X\rangle. \tag{2.21}$$

The fact that the effective value is defined in such a way that there is a one-to-one correspondence between the effective value and the corresponding cumulant-generating function implies that the whole set of the effective values can be converted to the corresponding probability distribution of the random variable $X$. In other words, the whole set of the effective values are equivalent to the other statistical representations we discussed earlier and can be used as alternatives of one another.

### 2.4.1. The effective values as generalised expectation values

An individual effective value can be interpreted as a generalisation of the *expectation value* or the *weighted arithmetic mean* of a random variable. This is due to the fact that the second equation in Eq.(2.20) is equivalent to the definition of a parameterised weighted Kolmogorov-Nagumo $f$-mean of $X$ [6, 7] where $f_\alpha(X) = e^{(\alpha-1)X}$ is the parameterised function with a parameter $\alpha$ in this particular case.

#### Kolmogorov-Nagumo $f$-mean

The Kolmogorov-Nagumo $f$-mean or the quasi-arithmetic mean is a generalisation of various concepts of mean e.g. arithmetic, quadratic, harmonic, and geometric means. Given a strictly monotonic and continuous function

$f(X)$ of a random variable $X$, the weighted $f$-mean of $X$ is defined to be

$$\mu_f(X) = f^{-1}\langle f(X)\rangle, \tag{2.22}$$

where $\mu_f(X)$ stands for the weighted $f$-mean, $f^{-1}$ is the inverse of $f$, and the angle bracket denotes the arithmetic mean with respect to the corresponding probability distribution of the random variable. The existence of $f^{-1}$ is guaranteed since it can be proven that a monotonic and continuous function must also be injective[1]. Note that the value of an $f$-mean and some of its properties vary with the function $f$ being used.

**Exponential mean**

The exponential mean, $\mu_{\mathsf{exp}}(X)$, is a kind of Kolmogorov-Nagumo $f$-mean where $X$ is the random variable and $f(X)$ is an exponential function. It is special because it is the only kind of the $f$-mean with additivity property [8] which is described as follows. Suppose $X$ and $Y$ are two independent random variables, the exponential mean of $X+Y$ is equal to the sum between the exponential means of each variable, i.e.

$$\begin{aligned}\mu_{\mathsf{exp}}(X+Y) &= \ln\langle e^{X+Y}\rangle \\ &= \ln\langle e^{X}\rangle + \ln\langle e^{Y}\rangle \\ &= \mu_{\mathsf{exp}}(X) + \mu_{\mathsf{exp}}(Y).\end{aligned} \tag{2.23}$$

### 2.4.2. The effective values and the fluctuation

From Eq.(2.21), we see that the effective value of order 1 of a random variable is equal to its arithmetic mean. Therefore, from Eq.(2.20), the effective value of any order $\alpha$ can be written as

$$X_\alpha = X_1 + \sum_{n=2}^{\infty} \frac{\kappa_n(X)}{n!}(\alpha-1)^{n-1} = \langle X\rangle + \sum_{n=2}^{\infty} \frac{\kappa_n(X)}{n!}(\alpha-1)^{n-1}. \tag{2.24}$$

[1]Strictly, an injective function is not equivalent to an invertible function which must be bijective (i.e. simultaneously be injective and surjective). However, since we are only interested in the reverse map from the image of $f(X)$ back to its domain, i.e. we choose the codomain of $f(X)$ to be its image, the function becomes bijective and the reverse map is equivalent to its inverse which is unique.

This relationship shows that an effective value is equal to a certain sum between the arithmetic mean ($\kappa_1(X)$) and the fluctuation around it (encoded in the other cumulants $\kappa_n(X)$ for $n > 1$). It is clear that the degree of contribution from the fluctuation part depends on the value of $\alpha$. In a special case where there is no fluctuation in the value of $X$, i.e. if $X$ is a constant, the effective values of all order become identical to the order 1 and the arithmetic mean[2].

### 2.4.3. Some properties of the effective values

#### Existence

It is obvious that, if a cumulant-generating function of a random variable diverges at some value of $\alpha$, then the effective value of that order does not exist as well. However, the reverse does not hold as can be seen in the case of $\alpha = 1$.

#### Sum of independent random variable at the same order

The effective value of order $\alpha$ corresponding to a joint probability distribution of independent random variables is equal to the sum of the effective values of order $\alpha$ of the individual variables. Suppose $Y = \sum_i a_i X_i$, where $\{X_i\}$ and $Y$ are random variables similar to what was previously done, one can show that their effective values of order $\alpha$ are related as follows.

$$Y_\alpha = \sum_{i=1}^{N} a_i \left(X_i\right)_\alpha , \tag{2.25}$$

where $\left(X_i\right)_\alpha$ stands for the effective value of order $\alpha$ of the random variable $X_i$. Note that this property directly inherits from that of the cumulant-generating function Eq.(A.12) as well as the exponential mean Eq.(2.23). It was also shown in the context of Kolmogorov-Nagumo $f$-mean that the only

[2] A hidden assumption imposed here is that the cumulant-generating function of the random variable must exist. We will use this assumption throughout our discussion in this thesis unless explicitly specify otherwise. A well-known example when this assumption *fails* is when the random variable has a Cauchy-Lorentz probability density, $P\left(x; x_0, \gamma\right) = \frac{1}{\pi\gamma\left[1+\left(\frac{x-x_0}{\gamma}\right)^2\right]}$, where $x_0$ and $\gamma$ are the location and scale parameters respectively. For such a distribution, not only the cumulant-generating function, but the moment-generating function and all the effective values also do not exist. Nevertheless, the characteristic function still does.

function $f$ which gives rise to this property is the exponential function [9], which is exactly corresponding to the effective values.

**Monotonicity**

Here, we will prove that the effective values have the following monotonic relation,

$$X_\mu \geq X_\nu, \tag{2.26}$$

which holds for arbitrary real parameters $\mu > \nu$. This fact can be proven by utilising Jensen's inequality which states that if $h(Y)$ is a *convex* function of a random variable $Y$, then

$$\langle h(Y) \rangle \geq h(\langle Y \rangle), \tag{2.27}$$

while if $h(Y)$ is a *concave* function, then

$$\langle h(Y) \rangle \leq h(\langle Y \rangle). \tag{2.28}$$

Our proof of Eq.(2.26) is the following. Let $\mu$ and $\nu$ be two non-zero real numbers and $Y \in \mathbb{R}^+$ be a positive real random variable. We can check whether $h(Y) = Y^{\nu/\mu}$ is a convex or concave function by examining its second derivative, $h''(Y) = \left(\frac{\nu}{\mu}\right)\left(\frac{\nu}{\mu} - 1\right) Y^{\frac{\nu}{\mu}-2}$. The function is strictly convex/concave if its second derivative is only positive/negative. Since the value of $Y^{\frac{\nu}{\mu}-2}$ is always positive, we have the following three cases.

1. If $\mu > \nu > 0$, the function $f(Y)$ is strictly concave. Thus,

$$\begin{aligned} [\langle Y \rangle]^{\nu/\mu} &\geq \langle Y^{\nu/\mu} \rangle \\ \therefore \frac{1}{\mu} \ln [\langle Y \rangle] &\geq \frac{1}{\nu} \ln \langle Y^{\nu/\mu} \rangle \end{aligned} \tag{2.29}$$

2. If $0 > \mu > \nu$, the function $f(Y)$ is strictly convex. Thus,

$$\begin{aligned} [\langle Y \rangle]^{\nu/\mu} &\leq \langle Y^{\nu/\mu} \rangle \\ \therefore \frac{1}{\mu} \ln [\langle Y \rangle] &\geq \frac{1}{\nu} \ln \langle Y^{\nu/\mu} \rangle \end{aligned} \tag{2.30}$$

3. If $\mu > 0 > \nu$, the function $f(Y)$ is also strictly convex. Thus,

$$\begin{aligned} [\langle Y \rangle]^{\nu/\mu} &\leq \langle Y^{\nu/\mu} \rangle \\ \therefore \frac{1}{\mu} \ln [\langle Y \rangle] &\geq \frac{1}{\nu} \ln \langle Y^{\nu/\mu} \rangle \end{aligned} \tag{2.31}$$

We see that the final inequalities of all the three cases are the same. Replace the variable $Y$ by $e^{\mu X}$, where $X$ is another random variable, we get

$$\begin{aligned} \frac{1}{\mu} \ln \left[ \langle e^{\mu X} \rangle \right] &\geq \frac{1}{\nu} \ln \left[ \langle e^{\nu X} \rangle \right] \\ X_{\mu+1} &\geq X_{\nu+1}. \end{aligned} \tag{2.32}$$

The last inequality comes from the definition of the effective values Eq.(2.20). Strictly, this proof validates the monotonicity for all $\mu > \nu$ except for $\mu = 0$ or $\nu = 0$. However, since $\lim_{\lambda \to 0} X_{\lambda+1} = \kappa_1(X)$ exists, one can interpolate the relation to cover the point, thus proving the inequality to hold everywhere. The monotonicity property of the effective values is an interesting and important property. We will show in the next chapter that it gives rise to a kind of the second law(s) of thermodynamics.

## 2.5. Some applications in physics

There are various concepts in different areas of physics that encode the statistics of their corresponding systems. In this section, some of them will be examined, namely, the partition function, Rényi entropy, relative Rényi entropy, Tsallis entropy, and relative Tsallis entropy. We will generalise some of these concepts and show explicitly how they all link to the various representations discussed earlier.

### 2.5.1. Partition function

A partition function $Z(\beta')$ is a mathematical object which encodes all the statistics of a thermal state in thermodynamics. For canonical ensemble, its expression is

$$Z\left(\beta'\right) = \sum_i e^{-\beta' E_i} = e^{-\beta' F'}. \tag{2.33}$$

Here, $\{E_i\}$ is the set of the energy the system can be found to have, $\beta'$ is a variable with the same dimension as the inverse temperature of the system $\beta$, and $F'$ is the free energy of the thermal state $\tau' = \sum_i e^{-\beta'(E_i - F')}|i\rangle\langle i|$, where $\{|i\rangle\langle i|\}$ is its eigenbasis. It should be emphasised that the variable $\beta'$ is not the same as $\beta$ because the latter is a property of the system that is fixed while the former is a variable. The partition function is at the heart of equilibrium thermodynamics since it encodes all there is to know about the thermal state, for example, internal energy, heat capacity, entropy, etc.

In this section, we will show how a partition function arises naturally as an object that encodes the statistics of a thermal state. Let us start by considering the moment-generating function of an arbitrary distribution where the random variable is the energy $E$ (cf. section 2.2). Without loss of generality, we may assume that the distribution is finite and discrete. Therefore, we have

$$M_E(\gamma) = \sum_i p_i \, e^{\gamma E_i}, \tag{2.34}$$

where $\gamma$ is our conjugate variable. Next, substitute the probability distribution of the thermal state $p_i = e^{-\beta(E_i - F)}$ in, we will have

$$\begin{aligned} M_{E_{thermal}}(\gamma) &= \sum_i e^{(\gamma-\beta)E_i + \beta F} \\ &= \sum_i e^{-\beta' E_i + \beta F} \\ &= \frac{Z(\beta')}{Z(\beta)}. \end{aligned} \tag{2.35}$$

where we assign $\beta' \equiv \beta - \gamma$. Thus the partition function is equivalent to the moment-generating function, $M_{E_{thermal}}$, of a thermal state up to a constant factor $e^{\beta F} = \frac{1}{Z(\beta)}$. This constant will not appear when one computes cumulants which explains how we can simply use the logarithm of a partition function in place of its corresponding cumulant-generating function (the logarithm of the moment-generation function) when dealing with a thermal state. To show this claim explicitly, let us examine a detailed calculation of the internal energy, which is the cumulant of the first order

(2.14), as an example:

$$\begin{aligned}\langle E\rangle &= \frac{\partial}{\partial\gamma}\ln M_E(\gamma)\bigg|_{\gamma=0} \\ &= -\frac{\partial}{\partial\beta'}\ln\left(\sum_i e^{-\beta' E_i+\beta F}\right)\bigg|_{\beta'=\beta} \\ &= \frac{\sum_i E_i e^{-\beta E_i}}{\sum_i e^{-\beta E_i}}.\end{aligned} \tag{2.36}$$

The second equation is valid since $\beta$ is a constant and $\gamma = 0$ is equivalent to $\beta' = \beta$. Notice how the two proportionality terms $e^{\beta F}$ cancel out. Thus, we can drop this factor from the beginning without affecting the result. In other words, we can just replace $M_E(\gamma)$ with $Z(\beta')$. Therefore,

$$\langle E\rangle = -\frac{\partial}{\partial\gamma}\ln M_E(\gamma)\bigg|_{\gamma=0} = -\frac{\partial}{\partial\beta'}\ln Z\left(\beta'\right)\bigg|_{\beta'=\beta}, \tag{2.37}$$

which is exactly the relationship between the partition function and the corresponding internal energy of the system. We would like to emphasise here again the difference between the *variable* $\beta'$ and the inverse temperature of the system which is *constant* $\beta$. This point is not always clearly stated, or is overlooked sometimes even, leading to the abuse of the inverse temperature $\beta$ as if it is a variable in the formula appearing in many standard textbooks which may lead to confusion.

Next, we will examine the concept of Rényi entropies and show that they are the effective values which effectively measure the uncertainty associated to a state.

### 2.5.2. Rényi entropy

Being a generalisation of Shannon entropy, Rényi entropy is discussed in many contexts, ranging from information theory [8, 10–13], statistical mechanics [14–19], and even in biodiversity [20, 21]. In this section, we will provide a new perspective to Rényi entropies by explicitly showing that they are the effective values which form a complete measure of the uncertainty of the system. This also implies that Shannon or von Neumann entropy,

being just a single instance of Rényi entropies, is generally not sufficient to capture all the uncertainty actually presented.

### Definition of Rényi entropy

The Rényi entropy of order $\alpha$ of a quantum state $\rho = \sum_i p_i |i\rangle\langle i|$ is defined as follows[3]

$$S_\alpha(\rho) = -\frac{1}{\alpha - 1} \ln \left[ \mathrm{Tr}\left(\rho^\alpha\right) \right] = -\frac{1}{\alpha - 1} \ln \left[ \sum_i p_i^\alpha \right]. \tag{2.38}$$

The definition of the Rényi entropy for classical system $S_\alpha(P(X))$ can be obtained from the same formula by replacing the density matrix with the probability distribution, $P(X) = \{p_i(x_i)\}$ for a random variable $X = \{x_i\}$. In most literature, Rényi entropy is commonly defined with the parameter $\alpha \in (0,1) \cup (1,\infty)$ [4]. The reason why the negative numbers are usually excluded is because, for any *non*-full rank density matrix (or equivalently any probability distribution with $p_i = 0$ for some $i$), the Rényi entropies with negative real order will diverge. Nevertheless, if one excludes all the non-full rank density matrices (or its classical counterparts) from consideration, then it is possible to define Rényi entropies where the parameters are negative. Thus, to ensure that all the allowed values of $\alpha$ are taken into account, let us agree that whenever we refer to "all" the Rényi entropies or related $\alpha$-parameterised quantities in this thesis, it is to be understood that we also include $\alpha < 0$ if the corresponding state is full rank. For convenience, let us also agree that, from now on, when we write $\alpha = 0$, what we actually mean is $\alpha = \lim_{a \to 0^+} a$ (The value at $\alpha = 0$ may strictly be ill-defined due to the discontinuity). Similar conventions will also be applied to $\alpha = 1$ and $\alpha = \pm\infty$.

Rényi entropy $S_\alpha(\rho)$ is a generalisation of Shannon or von Neumann

[3] This definition is different from what some other authors use. For example in Ref. [18], the authors choose to define Rényi entropies of positive order in the same way as we do. However, they add an extra minus sign in front of the whole expression for the negative orders. This is to ensure that the state with more uncertainty will never have a lower entropy than the state with less uncertainty at any order. We choose not to do that because it will make the identification of Rényi entropy as an effective value, which will be discussed later, complicated.

[4] This is not always the case though. For example, it is argued in Ref. [11] that the range of $\alpha$ can be extended to be a *complex* number where the function in (2.38) is analytic, except for $\alpha$ being a negative real value.

entropy $S(\rho)$. To be more precise, Shannon or von Neumann entropy is the Rényi entropy of order $\alpha$ in the limit $\alpha$ approaching 1, as is shown below.

$$\begin{aligned}
\lim_{\alpha\to 1} S_\alpha(\rho) &= \lim_{\alpha\to 1} -\frac{1}{\alpha-1}\ln\left[\sum_i p_i^\alpha\right] \\
&= \lim_{\alpha\to 1} -\frac{1}{\alpha-1}\ln\left[\sum_i p_i e^{(\alpha-1)\ln p_i}\right] \\
&\approx \lim_{\alpha\to 1} -\frac{1}{\alpha-1}\ln\left[\sum_i p_i\left(1+(\alpha-1)\ln p_i\right)\right] \\
&\approx -\sum_i p_i \ln p_i \\
&= S(\rho)\,. \qquad (2.39)
\end{aligned}$$

In the derivation, we Taylor-expand the exponential and the logarithm functions respectively, and keep only the first few terms. As per our agreement, from now on, we will drop the limit notation and write $S_1(\rho) = \lim_{\alpha\to 1} S_\alpha(\rho) = S(\rho)$ and we will use $S(\rho)$ and $S_1(\rho)$ interchangeably. Apart from order 1, the Rényi entropies of order 0 and $\infty$ are also interesting and being used extensively [15–19], since they are equivalent to the rank and maximum eigenvalue of the corresponding density matrix respectively. Moreover, some authors find the collision entropy which is the Rényi entropy of the parameter $\alpha = 2$ useful as well [11, 22].

**Rényi entropy as an alternative to Shannon entropy**

In Ref. [8], Rényi proposed the five postulates underlying the derivation of an uncertainty measure, the Shannon entropy $S(\mathcal{P})$, where $\mathcal{P} = \{p_1, p_2, \ldots, p_n\}$ is a generalised probability distribution, composed of the probabilities $p_i$, such that $W(\mathcal{P}) = \sum_{i=1}^n p_i \leq 1$. Suppose $S'(\mathcal{P})$ is an uncertainty measure, the five postulates state as follows.

**Postulate 1** $S'(\mathcal{P})$ is invariant under the permutation of the order of the elements of $\mathcal{P}$.

**Postulate 2** For a generalised probability distribution that is composed of only a single non-zero probability i.e. $\mathcal{P} = \{p\}$, where $p > 0$, the uncertainty measure $S'(\mathcal{P})$ is a continuous function of $p$.

**Postulate 3** For $\mathcal{P} = \left\{\frac{1}{2}\right\}$, $S'(\mathcal{P}) = \ln 2$.[5]

**Postulate 4** Given two *independent* generalised probability distributions, $\mathcal{P}$ and $\mathcal{Q}$, the uncertainty measure of the *joint distribution* is the sum of the individual measures i.e. $S'(\mathcal{P}, \mathcal{Q}) = S'(\mathcal{P}) + S'(\mathcal{Q})$.

**Postulate 5** Given two generalised probability distributions, $\mathcal{P}$ and $\mathcal{Q}$, such that $W(\mathcal{P}) + W(\mathcal{Q}) \leq 1$, then $S'(\mathcal{P} \cup \mathcal{Q}) = \frac{W(\mathcal{P})S'(\mathcal{P}) + W(\mathcal{Q})S'(\mathcal{Q})}{W(\mathcal{P}) + W(\mathcal{Q})}$.

Rényi showed that the first four postulates give the unique uncertainty measure for a *single outcome* with probability $\mathcal{P} = \{p\}$ in the form of $S'(\{p\}) = -\ln p$. This unique measure was explicitly called the *surprisal* for the first time in Ref. [23]. For convenience, we will use the notation $s(p)$ as the shorthand for $S'(\{p\})$ from now on. Taking multiple probabilistic outcomes together to form a generalised probability distribution $\mathcal{P} = \{p_1, p_2, \ldots, p_n\}$, Postulate 5 states that its uncertainty can be quantified by the arithmetic mean of the surprisals, i.e. $S'(\mathcal{P}) = \sum_{i=1}^{n} p_i \cdot s(p_i) = -\sum_{i=1}^{n} p_i \ln p_i$, which is exactly the Shannon entropy $S(\mathcal{P})$. Thus, $S'(\mathcal{P}) = S(\mathcal{P})$. In other words, the five postulates above uniquely determine the form of the uncertainty measure as that of the Shannon entropy. However, Rényi argued that the last postulate,"the uncertainty of the combined generalised probability distribution is equal to the weighted arithmetic mean of the uncertainties of its component", is too restricted and can be replaced by a more general postulate of a generalised mean (Kolmogorov-Nagumo $f$-mean). Keeping the first four postulates, he proposed that the fifth postulate should instead be,

**Postulate 5*** Given two generalised probability distributions, $\mathcal{P}$ and $\mathcal{Q}$, such that $W(\mathcal{P}) + W(\mathcal{Q}) \leq 1$, then

$$S'(\mathcal{P} \cup \mathcal{Q}) = g_\alpha^{-1} \frac{W(\mathcal{P})\, g_\alpha(S'(\mathcal{P})) + W(\mathcal{Q})\, g_\alpha(S'(\mathcal{Q}))}{W(\mathcal{P}) + W(\mathcal{Q})},$$

where $g_\alpha(x) = e^{(\alpha-1)x}$ for $\alpha \in (0,1) \cup (1,\infty)$.

The form of $g_\alpha(x)$ in Postulate 5* is not arbitrary. Rényi showed that it is the only form of the strictly monotonic and continuous function, with

[5] Logarithm base 2 is used in the original paper [8], so the original expression actually is $S'(\mathcal{P}) = 1$. The reason we choose to use the natural logarithm here instead is because it is more convenient in the context of thermodynamics.

respect to the parameter $\alpha \in (0,1) \cup (1,\infty)$, that does not violate the other four assumptions. With this, the new five postulates now uniquely determine the new form of the uncertainty measure with a parameter $\alpha \in (0,1) \cup (1,\infty)$ as $S'(\mathcal{P}) = -\frac{1}{\alpha-1} \ln \left[\sum_i p_i^\alpha\right] = S_\alpha(\mathcal{P})$, which is the Rényi entropy of order $\alpha$. In other words, the Rényi entropy of any order $\alpha \in (0,1) \cup (1,\infty)$ can be used as an uncertainty measure, according to Rényi's postulates. This includes the Shannon entropy as the special instance where the value of $\alpha$ is very close to 1 as is shown in (2.39). Note that Rényi himself did not state the reason why he did not include $\alpha < 0$ in his definition of Rényi entropy, but it is highly plausible because that will lead to a divergence when the probability distribution $\mathcal{P}$ contains some null probability $p_i = 0$. Nevertheless, as we discussed at the beginning of this section, this is not the case if the distribution does not contain any null probability. Thus it is totally fine to extend the definition of Rényi entropy of such a distribution to include $\alpha < 0$. We argue that these negative order Rényi entropies of a distribution that does not contain any null probability can also be used as an uncertainty measure as the Rényi entropies of positive order[6].

**Rényi entropies: the complete uncertainty measure in information theory**

The fact that Rényi entropy of any order can be used as an uncertainty measure of a state or a distribution naturally leads to a question. Since Rényi entropies of different orders generally have different values and there are infinitely many of them, which one should be used? We argue that *all* of them are needed in order to *completely* capture the uncertainty of a state.

To show this claim explicitly, let us start from the definition of Rényi entropy in (2.38). We can equivalently rewrite the probability $p_i$ on the

[6]To be precise, *if* Rényi entropies of negative order are defined according to Eq.(2.38), it is not the negative order relative Rényi entropies themselves but actually the *negative of their values* that are appropriate to be used as measures of the uncertainty. In other words, the negative order relative Rényi entropies themselves are not yet appropriate uncertainty measures until one multiplies them with $-1$. This is just the matter of convention. See footnote 3 for more detailed discussion on this point.

right-hand side in terms of the corresponding surprisal $s_i$ as

$$\begin{aligned} S_\alpha(\rho) &= -\frac{1}{\alpha-1}\ln\left[\sum_i p_i^\alpha\right] \\ &= -\frac{1}{\alpha-1}\ln\left[\sum_i p_i e^{(\alpha-1)\ln p_i}\right] \\ &= -\frac{1}{\alpha-1}\ln\left[\sum_i p_i e^{(\alpha-1)(-s_i)}\right] \\ &= -\frac{1}{\alpha-1}\ln\left[\left\langle e^{(\alpha-1)(-s)}\right\rangle\right]. \end{aligned} \tag{2.40}$$

The last equation is exactly the expression of a negative effective value, defined in (2.20), with the random variable $X$ being replaced by $-s$. This shows that the negative Rényi entropies are the effective values of the negative surprisal. In other words, the Rényi entropies of every order together form an equivalent representation of the probability distribution of the surprisal $P'(s)$[7], which contains all there is to know about the uncertainty of the state. Thus, by considering Rényi entropies, the "fluctuation in the uncertainty" is spontaneously taken into account. We see that Shannon entropy ($S_1$) becomes the limit of all the Rényi entropies when the fluctuation in the uncertainty is negligible, i.e. when the surprisals of all the possible outcomes are approximately the same. This can only occur in the vicinity of the maximally mixed state.

Indeed, the fact that a complete uncertainty of a state can only be captured by the whole set of Rényi entropies instead of any one of them alone was hinted earlier in the form of the second laws of thermodynamics proposed by Brandão *et al.* in Ref. [18]. In the particular case of trivial Hamiltonian, the laws state that, under catalytic noisy operations[8], a transforma-

[7]Note that $P'(s)$ is not the same as the probability associated to the state $\rho$ in the presence of some degeneracy. While the former is the probability distribution corresponding to different values of the surprisals, the latter is the probability distribution corresponding to different possible outcomes. Take, for example, the maximally mixed state. The fact that the surprisal of every possible outcome is the same means $P'(s)$ is a sharp distribution instead of a uniformly distributed one.

[8]The catalytic noisy operation is defined as a class of quantum operation which can be implemented on system $A$ by any global unitary operation which transforms a product state $\rho_A \otimes \frac{\mathbb{1}_N}{N}_B \otimes \omega_C$ to $\rho'_{AB} \otimes \omega_C$, where $N$ is the dimension of system $B$ which is arbitrary, $\mathbb{1}_N$ is the identity matrix of dimension $N$, and $\rho'_{AB}$ is the joint state of system $A$ and $B$ after the transformation. The system $C$, being absolutely unchanged after the transformation is called the catalyst. The state of the system $A$ after the

tion from a state $\rho$ to $\sigma$ is *certainly* possible if and only if the following two conditions, $\alpha > 0,\ S_\alpha(\rho) \leq S_\alpha(\sigma)$ and $\alpha < 0,\ S_\alpha(\rho) \geq S_\alpha(\sigma)$, are fulfilled simultaneously[9]. Note that these conditions cover the value of the parameter $\alpha$ from the whole real line (except at exactly 0 in which Rényi entropy may be discontinuous), not just the positive value. This is to ensure that the laws cover all the full-rank states. In the light of our interpretation, these second laws simply mean such a transformation is certainly possible if and only if the uncertainty of the final state is "the same or larger than" the uncertainty of the initial state even when fluctuation is taken into account.

### Some properties of Rényi entropy

#### Sum of product states

Given that $\rho$ and $\sigma$ are the states of two independent systems, the joint Rényi entropy of order $\alpha$ is equal to the sum between the individual Rényi entropies of the same order, i.e.

$$S_\alpha(\rho \otimes \sigma) = S_\alpha(\rho) + S_\alpha(\sigma) \tag{2.41}$$

Note that this property immediately follows from the corresponding property of the effective values.

#### Monotonicity in $\alpha$

transformation, $\sigma_A$, is obtained by tracing out the system $B$, i.e. $\sigma_A = \mathrm{Tr}_B \rho'_{AB}$. Some important properties of catalytic noisy operations are they can never decrease Rényi entropies of the individual states involving [18] and the only state they all commonly preserve is the maximally mixed state. In fact, it will be shown in section 2.5.3 that the maximally mixed state plays the role of the "equilibrium state", or the state that has the maximum Rényi entropy of all at every order.

[9] By its appearance, this condition for $\alpha < 0$ means the transformation is possible if and only if all the negative order Rényi entropies do not increase. This seems to be the opposite to the usual sense in which the transformation should only be possible if and only if entropies do not decrease. The reason for this is the way we choose to define Rényi entropies here, which is slightly different from how it is done in Ref. [18] when $\alpha < 0$, that makes our Rényi entropies of the negative order become the measures of the "negative uncertainty". This means the Rényi entropies of order $\alpha < 0$ of a state with more uncertainty are less than the Rényi entropies of the same order of another state with less uncertainty. Hence, even though the formula appears to be the opposite to the usual, the spirit of the second law that a transformation can only occur if and only if the uncertainty never decreases still holds.

Suppose $\rho$ is a full-rank state, $(\alpha, \alpha') \in \mathbb{R} \times \mathbb{R}$, and $\alpha > \alpha'$ then

$$S_\alpha(\rho) \leq S_{\alpha'}(\rho). \tag{2.42}$$

If the state $\rho$ is *not* full-rank however, its Rényi entropies will have a discontinuity at $\alpha = 0$ and all the negative orders will become divergent. This renders the monotonic property to hold properly only for the positive orders. Note that the sign is opposite to the monotonic relation of the effective values (Eq.(2.26)) due to the fact that Rényi entropies are negative effective values (cf.(2.5.2)).

**Non-negativity**

$$\forall\, \alpha \in \mathbb{R},\ S_\alpha(\rho) \geq 0. \tag{2.43}$$

**Asymptotic equipartition**

The fact that all Rényi entropies are needed in order to form a complete information measure of a state logically implies that Shannon entropy alone is insufficient, i.e. it is an *incomplete* information measure. A natural question then is, why does Shannon entropy, which is only a single instance of Rényi entropies, seem to be special? And how can it be applied in many situations as if it is a complete information measure? The key to answer to this question is the asymptotic equipartition property which states that the Rényi entropy rate of an independent and identically distributed source is asymptotically equal to the Shannon entropy, *if* one were to take only the typical sequences into account and disregard the non-typical ones [24]. This means, precisely, it is still true that Shannon entropy alone cannot completely capture all the information encoded in a distribution or state. However, it is guaranteed that there is only a negligible amount of information missing as long as the law of large number applies. This missing information is corresponding to the fluctuation which is also small in such limit.

The asymptotic equipartition property was first proved by Shannon in his original paper [25][10]. Its extension to conditional Rényi entropies

[10]Shannon himself used this property to justify how his notion of entropy (i.e. Shannon

was done for classical states by Renner and Wolf in Ref. [10] and for quantum states by Tomamichel *et al.* in Ref. [24].

### 2.5.3. Relative Rényi entropy

We see that all the Rényi entropies form *a* complete measure of the uncertainty associated to a system, where the random variable is the surprisal. We will now show that this is the measure that only arises when the maximally mixed state (equivalently, the uniform distribution) is used as the reference state (or the reference probability distribution). We will see that, apart from Rényi entropy and surprisal, there are actually many other uncertainty measures which arise naturally as a consequence of different choices of the reference state (or reference probability distribution). The concept of the reference state is similar to a reference point in the analysis of potential or a reference frame in the analysis of motion in mechanics. It is the state that acts as a reference where the uncertainty of all the other states are defined with respect to. To start, let us first review the concept of relative Rényi entropy.

#### Definitions of relative Rényi entropy

##### Classical states and commuting quantum states

In Ref. [8], Rényi himself did not only generalise the concept of Shannon entropy to Rényi entropy, but he also generalised the Kullback-Leibler divergence (or "relative entropy") to the *classical* relative Rényi entropy, which is defined as

$$S_\alpha\left(P||Q\right) = \frac{1}{\alpha - 1} \ln \left[ \sum_i \left( p_i^\alpha q_i^{1-\alpha} \right) \right], \tag{2.44}$$

where $P(X)$ and $Q(X)$ are probability distributions of the random variable $X$ with $\mathrm{supp}\left(P\left(X\right)\right) \subseteq \mathrm{supp}\left(Q\left(X\right)\right)$. We will call the probability distribution $Q(X)$ the *reference probability distribution*. Similar to Rényi entropy, relative Rényi entropy is originally defined with

entropy) is an appropriate measure of the information rate associated to independent and identically random variables in the asymptotic limit. Note that the notion of Rényi entropy was not included in that paper as the concept had yet to be discovered at that time.

$\alpha \in (0,1) \cup (1,\infty)$ to avoid the divergence, which arises when $\alpha < 0$ and the support of the distribution of interest is a strict subset of the support of the reference distribution, i.e. $\text{supp}(P(X)) \subset \text{supp}(Q(X))$. However, if the supports of the two distributions are identical, i.e. $\text{supp}(P(X)) = \text{supp}(Q(X))$, the relative Rényi entropy will always be finite for all $\alpha \in \mathbb{R}$, where the same conventions in terms of limiting values are applied for $\alpha \in \{0, 1, \pm\infty\}$ as was done previously in the definition of Rényi entropy in section 2.5.2. Thus, to ensure that all the valid values of $\alpha$ are included in our analysis, let us agree that we will always include $\alpha < 0$ in the case where $\text{supp}(P(X)) = \text{supp}(Q(X))$ from now on whenever we refer to "all" relative Rényi entropies of such kinds of distributions.

The definition of relative Rényi entropy in Eq.(2.44) can be extended to *commuting* quantum states by replacing the probability distributions $P$ and $Q$ respectively by two commuting density matrices $\rho = \sum_i p_i |i\rangle\langle i|$ and $\zeta = \sum_j q_j |j\rangle\langle j|$ i.e.

$$\begin{aligned} S_\alpha(\rho||\zeta) &= \frac{1}{\alpha - 1} \ln \left[ \text{Tr}\left(\rho^\alpha \zeta^{1-\alpha}\right) \right] \\ &= \frac{1}{\alpha - 1} \ln \left[ \sum_i \left(p_i^\alpha q_i^{1-\alpha}\right) \right]. \end{aligned} \tag{2.45}$$

Similar to before, we will call the state $\zeta$ the *reference state*. Again, this definition is well-defined only under the condition $\text{supp}(\rho) \subseteq \text{supp}(\zeta)$. We will always assume this condition for all the calculations in this thesis from now on and may not always explicitly mention it. Taking limit $\alpha \to 1$, one can show that the relative Rényi entropy

becomes equivalent to the relative entropy $S(P||Q)$.

$$\begin{aligned}
\lim_{\alpha\to 1} S_\alpha(P||Q) &= \lim_{\alpha\to 1} \frac{1}{\alpha-1} \ln\left[\sum_i p_i^\alpha q_i^{1-\alpha}\right] \\
&= \lim_{\alpha\to 1} \frac{1}{\alpha-1} \ln\left[\sum_i p_i e^{(\alpha-1)(\ln p_i - \ln q_i)}\right] \\
&\approx \lim_{\alpha\to 1} \frac{1}{\alpha-1} \ln\left[\sum_i p_i \left(1+(\alpha-1)(\ln p_i - \ln q_i)\right)\right] \\
&\approx \sum_i p_i (\ln p_i - \ln q_i) \\
&= S(P||Q)\,. \qquad (2.46)
\end{aligned}$$

One can also similarly prove that

$$\lim_{\alpha\to 1} S_\alpha(\rho||\zeta) = S(\rho||\zeta)\,. \qquad (2.47)$$

**Non-commuting states**

A crucial requirement for a valid definition of the relative Rényi entropy for general quantum states is it must reduce to (2.45) when the two states are commuting. However, that requirement alone does not uniquely determine the form of the definition in the non-commuting case. Additional requirements such as the satisfaction of the data-processing inequality must be taken into account [26]. However, even with that, there are still many possibilities and several different kinds of relative Rényi entropies have been put forward [13, 26–28]. Different definitions have different properties and to find a single definition that reduces to all these possibilities in suitable situations is still an ongoing research topic.To the best of our knowledge, the deepest result so far is presented by Audenaert and Datta in Ref. [28]. In that paper, the authors propose a notion called the $\alpha - z-$*relative Rényi entropies* ($\alpha - z-$RRE), the definition of which is

$$S_{\alpha,z}(\rho||\sigma) = \frac{1}{\alpha-1} \ln\left[\mathrm{Tr}\left(\rho^{\alpha/z}\sigma^{(1-\alpha)/z}\right)^z\right], \qquad (2.48)$$

where $\rho$ and $\sigma$ are two arbitrary quantum states in which $\mathrm{supp}(\rho) \subseteq \mathrm{supp}(\sigma)$, and a new parameter $z \in \mathbb{R}$ is introduced. It is shown in

the paper how this single definition reduces to two other previously proposed quantum extensions of the relative Rényi entropies, which are referred to in the same paper as the *α-relative Rényi entropy* ($\alpha$-RRE)

$$S_\alpha(\rho||\sigma) = \frac{1}{\alpha-1}\ln\left[\mathrm{Tr}\left(\rho^\alpha\sigma^{1-\alpha}\right)\right], \tag{2.49}$$

and the *sandwiched relative Rényi entropy* or *quantum Rényi divergence* ($\alpha$-QRD)

$$\widetilde{S}_\alpha(\rho||\sigma) = \frac{1}{\alpha-1}\ln\left[\mathrm{Tr}\left(\rho\sigma^{\frac{1-\alpha}{\alpha}}\right)^\alpha\right], \tag{2.50}$$

by setting $z = 1$ and $z = \alpha$ respectively. The $\alpha$-RRE was first presented in Ref. [27] while the $\alpha-$QRD was independently proposed in Ref. [13] and Ref. [26]. Note that the form of $\alpha$-RRE is just the same as in the case of commuting states (2.45). Moreover, still in Ref. [28], the authors also propose a new kind of relative Rényi entropy called the *reverse sandwiched relative Rényi entropy* which is defined as

$$\widehat{S}_\alpha(\rho||\sigma) = \frac{1}{\alpha-1}\ln\left[\mathrm{Tr}\left(\rho^{\frac{\alpha}{1-\alpha}}\sigma\right)^\alpha\right]. \tag{2.51}$$

Basically, this is the $\alpha - z-$RRE when $z = 1-\alpha$. Note that, when the two states are commuting, (2.48) becomes (2.45). In other words, the parameter $z$ does not play any role in commuting case.

In this thesis, we will mainly focus on the $\alpha$-RRE which, from its expression, is clearly the most straightforward generalisation from the concept of relative Rényi entropy of commuting states. For convenience, we will just refer to it simply as the relative Rényi entropy from now on, unless it is unclear from the context. The sandwiched and the reverse relative Rényi entropies will also be discussed briefly at times.

### Some properties of relative Rényi entropy

Here, some of the known properties of relative Rényi entropy are presented. Suppose $\rho$ and $\sigma$ are two arbitrary quantum states, where $\mathrm{supp}(\rho) \subseteq \mathrm{supp}(\sigma)$.

**Sum of product states**

$$S_\alpha\left(\rho\otimes\rho'||\sigma\otimes\sigma'\right)=S_\alpha\left(\rho||\sigma\right)+S_\alpha\left(\sigma||\sigma'\right). \tag{2.52}$$

**Monotonicity in $\alpha$**

Suppose the supports of $\rho$ and $\sigma$ are identical, i.e. $\mathrm{supp}(\rho)=\mathrm{supp}(\sigma)$, and $(\alpha,\alpha')\in\mathbb{R}\times\mathbb{R}$, then

$$S_\alpha\left(\rho||\sigma\right)\geq S_{\alpha'}\left(\rho||\sigma\right), \tag{2.53}$$

holds for $\alpha>\alpha'$. However, if the supports of the two states are not identical, i.e. $\mathrm{supp}\left(\rho\right)\subset\mathrm{supp}\left(\sigma\right)$, the relative Rényi entropy will have a discontinuity at $\alpha=0$. This renders the monotonic property to separately hold for positive and negative orders.

**Non-negativity for $\alpha>0$**

For $\alpha>0$,

$$S_\alpha\left(\rho||\sigma\right)\geq 0. \tag{2.54}$$

In a special case where $\rho=\sigma$, the relative Rényi entropy will be vanishing, i.e. $S_\alpha\left(\rho||\rho\right)=0$.

**Null value for $\alpha=0$ of identical support states**

Suppose the supports of $\rho$ and $\sigma$ are identical, i.e. $\mathrm{supp}(\rho)=\mathrm{supp}(\sigma)$, and $\alpha=0$, then

$$S_0\left(\rho||\sigma\right)=0. \tag{2.55}$$

This property can be proven straightforwardly from the definition of relative Rényi entropy of order 0. It basically follows from the fact that the result of the trace is 1 if the identical support holds and $\ln 1=0$.

**Non-positivity for $\alpha<0$ of identical support states**

Suppose the supports of $\rho$ and $\sigma$ are identical, i.e. $\mathrm{supp}(\rho)=\mathrm{supp}(\sigma)$, and $\alpha<0$, then

$$S_\alpha\left(\rho||\sigma\right)\leq 0. \tag{2.56}$$

This property follows immediately from the monotonicity in $\alpha$ and the null value for $\alpha = 0$ of identical support states that were discussed above.

**Invariance under joint unitary operations**

$$S_\alpha\left(\rho||\sigma\right) = S_\alpha\left(U\rho U^\dagger||U\sigma U^\dagger\right). \tag{2.57}$$

**Asymptotic equipartition**

Just like Rényi entropy, relative Rényi entropy also possesses the asymptotic equipartition property, i.e. the relative Rényi entropy rate of an independent and identically distributed source with respect to another independent and identically distributed one is asymptotically equal to the relative entropy, *if* one were to take only the typical sequences into account and disregard the non-typical ones.

**Data-processing inequality**

Suppose $\Phi$ is a completely positive trace preserving map, and the states $\rho$ and $\sigma$ are *non-commuting* i.e. $[\rho, \sigma] \neq 0$, the following inequality always holds [28–30]:

$$\forall\, \alpha \in (0, 2],\ S_\alpha\left(\rho||\sigma\right) \geq S_\alpha\left(\Phi\left(\rho\right)||\Phi\left(\sigma\right)\right). \tag{2.58}$$

However, if the states $\rho$ and $\sigma$ are *commuting*, i.e. $[\rho, \sigma] = 0$, the range of validity of the inequality is extended to $\alpha > 0$ as follows [12]:

$$\forall\, \alpha > 0,\ S_\alpha\left(\rho||\sigma\right) \geq S_\alpha\left(\Phi\left(\rho\right)||\Phi\left(\sigma\right)\right). \tag{2.59}$$

Before we continue our discussion about the $\alpha$-relative Rényi entropy further, for the sake of later reference, let us also add here the data-processing inequality for the other two kinds of quantum relative Rényi entropy, i.e. the sandwiched and the reverse sandwiched relative Rényi entropies of *non-commuting* states [30–32]:

$$\forall\, \alpha \geq 1/2,\ \widetilde{S}_\alpha\left(\rho||\sigma\right) \geq \widetilde{S}_\alpha\left(\Phi(\rho)||\Phi(\sigma)\right) \tag{2.60}$$

$$\forall\, \alpha \in (0, 1/2],\ \widehat{S}_\alpha\left(\rho||\sigma\right) \geq \widehat{S}_\alpha\left(\Phi(\rho)||\Phi(\sigma)\right) \tag{2.61}$$

Notice the difference in the range of validity of $\alpha$ between the three

kinds of quantum relative Rényi entropies of non-commuting states. For commuting cases, the three kinds of entropies become identical, thus the data-processing inequality of the sandwiched and the reverse sandwiched relative Rényi entropies in such cases are also represented by Eq.(2.59).

**Relative Rényi entropies as effective values**

Recall that $S_\alpha(\rho)$ is an effective value of the surprisals obtained from Laplace transform of the probability distribution corresponding to $\rho$, using the surprisal as the random variable. Here, we will show that one can similarly view relative Rényi entropies as effective values of the surprisals of a state relative to those of a given reference state. Being effective values signifies that one needs every order of relative Rényi entropy in order to completely capture the "relative surprisal" distribution.

Suppose $\rho = \sum_i p_i |i\rangle\langle i|$ and $\sigma = \sum_j q_j |\psi_j\rangle\langle\psi_j|$, we can rewrite (2.49) as the following

$$\begin{aligned} S_\alpha(\rho||\sigma) &= \frac{1}{\alpha-1} \ln \left[ \mathrm{Tr} \left( \sum_{i,j} p_i^\alpha |i\rangle\langle i| \cdot q_j^{1-\alpha} |\psi_j\rangle\langle\psi_j| \right) \right] \\ &= \frac{1}{\alpha-1} \ln \left[ \sum_{i,j} p_i |\langle i|\psi_j\rangle|^2 e^{(\alpha-1)(\ln p_i - \ln q_j)} \right] \\ &= \frac{1}{\alpha-1} \ln \left[ \sum_{i,j} p_{i,j} e^{-(\alpha-1)\left(s_i - s'_j\right)} \right], \end{aligned} \tag{2.62}$$

where $s_i \equiv -\ln p_i$ and $s'_j \equiv -\ln q_j$ are the corresponding surprisals, and $p_{i,j} = p_i |\langle i|\psi_j\rangle|^2$ is the joint probability of choosing the state $|i\rangle\langle i|$ and comparing it with the state $|\psi_j\rangle\langle\psi_j|$. We see that the random variable is now the "relative" surprisals of the state $\rho$ with respect to that of the reference state $\sigma$. The inclusion of the reference state allows one to link this mathematical concept closer to physical situations because most physical quantities are relative.

### The roles of the reference states

The uncertainty or information encoded in a state is a relative concept depending on the reference one chooses to measure it against. In this section, we will see how two different reference states give rise to two different uncertainty measures, each of which is an appropriate measure in its own context.

#### Maximally mixed state: relation to Rényi entropy

First, let us choose the maximally mixed state (or the uniform distribution in classical case) as the reference state, one can show how Rényi entropy is related to relative Rényi entropy by the following,

$$\begin{aligned} S_\alpha\left(\rho||\frac{\mathbb{1}_N}{N}\right) &= \frac{1}{\alpha-1}\ln\left[\sum_i^N p_i^\alpha N^{\alpha-1}\right] \\ &= \frac{1}{\alpha-1}\ln\left[\sum_i^N p_i e^{(\alpha-1)(-s_i)}\right] + \ln N \\ &= -S_\alpha(\rho) + \ln N, \end{aligned} \tag{2.63}$$

where $N$ is equal to the dimension of the Hilbert space of the state $\rho$. In words, this shows the relative Rényi entropy of order $\alpha$ of a state with a maximally mixed state as the reference is equal to the difference between the constant term, $\ln N$, and the Rényi entropy of the same order and the same state. The constant, $\ln N$, is an interesting quantity. From the non-negativity of Rényi entropies and relative Rényi entropies of positive order, we can immediately see that it is the strict *upper* bound of relative Rényi entropies of any state for $\alpha > 0$ and is also equal to the values of Rényi entropies of the maximally mixed state for all $\alpha \in \mathbb{R}$. Furthermore, we see that if the state of interest is full-rank, $\ln N$ is the strict *lower* bound of its relative Rényi entropies of negative order.

#### Thermal state: relation to $\alpha-$free energy

Now, let us change the reference state from the maximally mixed state to a thermal state $\tau = \sum_j e^{-\beta(E_j - F(\tau))}|\psi_j\rangle\langle\psi_j|$. The relative Rényi

entropy of a state $\rho$ with respect to $\tau$ is

$$\begin{aligned} S_\alpha\left(\rho||\tau\right) &= \frac{1}{\alpha-1}\ln\left[\mathrm{Tr}\left(\rho^\alpha\tau^{1-\alpha}\right)\right] \\ &= \frac{1}{\alpha-1}\ln\left[\sum_{i,j} p_i|\langle i|\psi_j\rangle|^2 e^{(\alpha-1)[(-s_i+\beta E_j)-\beta F(\tau)]}\right] \\ &= \frac{1}{\alpha-1}\ln\left[\sum_{i,j} p_{i,j} e^{(\alpha-1)\beta f_{i,j}}\right] - \beta F(\tau) \\ &= \beta F_\alpha(\rho,\tau) - \beta F(\tau), \end{aligned} \tag{2.64}$$

where we introduce a new function

$$\begin{aligned} f_{i,j} &\equiv \frac{1}{\beta}(\beta E_j - s_i) \\ &= \frac{1}{\beta}(\beta E_j + \ln p_i), \end{aligned} \tag{2.65}$$

which we will call the $f$-function and another new functional

$$F_\alpha(\rho,\tau) \equiv \frac{1}{(\alpha-1)\beta}\ln\left[\sum_{i,j} p_{i,j} e^{(\alpha-1)\beta f_{i,j}}\right], \tag{2.66}$$

which will be called the free energy of the state $\rho$ of order $\alpha$ with respect to the *thermal reference state* $\tau$. The thermal reference state is an essential part of this definition as it sets a reference Hamiltonian and temperature in which the free energies of the state of interest are defined with respect to. Different thermal reference states generally give different free energies. Therefore, to avoid an unambiguity, the thermal reference state must always be specified clearly wherever the concept of free energies is involved, unless it is clear from the context what the thermal reference state is.

The free energy of order $\alpha$ was discussed as a generalisation of the conventional Helmholtz free energy for the first time in Ref. [17] but was limited to only order 0, 1, and $\infty$. The consideration was extended to all real orders in Ref. [18] in an attempt to reformulate thermodynam-

ics as a resource theory and derive a generalisation of the second law[11]. Comparing this to the previous case where the reference state is the maximally mixed state, we can see the following. First, the fundamental measure of the uncertainty of a single outcome $i$ changes from $s_i$ to $-\beta f_{i,j}$. Note the inclusion of the reference index $j$. This indicates that it is generally not sufficient to discuss the uncertainty of an outcome without specifying the reference it is measured against. Next, $\beta F_\alpha(\rho, \tau)$ is the effective value of order $\alpha$ of $\beta f(\rho)$. This is equivalent to the relation between $S_\alpha(\rho)$ and $s(\rho)$ in the previous case. Also, the constant term changes from $\ln N$ to $-\beta F(\tau)$. This implies that all the free energies of the thermal state $\tau$ with respect to itself are identical and are equal to $F(\tau)$, i.e.

$$\forall\, \alpha \in \mathbb{R},\ F_\alpha(\tau, \tau) = F(\tau). \tag{2.69}$$

This fact explains why there seems to be only one free energy instead of the whole family that is parameterised by $\alpha$ in the near-equilibrium thermodynamics where the fluctuation is almost negligible. By the same argument, this also explains why it is sensible that the whole family of $\alpha$-free energy arises naturally in non-equilibrium circumstances. For the sake of convenience, we will then keep using the notation $F(\tau)$ for the free energy of any order $\alpha$ of the thermal state instead of $F_\alpha(\tau, \tau)$. Moreover, $F(\tau)$ also serves as the strict *lower* bound of the free energies of every positive order (as well as the strict *upper* bound of the free energies of every negative order if the support of the state of interest is identical to the support of the reference thermal state). The opposite to the previous case is due to the fact

[11] Actually, two different kinds of $\alpha$-free energy are discussed in Ref. [18]. The first one,

$$\bar{F}_\alpha(\rho, \tau) = \frac{\mathrm{sgn}(\alpha)}{\beta} S_\alpha\left(\rho||\tau\right) + F(\tau), \tag{2.67}$$

is based on the concept of $\alpha$-relative Rényi entropy while the other one,

$$\widetilde{F}_\alpha(\rho, \tau) = \frac{1}{\beta} \widetilde{S}_\alpha\left(\rho||\sigma\right) + F(\tau), \tag{2.68}$$

is based on the sandwiched relative Rényi entropy. Note that the notations we use here are different from the ones used in Ref. [18]. Note also that the definition of $\bar{F}_\alpha(\rho, \tau)$ is very close to our definition of $F_\alpha(\rho, \tau)$ in Eq.(2.64), except for the presence of the sign function, $\mathrm{sgn}(\alpha)$. Thus, the difference between our $\alpha$-free energy $F_\alpha(\rho, \tau)$ and $\bar{F}_\alpha(\rho, \tau)$ is manifest only when $\alpha < 0$.

that the $f$-function is defined with the negative value of the surprisal.

What do we learn from here? Basically, every reference state gives rise to its own notions of uncertainty measure, which are equivalent to the surprisal and Rényi entropy in the case of the maximally mixed state. As an example, what we have just done above is changing the reference state from the maximally mixed state to a thermal state. We see that, by the same line of analysis of the relationship between relative Rényi entropy and Rényi entropy, the uncertainty measure of a single outcome in this case becomes an $f-$function with the effective measures being the free energies.

Now that we learn there are many possible measures, i.e. representations, one may choose to quantify the uncertainty of a given system, each of which depends on the choice of the reference state, the questions to ask are, which one should be chosen?, actually why should we choose?, and is it not enough to stick with only one representation? The answer is, yes, one can just stick to one representation. However, a certain representation may ease the analysis of a certain situation at hand than the others. Again, this is comparable to the application of a transformation in mechanics.

### 2.5.4. Tsallis entropy and relative Tsallis entropy

Tsallis entropy is another generalisation of Shannon entropy, apart from Rényi entropy. It was first proposed by Constantino Tsallis in 1988 in Ref. [33] and are regarded as a "true generalisation of Boltzmann-Gibbs entropy" by many physicists, including Murray Gell-Mann [34]. Similarly, relative Tsallis entropy is another generalisation of relative entropy, apart from relative Rényi entropy. Both quantities have found many uses in physics in various contexts, ranging from astrophysics [35], high energy physics [36], plasma physics [37], cold atoms [38, 39], to quantum thermodynamics [40]. Unlike Rényi entropy and relative Rényi entropy, Tsallis entropy and relative Tsallis entropy are non-additive, meaning both Tsallis entropy and relative Tsallis entropy of independent random variables are not equal to the sum of the individual ones.

#### Definitions

##### Tsallis entropy

Suppose $P(X) = \{p_1, p_2, \ldots, p_n\}$ is the probability distribution of a

discrete variable $X$, where $\sum_i^n p_i = 1$, and $\alpha \in \mathbb{R}$, the Tsallis entropy of order $\alpha$ is defined as [33]

$$\mathcal{T}_\alpha(P(X)) \equiv \frac{1}{\alpha - 1}\left(1 - \sum_i^n p_i^\alpha\right). \tag{2.70}$$

Tsallis entropy can also be defined in terms of a density matrix. Suppose $\rho = \sum_i p_i |i\rangle\langle i|$, the Tsallis entropy of order $\alpha$ is defined as

$$\mathcal{T}_\alpha(\rho) \equiv \frac{1}{\alpha - 1}\left(1 - \mathrm{Tr}(\rho^\alpha)\right). \tag{2.71}$$

**Relative Tsallis entropy**

The relative Tsallis entropy of order $\alpha$ of the state $\rho$ with respect to another state $\sigma = \sum_j q_j |\psi_j\rangle\langle\psi_j|$ is defined as [41–44]

$$\mathcal{T}_\alpha(\rho||\sigma) \equiv \frac{1}{1-\alpha}\left(1 - \mathrm{Tr}(\rho^\alpha \sigma^{1-\alpha})\right) = \frac{1}{1-\alpha}\left(1 - \sum_{i,j} p_i^\alpha q_j^{1-\alpha} |\langle i|\psi_j\rangle|^2\right). \tag{2.72}$$

**Relation to moment-generating function**

From Eq.(2.10) and Eq.(2.71), it is clear that we can rewrite Tsallis entropy in terms of a moment-generating function as follows

$$\mathcal{T}_\alpha(\rho) = \frac{1}{\alpha - 1}\left(1 - M_{s(\rho)}(1-\alpha)\right), \tag{2.73}$$

where $s(\rho) \equiv -\ln \rho$ is treated as the random variable of the moment-generating function. This can as well be done for relative Tsallis entropy, i.e.

$$\mathcal{T}_\alpha(\rho||\sigma) = \frac{1}{1-\alpha}\left(1 - M_{\Delta s}(\alpha - 1)\right), \tag{2.74}$$

where now the random variable is $\Delta s \equiv s(\sigma) - s(\rho)$, the surprisal differences of the individual outcomes corresponding to the two states. Eq.(2.73) and Eq.(2.74) imply that all Tsallis entropies as well as all relative Tsallis entropies also form complete uncertainty measures.

### Rényi-Tsallis identities

#### Rényi-Tsallis entropy identity

From (2.38), the relation between Rényi entropy and Tsallis entropy of the same order $\alpha$ can be expressed nicely as an identity, i.e.

$$e^{(1-\alpha)S_\alpha(\rho)} - (1-\alpha)\,\mathcal{T}_\alpha(\rho) = 1. \tag{2.75}$$

It is noteworthy that this identity holds for all $\alpha$. We will call Eq.(2.75) the Rényi-Tsallis entropy identity. In the limit where $\alpha$ approaches 1, by Taylor-expanding the exponential function in (2.75), one can show that

$$S_1(\rho) = \mathcal{T}_1(\rho), \tag{2.76}$$

i.e. both kinds of entropies coincide at $\alpha = 1$, which is the limit where the fluctuation is disregarded and the two entropies become identical to Shannon entropy.

#### Rényi-Tsallis relative entropy identity

Similarly, the relation between relative Rényi entropy and relative Tsallis entropy of the same order forms another identity, i.e.

$$e^{(\alpha-1)S_\alpha(\rho||\sigma)} - (\alpha-1)\,\mathcal{T}_\alpha(\rho||\sigma) = 1. \tag{2.77}$$

Note the difference in the signs between the two identities. We will call this Rényi-Tsallis relative entropy identity. Again, this relation holds for all $\alpha$. Also, in the limit where $\alpha$ approaches 1, one can show that

$$S_1\left(\rho||\sigma\right) = \mathcal{T}_1(\rho||\sigma), \tag{2.78}$$

i.e. both the relative entropies coincide and become identical to the Kullback-Leibler divergence or relative entropy when the fluctuation is disregarded.

## 2.6. Chapter summary

Before we end this chapter, let us summarise what we have discussed so far. Starting by reviewing several mathematical concepts that are all equivalent to a probability distribution, we show that various existing physical concepts are actually variations of those equivalent representations. In particular, we show that the whole family of Rényi entropies, a generalisation of Shannon entropy which recently finds more and more uses in the context of entropy-related subjects such as thermodynamics and information theory, form an equivalent representation of the surprisal distribution. It thus encodes the uncertainty of the corresponding distribution completely. This gives Rényi entropy a new perspective and a more concrete reason of how it naturally shows up in those contexts in the first place. We also show that similar treatments apply to Tsallis entropy, and both Rényi and Tsallis relative entropies as well.

In the next chapter, we will discuss the $\alpha$-Jarzynski equalities which are our main theoretical result. These equalities form a generalisation of Jarzynski equality which give some more insight into non-equilibrium thermodynamics of both classical and quantum systems.

# 3. $\alpha$-Jarzynski equality: a Generalisation of Jarzynski equality

Jarzynski equality is an equality in non-equilibrium thermodynamics which provides an *exact* relationship between work, $W$, and free energy change, $\Delta F$, that is associated to a certain class of transition processes between two thermal states, both of which have the same inverse temperature $\beta$[1]. The expression of the equality is the following:

$$\langle e^{-\beta(W-\Delta F)} \rangle = 1. \tag{3.1}$$

The fact that Jarzynski equality gives an exact relation between work and free energy difference is very astonishing. This is because, before its discovery by Jarzynski in 1997 [45], the relationship between work and free energy difference was only known in the form of the inequality, $\langle W \rangle - \Delta F \geq 0$, which is a variation of the second law of thermodynamics. This was except for a special case where the work fluctuation is small that one could go beyond the inequality and had the relation $\langle W \rangle - \Delta F \simeq \frac{\beta}{2}(\langle W^2 \rangle - \langle W \rangle^2)$, which is a fluctuation-dissipation relation [46]. Jarzynski equality is superior to these previously known relations[2] because it holds no matter how far from equilibrium or how big the fluctuation of the work is. In fact, it has been shown that these two relations can be derived directly from Jarzynski equality by Jarzynski himself in Ref. [45]. As an application, Hummer and Szabo showed in Ref. [47] how Jarzynski equality allowed one to determine

[1] Depending on the detail of the protocol in which the work is done, the final state at the end of the process is not necessarily be a thermal state. The only role of the "fictitious final thermal state" in such a case is to provide the final free energy needed in the equality. We will discuss the precise setting and conditions where the equality is valid in further detail later in the chapter.

[2] These two free energy-work relations that are known before Jarzynkski equality will be discussed in a bit more detail in section 3.2.1 and section 3.2.2.

an unknown free energy landscape from the corresponding work distribution, which could be obtained directly from a set of repeated experiments.

In this chapter, based on the concepts we discussed earlier, mainly relative Rényi entropies and $\alpha$-free energies, we derive a generalisation of Jarzynski equality which leads naturally to a generalisation of the second law of thermodynamics and a generalisation of the fluctuation-dissipation relation. Also, on a practical side, our generalised Jarzynski equality allows one to obtain all the $\alpha$-free energies experimentally from the statistics of the work in a similar fashion to Hummer and Szabo's method.

## 3.1. Crooks fluctuation theorem

Before getting into more details about the Jarzynski equality and its generalisation, let us first give an overview of Crooks fluctuation theorem, another exact non-equilibrium relation which is more fundamental and can be used to derive the original Jarzynski equality. The following description of Crooks theorem is adapted from the setting discussed by Sagawa in Ref. [48]. Suppose, at the initial time $t = 0$, the system of interest is prepared in the state $\rho_0 = \sum_i p_i |i\rangle\langle i|$ with the initial bare Hamiltonian $H_S(t = 0) = \sum_i E^i_{S,0} |i\rangle\langle i|$. Here, $p_i$ is the probability of finding the system being in the eigenstate $|i\rangle\langle i|$ with the corresponding energy $E_i$, if an energy measurement is done to this system right at $t = 0$. The system is then put in contact with a heat bath of state $\tau_B = e^{-\beta(H_B - F(\tau_B))}$ of inverse temperature $\beta$, where $H_B = \sum_k E^k_B |\phi_k\rangle\langle\phi_k|$ is the bare bath Hamiltonian which is time-independent and $F(\tau_B)$ is its Helmholtz free energy. Here, $\{E^k_B\}$ and $\{|\phi_k\rangle\langle\phi_k|\}$ are the eigenvalues and eigenstates of the Hamiltonian $H_B$ respectively. After that, the system and the bath are then subjected to a non-adaptive, pre-specified protocol, which is called the *forward protocol*. The protocol can be divided into 3 steps. First, both the system and the bath are individually measured in their respective eigenbases, $\{|i\rangle\langle i|\}$ and $\{|\phi_k\rangle\langle\phi_k|\}$, to determine their actual initial states. Then both of them are driven by a unitary operator $U = \mathbb{T} e^{-i \int_0^T H(t)\, dt}$ which causes them to evolve from time $t = 0$ to $t = T$, where $\mathbb{T}$ is the time-ordering operator and $H(t) = H_S(t) + H_{SB} + H_B$ is the total Hamiltonian. It is assumed here that the interaction Hamiltonian will be "switched on", i.e. $H_{SB} \neq 0$, only during the interval $0 \leq t \leq T$ and "switched off", i.e. $H_{SB} = 0$, for

the rest of the time outside that interval. Note that it is also possible to choose $H_{SB} = 0$ all the time. The system and the bath will evolve independently in such a case, and one can simply ignore the bath altogether. Note also that, during the interaction interval, only the bare system Hamiltonian $H_S$ is time-dependent and the details about how it varies with time is also a part of the protocol. Physically, this is done by manipulating only some controllable parameters of the system Hamiltonian in the same manner every time the protocol is run. Finally, at time $t = T$, the total state becomes $U(\rho_0 \otimes \tau_B)U^\dagger$ and the interaction Hamiltonian is "switched off". At this moment, the system and the bath are *individually* measured again. The measurement basis for the bath state is chosen to be the eigenbasis of the bath Hamiltonian $\{|\phi_k\rangle\langle\phi_k|\}$, i.e. it is the same as the bath measurement performed at the start of the protocol. For the system, there is no restriction. Any choice of basis is valid, as long as it is chosen beforehand, also as a part of the protocol. Suppose that the final system measurement basis is $\{|\psi_j\rangle\langle\psi_j|\}$, the probability of realising the transition $|a\rangle\langle a| \otimes |\phi_b\rangle\langle\phi_b| \longrightarrow |\psi_c\rangle\langle\psi_c| \otimes |\phi_d\rangle\langle\phi_d|$ via the forward protocol will be

$$\begin{aligned} p_{fwd}((a,b) \to (c,d)) =& \langle a|\rho_0|a\rangle\langle\phi_b|\tau_B|\phi_b\rangle \times \\ & \Big[(\langle\psi_c| \otimes \langle\phi_d|)U(|a\rangle\langle a| \otimes |\phi_b\rangle\langle\phi_b|)U^\dagger(|\psi_c\rangle \otimes |\phi_d\rangle)\Big] \\ =& (p_a e^{-\beta(E_B^b - F(\tau_B))}) \left|(\langle\psi_c| \otimes \langle\phi_d|)U(|a\rangle \otimes |\phi_b\rangle)\right|^2 . \end{aligned} \tag{3.2}$$

Now, assume that the system is prepared in a new state $\tilde{\sigma}_T = \sum_j q_j |\tilde{\psi}_j\rangle\langle\tilde{\psi}_j|$ called the *reference state*[3] and it is put in thermal contact with the heat bath $\tilde{\tau}_B = e^{-\beta(\tilde{H}_B - F(\tilde{\tau}_B))}$ of inverse temperature $\beta$ and Hamiltonian $\tilde{H}_B = \sum_k E_B^k |\tilde{\phi}_k\rangle\langle\tilde{\phi}_k|$. Here, $\tilde{A}$ is the time-reversed counterpart of an operator $A$, i.e. $\tilde{A} = \theta A \theta^\dagger$ where $\theta$ is the time-reversal operator. Then the *backward protocol*, the *time reversal* of the forward protocol, is executed. By time reversal, it means the temporal order in which the steps of the forward protocol are implemented is reversed, and all the even-temporal-symmetry parameters keep their directions while all the odd-temporal-symmetry parameters

[3]Note that we previously discuss another concept also called the reference state as part of the definition of relative Rényi entropies. That these two concepts have the same name is not the result of no creativity, but it is because the two concepts are actually identical. This will become clear in section 3.3.

have their directions switched to the opposite. The backward protocol is also composed of 3 steps: initial measurement, unitary drive, and final measurement. To be able to properly compare it to the forward protocol, all the measurement bases chosen for the backward protocol must be the time reversal of those used in its forward protocol counterpart. Moreover, with the time-reversed total Hamiltonian $\tilde{H}(t) = \tilde{H}_S(t) + \tilde{H}_{SB} + \tilde{H}_B$, the time-reversed unitary operator for the backward protocol is $\widetilde{U} = \mathbb{T}e^{-i\int_0^T \tilde{H}(T-t)\,dt}$. Suppose the state after the first measurement is $|\tilde{\psi}_{c'}\rangle\langle\tilde{\psi}_{c'}| \otimes |\tilde{\phi}_{d'}\rangle\langle\tilde{\phi}_{d'}|$ and the state after the second measurement is $|\tilde{a}'\rangle\langle\tilde{a}'| \otimes |\tilde{\phi}_{b'}\rangle\langle\tilde{\phi}_{b'}|$, the probability of realising the transition $|\tilde{\psi}_{c'}\rangle\langle\tilde{\psi}_{c'}| \otimes |\tilde{\phi}_{d'}\rangle\langle\tilde{\phi}_{d'}| \longrightarrow |\tilde{a}'\rangle\langle\tilde{a}'| \otimes |\tilde{\phi}_{b'}\rangle\langle\tilde{\phi}_{b'}|$ via the backward protocol will be

$$\begin{aligned}
p_{bwd}((c',d') \to (a',b')) =& \langle\tilde{\psi}_{c'}|\tilde{\sigma}_T|\tilde{\psi}_{c'}\rangle\langle\tilde{\phi}_{d'}|\tilde{\tau}_B|\tilde{\phi}_{d'}\rangle\times \\
& \Big[(\langle\tilde{a}'| \otimes \langle\tilde{\phi}_{b'}|)\widetilde{U}(|\tilde{\psi}_{c'}\rangle\langle\tilde{\psi}_{c'}| \otimes |\tilde{\phi}_{d'}\rangle\langle\tilde{\phi}_{d'}|)\widetilde{U}^\dagger(|\tilde{a}'\rangle \otimes |\tilde{\phi}_{b'}\rangle)\Big] \\
=& \langle\psi_{c'}|\sigma_T|\psi_{c'}\rangle\langle\phi_{d'}|\tau_B|\phi_{d'}\rangle\times \\
& \Big[(\langle a'| \otimes \langle\phi_{b'}|)U^\dagger(|\psi_{c'}\rangle\langle\psi_{c'}| \otimes |\phi_{d'}\rangle\langle\phi_{d'}|)U(|a'\rangle \otimes |\phi_{b'}\rangle)\Big] \\
=& (q_{c'}e^{-\beta(E_B^{d'} - F(\tilde{\tau}_B))})\left|\langle\psi_{c'}| \otimes \langle\phi_{d'}|U|a'\rangle \otimes |\phi_{b'}\rangle\right|^2 .
\end{aligned} \tag{3.3}$$

One obtains the second line due to the fact that

$$|\langle\eta|\theta^\dagger\theta|\eta'\rangle|^2 = |\langle\eta|\eta'\rangle|^2, \tag{3.4}$$

for arbitrary states $|\eta\rangle$ and $|\eta'\rangle$, and

$$\begin{aligned}
\theta\widetilde{U}\theta^\dagger &= \mathbb{T}e^{\int_0^T \theta(-i\tilde{H}(T-t))\theta^\dagger\,dt} \\
&= \mathbb{T}e^{i\int_0^T H(T-t)\,dt} \\
&= U^\dagger.
\end{aligned} \tag{3.5}$$

We see from Eq.(3.2) and Eq.(3.3) that the ratio between the forward and backward transition probabilities between arbitrary two pairs of states

$|a\rangle\langle a| \otimes |\phi_b\rangle\langle\phi_b| \rightleftharpoons |\psi_c\rangle\langle\psi_c| \otimes |\phi_d\rangle\langle\phi_d|$ is

$$\begin{aligned}\frac{p_{fwd}((a,b)\to(c,d))}{p_{bwd}((c,d)\to(a,b))} &= e^{\beta[(E_B^d - E_B^b) - (F(\tilde{\tau}_B) - F(\tau_B))]} \cdot e^{\ln p_a - \ln q_c} \\ &= e^{s_c - s_a - \beta Q_{b\to d}} \\ &= e^{\nu_{(a,b)\to(c,d)}}, \end{aligned} \tag{3.6}$$

where $s_a$ and $s_c$ are the surprisals of the outcomes $a$ and $c$ respectively, $Q_{b\to d} \equiv E_B^b - E_B^d$ is the corresponding heat *absorbed by the system from the bath* in the *forward* transition, and $\nu_{(a,b)\to(c,d)} \equiv s_c - s_a - \beta Q_{b\to d}$ is the entropy production associated to the *forward* transition[4]. Note that the free energy terms cancel each other out because $H_B$ and $\tilde{H}_B$ have the same spectrum. Now, suppose $\nu'$ is an arbitrary real constant, the total probability $p_{fwd}(\nu')$ of yielding entropy production equal to $\nu'$ from the forward protocol can be computed as follows,

$$\begin{aligned} p_{fwd}(\nu') &= \sum_{a,b,c,d} p_{fwd}((a,b)\to(c,d))\, \delta_{\nu',\nu_{(a,b)\to(c,d)}} \\ &= \sum_{a,b,c,d} p_{bwd}((c,d)\to(a,b))\, e^{\nu_{(a,b)\to(c,d)}} \delta_{\nu',\nu_{(a,b)\to(c,d)}} \\ &= p_{bwd}(-\nu')\, e^{\nu'}. \end{aligned} \tag{3.7}$$

In the above derivation, the relation from Eq.(3.6) is exploited in the second line. In the third line, the fact that the entropy production associated to a backward transition is the negative of that of the forward transition between the same pairs is used, i.e. $\nu_{(c,d)\to(a,b)} = -\nu_{(a,b)\to(c,d)}$. Finally, Crooks theorem states that

$$\frac{p_{fwd}(\nu')}{p_{bwd}(-\nu')} = e^{\nu'}. \tag{3.8}$$

The theorem manifestly shows that, even though it is possible that a system may evolve in such a direction that decreases its entropy, it is exponentially

[4]Note that, the term $\beta Q_{b\to d}$ is the surprisal difference between the outcomes $b$ and $d$ of the bath. If instead of the thermal state $\tau_B$, one connects the system to an arbitrary state $\rho_0'$ at the start of the forward protocol and $\tilde{\sigma}'$ at the start of the backward protocol, the heat term $\beta Q_{b\to d}$ in the entropy production will change to be the corresponding surprisal difference between the outcomes $b$ and $d$ and the fluctuation theorem derived thereafter will still hold accordingly.

more likely to evolve in the opposite direction where its entropy increases. To compare this derivation to those found in other literature (for example, [45, 49, 50]), note that the transitions between different states here are equivalent to the different trajectories or paths, and the states of the thermal bath in this case are equivalent to the uncontrollable degrees of freedom.

Crooks fluctuation theorem was initially proved in classical stochastic, microscopically reversible processes [49, 50]. It was later shown to also be valid in quantum systems coupling weakly to a heat bath [51–54]. Furthermore, with a generalisation of the concept of the system free energy in strong coupling regime, the theorem has been proven to hold theoretically even in strong coupling quantum systems [55]. Apart from the theoretical aspect, Crooks fluctuation theorem has been tested experimentally in various settings, both classical [56–60] and quantum [61].

## 3.2. The original Jarzynski equality

Consider a special case where both the initial state and the reference state are also thermal with inverse temperature $\beta$, i.e. $\rho_0 = \tau_{S,0} = e^{-\beta(H_S(0)-F(\tau_{S,0}))}$ and $\sigma_T = \tau_{S,T} = e^{-\beta(H_S(T)-F(\tau_{S,T}))}$, where $H_S(0) = \sum_i E^i_{S,0}|i\rangle\langle i|$ and $H_S(T) = \sum_j E^j_{S,T}|\psi_j\rangle\langle\psi_j|$ are the initial and final system Hamiltonians with spectra $\{E^i_{S,0}\}$ and $\{E^j_{S,T}\}$ respectively, and $F(\tau_{S,0})$ and $F(\tau_{S,T})$ are the corresponding system free energies. Then Eq.(3.6) becomes

$$\begin{aligned}\frac{p_{fwd}((a,b)\to(c,d))}{p_{bwd}((c,d)\to(a,b))} &= e^{\beta((E^c_{S,T}-E^a_{S,0}-Q_{b\to d})-(F(\tau_{S,T})-F(\tau_{S,0})))} \\ &= e^{\beta(W_{(a,b)\to(c,d)}-\Delta F_S)},\end{aligned} \tag{3.9}$$

where $\Delta F_S \equiv F(\tau_{S,T}) - F(\tau_{S,0})$ is the Helmholtz free energy difference between the reference and the initial states of the system and $W_{(a,b)\to(c,d)} = E^c_{S,T} - E^a_{S,0} - Q_{b\to d}$ is the work that is *done on the system* and is associated to the *forward* transition $|a\rangle\langle a| \otimes |\phi_b\rangle\langle\phi_b| \longrightarrow |\psi_c\rangle\langle\psi_c| \otimes |\phi_d\rangle\langle\phi_d|$. A reason the latter is justified to be the work done on the system is the following. First, since the heat $Q_{b\to d} \equiv E^b_B E^d_B$ is defined as the negative of the bath energy difference, $W_{(a,b)\to(c,d)}$ is fundamentally the *global* energy change, by definition. Then, because the global state evolves unitarily, $W_{(a,b)\to(c,d)}$ can also be considered as the work *done on the global state*. Finally, due to the

fact that the only time-dependent part of the total Hamiltonian is the system Hamiltonian, which means the protocol only "actively" changes the energy of the system, the global work becomes equal to the local work done on the system. This argument was raised in Ref. [55] as part of the analysis of Crooks theorem and Jarzynski equality for arbitrary open quantum systems. Another way to see that $W_{(a,b)\to(c,d)}$ really is the work done on the system is to follow the first law of thermodynamics, i.e. the energy change of the system subtracted by the heat it absorbs is equal to the work acted on it. This argument follows Ref. [48][5]. From Eq.(3.9), we see that the entropy production corresponding to this setting then is proportional to the difference between the work and the free energy difference. Crooks theorem thus dictates that

$$\frac{p_{fwd}(\beta(W' - \Delta F_S))}{p_{bwd}(-\beta(W' - \Delta F_S))} = e^{\beta(W' - \Delta F_S)}, \tag{3.10}$$

where $p_{fwd}(\beta(W' - \Delta F_S)) = \sum_{a,b,c,d} p_{fwd}((a,b) \to (c,d))\delta_{W',W_{(a,b)\to(c,d)}}$ is the marginal probability of having to *input* a certain amount of work $W'$ to the system during the forward protocol while $p_{bwd}(-\beta(W' - \Delta F_S)) = \sum_{a,b,c,d} p_{bwd}((c,d) \to (a,b))\delta_{W',-W_{(a,b)\to(c,d)}}$ is the marginal probability of having to *draw out* the same amount of work $W'$ from the system during the backward protocol. Since the temperature and the free energies are assumed to be known implicitly and are constant in this setting, it is clear that $p_{fwd}(+W') = p_{fwd}(\beta(W' - \Delta F_S))$ and $p_{bwd}(-W') = p_{bwd}(-\beta(W' - \Delta F_S))$, where $p_{fwd}(+W')$ and $p_{bwd}(-W')$ are the forward and backward work probability distributions respectively. One may then rewrite Crooks theorem above as

$$\frac{p_{fwd}(+W')}{p_{bwd}(-W')} = e^{\beta(W' - \Delta F_S)}. \tag{3.11}$$

Note that, since the free energy of the bath does not change, the total free energy difference $\Delta F = F(\tau_{S,T} \otimes \tau_B) - F(\tau_{S,0} \otimes \tau_B)$ is equal to the system free energy difference $\Delta F_S$, hence we will drop the subscript $S$ from now on.

[5] The appropriateness of defining $W_{(a,b)\to(c,d)}$ as work has been concerned however due to its intrinsic probabilistic nature [16]. This leads to the study of maximum/minimum deterministic single-shot work which is a part of the emerging field of single-shot thermodynamics as is discussed, for example, in [15–18, 62–65]. We will not concern about that subtle point in this thesis, nevertheless, and will just treat $W_{(a,b)\to(c,d)}$ as work.

By rearranging terms and computing the average, it was straightforwardly proven in Ref. [49, 50] that the above expression leads to Jarzynski equality [45], i.e.

$$\langle e^{-\beta(W-\Delta F)}\rangle_{fwd} = 1, \tag{3.12}$$

where the average on the left-hand side of the equation is computed with respect to the forward probability. We will drop the subscript $fwd$ from now on and use only the angle brackets to represent the average with respect to the forward transition probability, unless there are more than one probability distribution involved and it is unclear which one is being considered. Just like Crooks theorem, it has been proven theoretically that Jarzynski equality holds in various different settings, both classical [45,49,50,60,66,67] and quantum [51, 54, 68, 69]. Moreover, a number of experiments have been performed to verify the equality in various classical setups, for instance, single-molecule folding/unfolding experiments [58, 70–75], oscillating torsion pendulum [57], and single-electron box [76]. Recently, a proposal to test the quantum version of the equality using an ion trap was proposed [77] and also experimentally verified [78].

What is interesting about the Jarzynski equality is the fact that it shows an unexpected relationship between a non-equilibrium quantity, i.e. work, and an equilibrium quantity, i.e. the equilibrium Helmholtz free energy, and that it always holds true no matter how far from the local equilibrium the state is during the evolution. This allows one to find the equilibrium free energy of a system with a complicated configuration by repetitively measuring the amount of work done on the system via an arbitrary non-equilibrium process that brings the system from a certain thermal state, the free energy of which is known, to the target configuration, the free energy of which is what one would like to determine [45, 47, 79]. In fact, this point was used in order to experimentally validate Jarzynski equality and Crooks theorem as shown in the references mentioned above.

### 3.2.1. A free energy-work inequality

As an equality that is valid for even far from equilibrium situations, it has been shown by means of a Jensen inequality, $\langle e^X\rangle \geq e^{\langle X\rangle}$, that Jarzynski equality implies the following relation between work and free energy differ-

ence [45],

$$\langle W \rangle \geq \Delta F. \tag{3.13}$$

This relation states that: "*In average*, in order to increase the free energy of a system which is initially in a thermal state, one requires to do work *at least* equal to the amount of free energy increase itself", or, equivalently: "The amount of work one can extract from a thermal state is *at most* equal to the free energy decrease, *in average*". This is a variation of the second law relation that appears in the standard thermodynamics, which is achieved simply by applying Jensen inequality to Eq.(3.12). For a finite temperature, the only case where this relation becomes an equality is when the corresponding process is quasi-static, i.e. when the system stays very close to its local thermal equilibrium at all times.

### 3.2.2. A fluctuation-dissipation relation

By defining the dissipated work[6],

$$W_{diss} \equiv W - \Delta F, \tag{3.14}$$

it has also been shown in Ref. [45] that a fluctuation-dissipation relation[7] that was previously presented in Ref. [46],

$$\langle W_{diss} \rangle \simeq \frac{\beta}{2} \operatorname{Var}(W), \tag{3.15}$$

arises naturally from Jarzynski equality in the limit of small fluctuation. Here, $\operatorname{Var}(W) \equiv \langle W^2 \rangle - \langle W \rangle^2$ stands for the variance of the work and it

[6]The dissipated work $W_{diss}$ is defined here as the difference in value between the actual amount of work $W$ that is done on/extracted from the system in an individual transition between two thermal states of the same inverse temperature $\beta$, and the free energy difference between the two, $\Delta F$. Note that Eq.(3.13) suggests that the value of the dissipated work is non-negative *in average*. This means the average work required to accomplish such a transition can never be less than the free energy difference between the two states. It can, however, be negative sometimes in an individual transition. The dissipated work is proportional to the entropy production, with the inverse temperature $\beta$ being the proportionality constant

[7]Fluctuation-dissipation theorem is a non-equilibrium relation that was discovered long before fluctuation theorem and is one of the key principles to explain many phenomena, including the analysis of Brownian motion by Einstein [80] and Johnson noise by Nyquist [81].

is easy to see that this is equal to the variance of the dissipated work, i.e. $\mathrm{Var}(W) = \mathrm{Var}(W_{diss})$. Eq.(3.15) shows that the average dissipated work that is corresponding to a protocol that does not drive the system too far away from equilibrium (hence, the corresponding fluctuation is small) is directly proportional to its fluctuation. For this relation to be valid, the fluctuation must be small enough such that it can be effectively measured by the variance of the distribution alone. If this condition does not hold, then the fluctuation-dissipation relation does not provide an accurate description of the behaviour of the system anymore and one needs to resort to Jarzynski equality instead. Since both the variance and the inverse temperature are non-negative, this again shows that the dissipation is non-negative in average, which is precisely what Eq.(3.13) states. Note that Eq.(3.15) can be seen as an equality between the cumulants of the first order (i.e. the arithmetic mean) and the second order (i.e. the variance) of $W_{diss}$.

## 3.3. $\alpha$-Jarzynski equality

We are now ready to show how to rewrite the Jarzynski equality in terms of relative Rényi entropies. Under the same setting as the original Jarzynski equality, the ratio between the forward and backward transition probabilities between two given pairs of states is shown in Eq.(3.9). Starting from this equation, it is trivial to see that

$$\left(\frac{p_{fwd}((a,b)\to(c,d))}{p_{bwd}((c,d)\to(a,b))}\right)^{\alpha} = e^{\alpha\beta(W_{(a,b)\to(c,d)}-\Delta F)}. \tag{3.16}$$

Rearranging and rewriting terms slightly, we will then get the following two equivalent expressions,

$$\frac{[p_{fwd}((a,b)\to(c,d))]^{\alpha}}{[p_{bwd}((c,d)\to(a,b))]^{\alpha-1}} = p_{fwd}((a,b)\to(c,d))\, e^{(\alpha-1)\beta(W_{(a,b)\to(c,d)}-\Delta F)} \tag{3.17}$$

$$= p_{bwd}((c,d)\to(a,b))\, e^{\alpha\beta(W_{(a,b)\to(c,d)}-\Delta F)}. \tag{3.18}$$

We will keep Eq.(3.18) for later reference. For now, let us sum Eq.(3.17) over all the possible states. The term on the right-hand side will become

$$\sum_{a,b,c,d} p_{fwd}((a,b)\to(c,d))\, e^{(\alpha-1)\beta(W_{(a,b)\to(c,d)}-\Delta F)} = \langle e^{(\alpha-1)\beta(W-\Delta F)}\rangle_{fwd}. \tag{3.19}$$

Meanwhile, using the explicit expressions of $p_{fwd}((a,b)\to(c,d))$ and $p_{bwd}((c,d)\to(a,b))$ as are shown in Eq.(3.2) and Eq.(3.3) respectively, we can rewrite the term on the left-hand side of the equations as a trace as follows,

$$\begin{aligned}\sum_{a,b,c,d} \frac{[p_{fwd}((a,b)\to(c,d))]^{\alpha}}{[p_{bwd}((c,d)\to(a,b))]^{\alpha-1}} &= \mathrm{Tr}\left[U(\tau_{S,0}^{\alpha}\otimes\tau_B^{\alpha})U^{\dagger}(\tau_{S,T}^{1-\alpha}\otimes\tau_B^{1-\alpha})\right] \\ &= e^{(\alpha-1)S_{\alpha}\left(U(\tau_{S,0}\otimes\tau_B)U^{\dagger}||\tau_{S,T}\otimes\tau_B\right)}. \end{aligned} \tag{3.20}$$

Note that the last expression follows from Eq.(2.49), where we also use the fact that $U(\tau_{S,0}^{\alpha}\otimes\tau_B^{\alpha})U^{\dagger} = (U\tau_{S,0}\otimes\tau_B U^{\dagger})^{\alpha}$. To simplify the analysis, let us define the global states $\tau_0 \equiv \tau_{S,0}\otimes\tau_B$ and $\tau_T \equiv \tau_{S,T}\otimes\tau_B$. Thus, we will finally have a set of $\alpha$-parameterised equations which we will call *the $\alpha$-Jarzynski equalities*:

$$e^{(\alpha-1)S_{\alpha}\left(U\tau_0U^{\dagger}||\tau_T\right)} = \langle e^{(\alpha-1)\beta(W-\Delta F)}\rangle_{fwd}. \tag{3.21}$$

There are several points to note here. Firstly, the $\alpha$-Jarzynski equalities do not only generalise the original equality, they also provide a novel link between fluctuation relation and relative Rényi entropies. This is interesting because relative Rényi entropies are usually discussed in the context of single-shot thermodynamics while they are rarely used in the context of fluctuation theorem. These two subfields are usually studied separately, but, recently, there is an interest in combining them together as is presented, for example, in Ref. [19]. The appearance of relative Rényi entropies in the formulation of a fluctuation relation like the $\alpha$-Jarzynski equality then is another hint to a potential unification between the two subfields, which will help to expand our understanding of non-equilibrium thermodynamics further. Secondly, unlike the original Jarzynski equality, the relations between work and free energy described by the $\alpha$-Jarzynski equality are generally process-*dependent*. This is because the values of the relative Rényi

entropies in the formulation do depend on the unitary process $U$. We will discuss this point in more detail later in section 3.3.1. Thirdly, we can see clearly now the equivalence between the reference state defined in the context of the fluctuation theorem and the reference state defined in the context of relative Rényi entropy. This explains why it is justified to call the two concepts from two different contexts with the same name. Fourthly, we see that we can replace the product states $\tau_{S,0} \otimes \tau_B$ and $\tau_{S,T} \otimes \tau_B$ to the global states $\tau_0$ and $\tau_T$ respectively, without loss of generality. This is based on the equivalence between the work done locally on the system and the total work done on the global state in this setting. The advantages of dealing with the global state is not just the simplicity in the expression, but the fact that it is subjected to a unitary evolution helps to simplify the analysis as well. In fact, one can even redefine the global state to be the system that is subjected to a unitary evolution, without any interaction with any bath at all during the forward protocol. The final noteworthy point is the natural emerging of the state $U\tau_0 U^\dagger$ in the relative Rényi entropy. This is quite interesting in the *quantum* setting because $U\tau_0 U^\dagger$ may *not* commute either with the initial or final Hamiltonians, rendering its corresponding energy somewhat *ill-defined*. In such a situation, $U\tau_0 U^\dagger$ is not really the final state of the forward protocol but an intermediate state just before the final energy measurement is done. The natural emerging of this state reflects the fact that, in general, the randomness in quantum setting does not only arise from the uncertainty associated to the initial state, but also the intrinsic indeterminism of the final measurement outcome.

Let us next discuss several interesting features and consequences of the $\alpha$-Jarzynski equality.

### 3.3.1. $\alpha$-Jarzynski equality as a generalisation of Jarzynski equality and a meaning of relative Tsallis entropy of order $0$

First, we will show that the original Jarzynski equality really is a very special case of $\alpha$-Jarzynski equality. To show this explicitly, let us consider Eq.(3.21) for $\alpha = 0$,

$$\langle e^{-\beta(W-\Delta F)} \rangle = e^{-S_0\left(U\tau_0 U^\dagger || \tau_T\right)}. \tag{3.22}$$

We see that the left-hand side of this equation resembles the original Jarzynski equality in Eq.(3.12), however the term on the right-hand side is not simply 1, but is more general. It becomes 1 only under a special condition,

$$\mathrm{supp}\left(U\tau_0 U^\dagger\right) = \mathrm{supp}\left(\tau_T\right), \tag{3.23}$$

which results in $S_0\left(U\tau_0 U^\dagger||\tau_T\right) = 0$, and thus (3.22) becomes equivalent to the original equality. We will refer to this condition as *the identical support condition* from now on. If, however, $\mathrm{supp}\left(U\tau_0 U^\dagger\right) \subset \mathrm{supp}\left(\tau_T\right)$, then the zeroth order relative Rényi entropy will strictly be greater than zero, i.e. $S_0\left(U\tau_0 U^\dagger||\tau_T\right) > 0$. In this case, the value on the right-hand side of the equality will be less than 1, but still be strictly greater than 0, and the original Jarzynski equality does not hold anymore. In other words, general relations between work and free energy difference are described by the $\alpha$-Jarzynski equality (Eq.(3.21)), which include the relation shown in Eq.(3.22) for $\alpha = 0$. The original Jarzynski equality (Eq.(3.12)) is only a special case for $\alpha = 0$ with an additional condition that the support of the state just before the final energy measurement in the forward protocol and the support of the initial state of the backward protocol (the reference state) are identical. Since thermal states as well as their unitary transforms are usually full-rank, the condition of identical support is usually fulfilled automatically and is trivial in a general setting of Jarzynski equality. This explains why Jarzynski equality satisfies in those cases and also why it is process-independent. However, there is an exception, i.e. when the initial state of the system in the forward protocol is prepared under some constraints such that it is thermal with respect to a Hilbert space $\mathcal{S}$ while the reference state of the system is thermal with respect to another Hilbert space $\mathcal{H}$, where $\mathcal{S} \subset \mathcal{H}$ [8]. Since a unitary operator cannot change the rank of a state, the support of the state right before the final energy measurement of the forward protocol can only be a proper subset of the support of the reference state in this case[9], leading to the failure of the original Jarzynski equality. Note that, even though we have been using the

[8] For later reference, we will call this kind of state together with the ordinary thermal state, where $\mathcal{S} = \mathcal{H}$, a"generalised thermal state" (with respect to the Hilbert space $\mathcal{H}$). In other words, a generalised thermal state is a thermal state with respect to a Hilbert space $\mathcal{S}$, where $\mathcal{S} \subseteq \mathcal{H}$.

[9] To be rigorous, we consider here only the unitary operator that is defined on $\mathcal{H}$, so it cannot bring any state in or out of $\mathcal{H}$ by definition.

language of quantum mechanics so far for our discussion, the failure of the original Jarzynski equality when the relavant states fail to satisfy the identical support condition does not restricted to the realm of quantum system. A classical analogue of such a situation is an isothermal expansion of a thermal ideal gas which is discussed extensively in [82–85], where the constraint here is rendered by a partition which prevents the gas from expanding at the beginning. Note that, in such a classical case, the states defined on the Hilbert spaces are replaced by probability distributions defined on phase spaces, and the unitary evolution is replaced by an isentropic process. In Ref. [86] and Ref. [87], studies similar to ours were done independently by examining the entropy production associated to arbitrary unitary forward and backward processes. Instead of utilising relative Rényi entropies, the authors of these two works present the deviation from the original equality in terms of the probability $\lambda$ that the final state of the backward process lies outside of the support of the initial state of the forward process. Thus, from Eq.(3.11) and Eq.(3.22), it is clear that we can rewrite their $\lambda$ in terms of the zeroth order relative Rényi entropies as

$$\lambda = 1 - e^{-S_0\left(U\tau_0 U^\dagger || \tau_T\right)}. \tag{3.24}$$

With the Rényi-Tsallis relative entropy identity (Eq.(2.77)), it is easy to see that $\lambda$ is exactly the corresponding relative Tsallis entropy of order 0, i.e.

$$\lambda = \mathcal{T}_0(U\tau_0 U^\dagger || \tau_T). \tag{3.25}$$

This result gives an interpretation to relative Tsallis entropy of order 0 as being a measure of the "absolute irreversibility"[10] and shows its relevance to thermodynamics and fluctuation theorem. Whether there exists any other relationships between relative Tsallis entropy of other orders and fluctuation theorem is an interesting topic that is worth investigating further later.

[10]The term "absolute irreversibility" is defined in Ref. [87] as the fact that "in the backward process the density matrix does not return to the subspace spanned by those eigenvectors that have nonzero weight in the initial density matrix.". This occurs according to the fact that a unitary process preserves the rank of a state, but the rank of $\tau_T$ is greater than the rank of $\tau_0$ by the nature of the setting, hence it is impossible to unitarily reverse $\tau_T$ to a state that has the same support as $\tau_0$.

### 3.3.2. $\alpha$-Jarzynski equality as equivalent representations of forward and backward work distributions

We argue that a forward work distribution $p_{fwd}(W)$ can equivalently be represented by the whole set of its corresponding $\alpha$-Jarzynski equalities. Furthermore, *if* the initial state of the forward protocol is full rank, we argue that this same whole set of $\alpha$-Jarzynski equalities also completely captures the entire information encoded in its backward work distribution counterpart $p_{bwd}(\mathcal{W})$. Note that we choose to distinguish the notations between the forward work ($W$) and the backward work ($\mathcal{W}$) here for convenience in the subsequent discussion.

To prove our claim, let us start by summing Eq.(3.18) above over all the possible states using the explicit expressions of $p_{bwd}((c,d) \to (a,b))$ as is shown in Eq.(3.3). This is similar to what we did previously in the derivation of Eq.(3.21) except from the fact that we start from Eq.(3.18) instead of Eq.(3.17). We will then have

$$e^{-\alpha S_{1-\alpha}\left(U^\dagger \tau_T U || \tau_0\right)} = \langle e^{\alpha\beta(W-\Delta F)} \rangle_{bwd}, \tag{3.26}$$

This is the $\alpha-$Jarzynski equality that is rewritten in terms of an average over the backward protocol instead of the forward protocol as is expressed in Eq.(3.21). The left-hand side of the equality follows from the identity, $(\alpha-1)S_\alpha(\rho||\sigma) = -\alpha S_{1-\alpha}(\sigma||\rho)$, and the cyclic property of a trace. The proof of this identity is straightforward from the definition of relative Rényi entropies. Note that the subscript *bwd* of the angle bracket means that the average is taken with respect to the backward protocol. Note also that the work $W$ that appears in both Eq.(3.21) and Eq.(3.26) is the forward work.

Let us suppose for now that every state involved in both the forward and backward protocols are full rank. One can see that $W = -\mathcal{W}$ in this case and the right-hand sides of Eq.(3.21) and Eq.(3.26) can be considered to be the moment-generating functions of the product between the inverse temperature $\beta$ and the dissipated work $W_{diss}$ with respect to the forward and backward probabilities, $p_{fwd}(+\beta W_{diss})$ and $p_{bwd}(-\beta W_{diss})$, respectively (cf. Eq.(2.10))[11]. Since the inverse temperature $\beta$ and the free energy difference

[11] $W_{diss} = W - \Delta F$ is the dissipated work in the forward protocol while $-W_{diss} = \mathcal{W} + \Delta F$ is the dissipated work in the backward protocol. Note that we define the free energy difference $\Delta F$ here as the free energy of the initial state of the backward protocol

$\Delta F$ are fixed and known, it is clear that the $\alpha$-Jarzynski equality can also be considered to be the moment-generating functions of both $p_{fwd}(W)$ and $p_{bwd}(\mathcal{W})$. In other words, for the full rank case, the set of equalities forms an equivalent representation of the forward work distribution as well as an equivalent representation of the backward work distribution simultaneously. Thus, all the statistics of the work involved and how the forward ones are related to the backward ones are, in principle, encoded in this generalisation of Jarzynski equality.

Let us now analyse the case where the initial state of the system in the forward protocol is not full rank. Consider the forward protocol first. One sees that the non-full rank property does not change the fact that the right-hand side of Eq.(3.21) is the moment-generating function of the forward work distribution, hence the $\alpha$-Jarzynski equality always represent all of its corresponding statistics completely. In contrast, this is *not* the case for the backward protocol. The complication in this situation arises from the fact that the backward work is not simply the negative of the forward work, i.e. $\mathcal{W} \neq -W$. The explanation for this is the following. In the same way as in the forward protocol, the backward work $\mathcal{W}$ is determined by the energy difference between the final and the initial states of the backward protocol. Since the initial state in the backward protocol is the reference state, which is full-rank, the final state will also be full-rank. This means the support of the final state of the backward protocol is larger than the support of the initial state of the forward protocol, i.e. $\text{supp}(U^\dagger \tau_T U) \supset \text{supp}(\tau_0)$. Therefore, the set of values of the backward work is not identical to, but is a superset of the set of the negative of the forward work, i.e. $\{\mathcal{W}\} \supset \{-W\}$. Suppose the set of the backward work can be decomposed into the union of two non-intersecting subsets, $\{\mathcal{W}\} = \{\mathcal{V}\} \cup \{\mathcal{V}\}'$, where $\{\mathcal{V}\} = \{-W\}$ is the subset of the backward work values that is identical to the negative of the forward work and $\{\mathcal{V}\}'$ is its complement. Then we can rewrite the right-hand side of Eq.(3.26) in terms of $\mathcal{V}$ explicitly as $\langle e^{\alpha\beta(W-\Delta F)} \rangle_{bwd} = \sum_{\mathcal{V}} p_{bwd}(\mathcal{V}) e^{-\alpha\beta(\mathcal{V}+F(\tau_{S,T})-F(\tau_{S,0}))}$. The fact that the sum does not include all values of the backward work $\mathcal{W}$ hence means that Eq.(3.26) is not the moment-generating function of the backward work when $\tau_0$ is not full rank. In other words, unlike its forward counterpart, $\alpha$-Jarzynski equality does not completely encode the statistics associated to

subtracted by the free energy of the initial state of the forward protocol.

the backward work distribution $p_{bwd}(\mathcal{W})$ in this case.

### 3.3.3. $\alpha$-Jarzynski equality in terms of $\alpha$-free energy difference

The expression of the original Jarzynski equality is neat and concise since it involves only the exponential of the forward work $W$ and the free energy difference $\Delta F$ in the forward direction on one side, while the other side is simply 1. We will now show that we can actually rewrite the expression of our $\alpha$-Jarzynski equality in a similar way. This reduces the whole family of the $\alpha$-parameterised equalities to just a single identity that not only look nicer than Eq.(3.21), but they also give some more insight. The key idea here is the concept of the $\alpha$-free energy, a generalisation of the concept of Helmholtz free energy to non-equilibrium states which is introduced and discussed briefly in section 2.5.3. From the relation between the free energy of order $\alpha$ and the relative Rényi entropies of the same order in Eq.(2.64), it is clear that one may choose to rewrite the $\alpha$-Jarzynski equality (Eq.(3.21)) further in terms of the $\alpha$-free energy instead of relative Rényi entropies by multiplying both sides of Eq.(3.21) with $e^{(\alpha-1)\beta F(\tau_T)}$ as follows,

$$e^{(\alpha-1)(S_\alpha\left(U\tau_0U^\dagger||\tau_T\right)+\beta F(\tau_T))} = \langle e^{(\alpha-1)\beta(W-\Delta F+F(\tau_T))}\rangle. \tag{3.27}$$

Therefore,

$$e^{(\alpha-1)\beta F_\alpha(U\tau_0U^\dagger,\tau_T)} = \langle e^{(\alpha-1)\beta(W+F(\tau_0))}\rangle, \tag{3.28}$$

where $F_\alpha(U\tau_0U^\dagger,\tau_T) = S_\alpha\left(U\tau_0U^\dagger||\tau_T\right) + F(\tau_T)$ is the free energy of order $\alpha$ of the state $U\tau_0U^\dagger$ with respect to the thermal state $\tau_T$. Note that we arrive at the right-hand side of the equation above from the fact that $\Delta F \equiv F(\tau_T) - F(\tau_0)$. Thus, we finally have

$$\langle e^{(\alpha-1)\beta(W-\Delta F_\alpha)}\rangle = 1, \tag{3.29}$$

where $\Delta F_\alpha \equiv F_\alpha(U\tau_0U^\dagger,\tau_T) - F(\tau_0)$ is the difference between the free energy of order $\alpha$ of the state $U\tau_0U^\dagger$ (with respect to the reference state $\tau_T$) and the free energy of the initial thermal state $\tau_0$. Note that, similar to how relative Rényi entropies play the role of the effective values of the

dissipated work $W_{diss}$, one can see that the $\alpha$-free energy differences play the role of the effective values of the forward work $W$ here.

**Finding all the $\alpha$-free energies of an arbitrary state**

The $\alpha$-Jarzynski equalities in the form of Eq.(3.29) allow one to determine *all* the $\alpha$-free energies $F_\alpha(\rho, \tau)$ of a system, which is in an *arbitrary quantum state* $\rho$, from the statistics of the work that is done on the system via a certain forward protocol. Note that the free energies of $\rho$ considered here are defined with respect to the thermal reference state $\tau$, which is a thermal state of a certain temperature that has the same Hamiltonian as $\rho$. A trick to do this is the following. First, prepare $\tau_a$, an arbitrary thermal state with Hamiltonian $H(\lambda_a)$ which has the same temperature as $\tau$, and $\lambda(t)$, a time-dependent parameter of the Hamiltonian which is engineered such that it satisfies the following requirements:

1. At time $t = 0$, $\lambda(0) = \lambda_a$.

2. There exists a time $t = T$ such that $\lambda(T) = \lambda_\tau$, where $H_\tau = H(\lambda_\tau)$ is the Hamiltonian of the thermal reference state $\tau$ (which is the same as the Hamiltonian of the state $\rho$), and $\rho = V\tau_a V^\dagger$, where $V = \mathbb{T}e^{-i\int_0^T H(\lambda(t))\,dt}$ is the time-evolution operator generated by $H(\lambda(t))$ that drives the system from time $t = 0$ to $t = T$. Note that the notation $\mathbb{T}$ stands for the time-ordering operator.

Next, treat $\tau_a$ as the initial state, $V$ as the evolution, and follow the usual three steps of the forward protocol (i.e. initial energy measurement $\rightarrow$ unitary evolution $\rightarrow$ final energy measurement) many times until the number of collected data is enough to appropriately infer the underlying statistics of the work. In principle, all the $\alpha$-free energies $F_\alpha(\rho, \tau)$ of $\rho$ with respect to $\tau$ can then be found by Eq.(3.29), given that one knows the free energy $F(\tau_a)$ of the state $\tau_a$ beforehand. Note however that, it may not be an easy task to implement this method experimentally. Even though the fact that one can choose an arbitrary thermal state $\tau_a$ at the start as long as it has the same temperature as $\tau$ is an advantage, a potential difficulty lies in the fact that one still needs to have a good enough control over the parameter $\lambda(t)$ of the system Hamiltonian to be able to implement the required unitary $V$ that will transform $\tau_a$ to $\rho$.

It should be noted that the whole procedure we described above does not generally involve $F(\tau)$ at all. By that, we mean one neither require to know $F(\tau)$ beforehand nor can one find $F(\tau)$ from this method in general. This may seem puzzling at first, as the original Jarzynski equality which is a special instance of Eq.(3.29) does not seem to provide any $\alpha$-free energies $F_\alpha(\rho,\tau)$ of the state $\rho$ with respect to $\tau$, but instead the free energy $F(\tau)$ of the reference state $\tau$ itself. To resolve this issue, consider a special case where the identical support condition holds, i.e. $\mathrm{supp}(\rho) = \mathrm{supp}(\tau)$, we will have $S_0\left(\rho||\tau\right) = 0$ and hence $F_0(\rho,\tau) = F(\tau)$, according to Eq.(2.64). In words, this means the zeroth order free energy of any state $\rho$ with respect to a thermal reference state $\tau$ is equal to the free energy of $\tau$ itself as long as the support of $\rho$ is identical to the support of $\tau$. This implies that, by setting $\alpha = 0$, one can also determine the thermal free energy $F(\tau)$ of the state $\tau$ using Eq.(3.29), no matter what the state $\rho$ actually is, as long as the identical support conditions are fulfilled. Actually, by substituting $F(\tau)$ for $F_\alpha(\rho,\tau)$ in Eq.(3.29) and setting $\alpha = 0$, one sees that the equality reduces to the original Jarzynski equality. This therefore explains how the original Jarzynski equality allows one to determine the free energy of a thermal state, which is an "equilibrium" property, from the statistics of the "non-equilibrium" work. It should be noted that the key to this extra feature of the original Jarzynski equality is, once again, the underlying identical support condition.

### 3.3.4. $\alpha$-monotonicity as a kind of generalised second law relations

Similar to how one obtains the second law relation $\langle W\rangle \geq \Delta F$ from the original Jarzynski equality by means of a Jensen inequality, $\langle e^X\rangle \geq e^{\langle X\rangle}$, let us demonstrate how a generalisation of the second law relation can be achieved by applying the Jensen inequality to $\alpha$-Jarzynski equality in Eq.(3.21):

$$e^{(\alpha-1)S_\alpha\left(U\tau_0U^\dagger||\tau_T\right)} \geq e^{\beta(\alpha-1)\langle(W-\Delta F)\rangle}. \tag{3.30}$$

Thus,

$$(\alpha-1)S_\alpha\left(U\tau_0U^\dagger||\tau_T\right) \geq \beta(\alpha-1)(\langle W\rangle - \Delta F), \tag{3.31}$$

which gives

$$\frac{1}{\beta}S_\gamma\left(U\tau_0U^\dagger||\tau_T\right) \leq \langle W\rangle - \Delta F \leq \frac{1}{\beta}S_\delta\left(U\tau_0U^\dagger||\tau_T\right), \tag{3.32}$$

where $\gamma < 1$ and $\delta > 1$ are order parameters of the relative Rényi entropies. Recall that, if $\mathrm{supp}(U\tau_0U^\dagger)$ is a *strict* subset of $\mathrm{supp}(\tau_T)$, the relative Rényi entropies of negative order will become ill-defined. Hence the parameter $\gamma$ in such a case must also be bounded from below by 0, i.e. $0 < \gamma < 1$. By rearranging terms a bit, one may as well rewrite Ineq.(3.32) further in terms the generalised free energies instead of relative Rényi entropies as

$$\Delta F_\gamma \leq \langle W\rangle \leq \Delta F_\delta, \tag{3.33}$$

where

$$\Delta F_\alpha \equiv \frac{1}{\beta}S_\alpha(U\tau_0U^\dagger, \tau_T) + \Delta F \tag{3.34}$$

$$= F_\alpha(U\tau_0U^\dagger, \tau_T) - F(\tau_0) \tag{3.35}$$

is the difference in the free energies of order $\alpha$ between the states $U\tau_0U^\dagger$ (with respect to $\tau_T$) and $\tau_0$. We see that this is a family of parameterised inequalities that set up the bounds for the average forward work. We argue that these inequalities form *a kind of generalised second law relations* or, more precisely, *a set of generalised free energy-work inequalities*, which states that: "For a system initially prepared in a generalised thermal state of a certain temperature (cf. footnote 8), its free energies of order (greater/less) than 1 can never increase (less/more) than the average of the corresponding work that is done on the system via an arbitrary forward protocol".

Let us now discuss several aspects of these generalised second law relations. First, we argue that these relations, which state in terms of $\alpha$-free energy differences $\Delta F_\alpha = F_\alpha(U\tau_0U^\dagger, \tau_T) - F(\tau_0)$, are more sensible than the original relation, which instead employs the free energy difference $\Delta F = F(\tau_T) - F(\tau_0)$. This is because, in a forward protocol, the work $W$ is done only during the unitary evolution $U$ that evolves the initial thermal state $\tau_0$ to the state $U\tau_0U^\dagger$. Therefore, it is more sensible to compare the average work $\langle W\rangle$ with the free energy differences between $U\tau_0U^\dagger$ and

$\tau_0$, rather than the free energy difference between $\tau_T$ and $\tau_0$. Next, let us consider, in particular, the generalised free energy-work inequality at order zero which states that

$$\langle W \rangle \geq \Delta F_0, \tag{3.36}$$

where $\Delta F_0$ is the free energy difference of order zero between the states $U\tau_0 U^\dagger$ and $\tau_0$. We see that this relation reduces to the second law relation $\langle W \rangle \geq \Delta F$ in the same way as how $\alpha$-Jarzynski equalities reduce to the original Jarzynski equality as is discussed in section 3.3.1, owing to the fact that $\Delta F_0 = \Delta F$ or, equivalently, $S_0\left(U\tau_0 U^\dagger || \tau_T\right) = 0$ when the identical support condition holds (according to Eq.(3.34)). It should be emphasised that this result does not necessarily mean the state $U\tau_0 U^\dagger$ and the thermal reference state $\tau_T$ are the same. It simply means their supports are identical as is stated by the identical support condition. However, if the identical support condition does not hold, we will have $\langle W \rangle \geq \Delta F_0 > \Delta F$ because $S_0\left(U\tau_0 U^\dagger || \tau_T\right) > 0$. This shows that Ineq.(3.36) provides a tighter lower bound to the average work $\langle W \rangle$ than Ineq.(3.13) does in this case. Thus we see that, just by replacing the free energy $\Delta F$ with $\Delta F_0$, which only changes the original free energy-work inequality to a single instance of the generalised free energy-work inequalities, we can already go beyond the original second law relation. Not only do we recover $\langle W \rangle \geq \Delta F$ when the identical support condition is satisfied, but we also get a tighter lower bound for the average work in general. In fact, it is clear that even more tighter lower bounds (as well as upper bounds) can be achieved from Ineq.(3.33) if one considers the free energy-work relation at other orders that are closer to 1.

The free energy difference of order 1 is special. We can see from Ineq.(3.33) that, by taking the limit where the order parameter approaches 1, the free energy becomes exactly equal to the average work, i.e. $\lim_{\alpha \to 1} \Delta F_\alpha = \langle W \rangle$. Thus, we see that Ineq.(3.33) may be rewritten as

$$\Delta F_\gamma \leq \Delta F_1 \leq \Delta F_\delta, \tag{3.37}$$

or, equivalently, in terms of relative Rényi entropies instead of $\alpha$-free ener-

gies,

$$S_\gamma\left(U\tau_0U^\dagger||\tau_T\right) \leq S_1\left(U\tau_0U^\dagger||\tau_T\right) \leq S_\delta\left(U\tau_0U^\dagger||\tau_T\right). \tag{3.38}$$

Notice that the relations above are actually identical to the $\alpha$-monotonic relations of relative Rényi entropies (Eq.(2.53)), where one of them is of order 1. In other words, we see that the generalised free energy-work inequalities (Ineq.(3.33)) are just the $\alpha$-monotonic relations in disguise. Moreover, recall that a relative Rényi entropy can also be considered an effective value. Therefore, following the discussion about the relation between the effective values and the fluctuation in section 2.4.2, we can imply that the origin of this kind of generalised second law relations is the ignorance of the work fluctuation. While the average work (the free energy difference of order 1) does not contain any information concerning the fluctuation of the work, all the other orders of the free energy difference do, to individually different degrees.

### Data-processing inequality as another kind of generalised second law relations

It should be noted that there is another kind of generalised second law relations which is studied in the context of catalytic thermal operation by Brandão *et al.* and is presented in Ref. [18]. Those second laws are based on the data-processing inequality, which is *another* monotonic property of relative Rényi entropies (cf. section 2.5.3). To be precise, to formulate their second laws in Ref. [18], Brandão *et al.* employs not only the $\alpha$-relative Rényi entropy, but also the sandwiched and the reverse sandwiched relative Rényi entropies.

### Remarks on the two kinds of generalised second law relations

While our second laws relation arise due to the ignorance of the fluctuation of the work value (cf. section 2.4.2) and involves only one kind of quantum relative Rényi entropy, the "Brandão *et al.*'s second laws" arise from the restricted transformation according to the corresponding resource theory and involves all kinds of quantum relative Rényi entropies that are currently known. It is an interesting question whether these two kinds of the second

laws can be unified. A hint comes from the results in Ref. [17], where several second-law-like relations similar to ours are discussed. They are similar because those relations can also be stated in terms of the monotonic relation between relative Rényi entropies, but only the orders 0, 1, and $\infty$ of *commuting* states are considered[12]. The fact that the results in Ref. [17] can be derived directly from Brandão *et al.*'s second laws as is shown in Ref. [18] seems to suggest that the unification should be possible, at least, in commuting cases.

### 3.3.5. Support expansion and fluctuation-dissipation relations

The fact that $\alpha$-Jarzynski equality can be treated as a moment-generating function for every forward protocol means that its logarithm is a cumulant-generating function. From Eq.(2.12) and Eq.(3.21), we see that

$$S_\alpha\left(U\tau_0U^\dagger||\tau_T\right) = \beta\langle W_{diss}\rangle + \frac{\beta^2\,\mathrm{Var}(W_{diss})}{2}(\alpha-1) + \sum_{n=3}^{\infty}\frac{\kappa_n(W_{diss})}{n!}(\alpha-1)^{n-1}, \tag{3.39}$$

where we use the fact that the first two cumulants of the dissipated work, i.e. $\kappa_1(W_{diss})$ and $\kappa_2(W_{diss})$, are the arithmetic mean and the variance of the dissipated work $W_{diss}$ respectively (cf. section 2.3.1). It is clear that the fluctuation of the dissipated work is characterised by all the cumulants $\kappa_n(W_{diss})$ apart from the order $n = 1$. Now, suppose that the fluctuation is very small such that all the cumulants of order higher than $n = 2$ become negligible, i.e. the dissipated work distribution can be well-approximated by a Gaussian distribution. For convenience, we will refer to this as the

[12]Suppose $\tau'$ is a thermal state with a certain inverse temperature $\beta$ and a Hamiltonian $H$, whereas $\rho'$ is an arbitrary state with the same corresponding Hamiltonian $H$ and $[\rho', \tau'] = 0$. It is shown by Horodecki and Oppenheim in Ref. [17], using the resource theory framework, that the *minimum* amount of work one needs to perform to ensure a successful transformation from $\tau'$ to $\rho'$ is equal to $\frac{1}{\beta}S_\infty(\rho'||\tau')$, whereas the *maximum* amount of work one can certainly extract from the transformation from $\rho'$ back to $\tau'$ is equal to $\frac{1}{\beta}S_0(\rho||\sigma)$. Based on the fact that $S_\infty(\rho'||\tau') \geq S_0(\rho'||\tau')$, they then conclude that this signifies a fundamental second-law-like relation. Note that, this can also be viewed as the monotonic relation in $\alpha$ between relative Rényi entropies of order 0 and $\infty$. The relative Rényi entropy of order 1 gets into this picture when the asymptotic equipartition property applies, which gives $S_0(\rho'||\tau') = S_\infty(\rho'||\tau') = S_1(\rho'||\tau')$. This is what happens in standard equilibrium thermodynamics when fluctuation is negligible.

*Gaussian limit.* Then we will have

$$\beta\langle W_{diss}\rangle \simeq S_\alpha\left(U\tau_0U^\dagger||\tau_T\right) + \frac{(1-\alpha)}{2}\beta^2\,\mathrm{Var}(W), \tag{3.40}$$

where we use the fact that $\mathrm{Var}(W_{diss}) = \mathrm{Var}(W)$. The fluctuation-dissipation theorem in Eq.(3.15) is recovered from this relation by setting $\alpha = 0$ first, i.e.

$$\beta\langle W_{diss}\rangle \simeq S_0\left(U\tau_0U^\dagger||\tau_T\right) + \frac{\beta^2}{2}\,\mathrm{Var}(W), \tag{3.41}$$

then assuming that the identical support condition (Eq.(3.23)) is satisfied which will cause the zeroth order relative Rényi entropies to vanish. In general, however, the identical support condition may not hold due to some constraints in the initial setting as was previously discussed in section 3.3.1.

The fact that Eq.(3.41) holds independently of the identical support condition suggests that the relation between dissipation and fluctuation in Gaussian limit is not always directly proportional to each other. However, they always have a linear relation in this limit. The relative Rényi entropy of order 0 represents the part of the dissipation that arises from the expansion of the support of the state.

To restore the proportional relation between the dissipated work and the work fluctuation, we propose the concept of *the non-expanding dissipated work* denoted by $W_{diss,nex}$. It is defined and links to other previously discussed concepts as follows,

$$\begin{aligned} W_{diss,nex} &\equiv W_{diss} - \frac{S_0\left(U\tau_0U^\dagger||\tau_T\right)}{\beta} && (3.42)\\ &= W - \Delta F_0 && (3.43)\\ &= \frac{S_1\left(U\tau_0U^\dagger||\tau_T\right) - S_0\left(U\tau_0U^\dagger||\tau_T\right)}{\beta} && (3.44)\\ &= F_1(U\tau_0U^\dagger,\tau_T) - F_0(U\tau_0U^\dagger,\tau_T) && (3.45)\end{aligned}$$

In terms of the non-expanding dissipated work, Eq.(3.41) then becomes

$$\langle W_{diss,nex}\rangle \simeq \frac{\beta}{2}\,\mathrm{Var}(W), \tag{3.46}$$

We will call this relation *the non-expanding fluctuation-dissipation theo-*

*rem*, while the one in Eq.(3.41) will be called *the absolute fluctuation-dissipation theorem*. Note that, since the variance is non-negative the non-expanding dissipated work is also non-negative in average. This is confirmed by Eq.(3.33) for $\alpha = 0$. We see that, by taking out the contribution from the support expansion, the direct proportionality between the dissipation and the work fluctuation in the Gaussian limit is restored. It is interesting to see that this non-expanding dissipated work is mathematically captured by the difference between the $\alpha$-free energies (as well as relative Rényi entropies) of order 0 and 1. This gives an operational meaning to the difference between the $\alpha$-free energies (and relative Rényi entropies) of these particular orders.

## 3.4. Chapter summary

Before we end this chapter, let us summarise what we have shown so far one more time. With the aid of relative Rényi entropies and related concepts, we have derived a family of parameterised equalities, called the $\alpha$-Jarzynski equality, that does not only capture the relationship between work and free energy difference in an arbitrary non-equilibrium transformation between two certain thermal states, but also completely encodes the statistics of the work. It is shown that the original Jarzynski equality, both in classical and quantum settings, is a special instance of our generalised relations, obtained by also assuming an often-overlooked condition of identical support. Unlike the original equality however, the $\alpha$-Jarzynski equality is generally process-dependent, which is manifest in the presence of the unitary matrix $U$ in the relative Rényi entropy. The fact that the equality can also be expressed in terms of the $\alpha$-free energy suggests that one may be able to experimentally determine every order of the $\alpha$-free energy of a system in a particular state, similar to how the original equality allows one to determine the equilibrium free energy. With the $\alpha$-Jarzynski equality, we also show how the $\alpha$-monotonicity relation of the relative Rényi entropies may be treated as a generalisation of the second law of thermodynamics. The origin of this kind of generalised second law arises from the ignorance of work fluctuation, which can be perceived through the relation between effective values and fluctuation discussed in the previous chapter (cf. section 2.4.2). The fact that another kind of generalisation of the second law can be phrased as the data-processing inequalities, another kind of monotonic relation of

relative Rényi entropy, strongly supports the appropriateness of the use of relative Rényi entropy in non-equilibrium thermodynamics and also suggests that the two kinds of second laws may be related somehow. Moreover, we show that in the Gaussian limit, i.e. when the work fluctuation is so small that it can be effectively captured by its variance alone, the original fluctuation-dissipation theorem holds only when the identical support condition (Eq.(3.23)) is satisfied. When the identical support condition does not hold however, a correction term in the form of the relative Rényi entropy of order 0 must be added to compensate for it, thus leading to the new concept of the non-expanding dissipated work and an operational meaning of the difference between the $\alpha$-free energy of order 0 and 1. The dissatisfaction of the identical support condition is related to the notion of absolute irreversibility recently proposed and discussed in Ref. [86] and Ref. [87]. By utilising the Rényi-Tsallis relative entropy identity, we demonstrate how this notion can be quantified by the relative Tsallis entropy of order 0. This serves as a new operational meaning to the relative Tsallis entropy of order 0.

In the next chapter, we will discuss the more practical side of our work which is an experimental study of the non-equilibrium dynamics of an optically levitated nanosphere.

# 4. A non-equilibrium thermodynamic analysis of an optically levitated nanosphere

## 4.1. Overview and motivation

Temperature is one of the most important thermodynamical quantities. The state in which temperature is well-defined, i.e. the thermal state, is special because its energy has a Boltzmann distribution (or rather Bose-Einstein or Fermi-Dirac distributions, for equilibrium quantum statistical ensemble), giving rise to a partition function which is a moment-generating function that completely encodes the statistics associated to the thermal state and can thus be used to conveniently extract properties of the system.

Strictly, temperature is a property associated to a degree of freedom, so different degrees of freedom may have different temperatures. An example of such a system is an anisothermal plasma where the temperatures associated to different modes of motion of the plasma (and its constituents) are different. A "thermal equilibrium between two degrees of freedom" is thus a condition when the two degrees of freedom couple to each other and their temperatures become equal. Conventionally, the term "thermal equilibrium" without any degrees of freedom explicitly specified usually means a special case where all the degrees of freedom of interest are in the same thermal equilibrium, allowing one to be able to speak of "the temperature of the system" as a single entity. In many realistic situations, however, the systems of interest are not in thermal equilibrium, so the concept of temperature as a global property is not well-defined. Nevertheless, there are situations where local equilibriums are established, leading to the emergence of local temperatures, such as those being in steady states.

In this chapter, we discuss our study of the *classical* non-equilibrium dy-

namics of an optically levitated nanosphere and show how this setup could be used in thermometry to estimate both the local temperatures of a dilute gas which is in a non-equilibrium steady state around the sphere and also the surface temperature of the nanosphere itself. This investigation was initially done alongside the theoretical study that was discussed in Chapter 3, with the original aim being to experimentally verify Jarzynski equality and its variations both in classical and quantum circumstances using an optically levitated nanosphere setup. The reason we chose to work with this particular kind of setup was not only because it was convenient, but also because it is widely believed that such a system can potentially exhibit quantum effects at a macroscopic scale [88–97]. Thus we expected that it should allow a systematic study of the equalities both in the classical and quantum regimes, as well as the transition between them. However, in order to devise a suitable protocol for the verification, one must understand the dynamics of the levitated nanosphere thoroughly first. To this end, we propose a theoretical model called "the non-interacting baths model" and show that it fits well with the data from the actual experiment, hence contributing some more insight into the non-equilibrium nature of this kind of setup.

Our study reveals that the *classical* dynamics of an optically levitated nanosphere is quite rich in detail and the system is highly far from equilibrium, with the presence of 4 distinct temperatures, each of which arises from different degree of freedom of the setup. We find that the main cause of this complexity is the interplay between the laser and the surrounding gas. To put it briefly, the laser does not only trap the sphere but also heats it up as part of the laser is absorbed by the impurities in its body. Meanwhile, the surrounding gas does not only provide a drag force but also cools the body of the sphere down by taking some heat away through its molecular collisions with the sphere. We show that, depending on the parameters of the setup, what eventually happens to the system is either that the particle leaks from the optical trap or the system assumes a non-equilibrium steady state. Our analysis also shows that the coupling between the centre of mass and the bulk degrees of freedom of the sphere via the interaction with the gas allows one to estimate $T_{\mathsf{sur}}$, the surface temperature of the sphere, from $T_{\mathsf{CM}}$, the temperature corresponding to the random motion of the centre

of mass[1]. Using this estimation method, we find that the surface temperature of the sphere rises when the intensity of the trapping laser increases and/or the gas pressure decreases and vice versa. We also find that the rising surface temperature can even reach the melting point of the material when the intensity of the trapping laser is high and/or the surrounding gas pressure is low enough. This discovery thus resolves a wide suspicion that the laser heating is an underlying cause of the nanosphere leakage in the low pressure regime [94, 98, 99], which is one of the obstacles to the success of the ground state cooling experiments that are implemented on optically levitated nanosphere setups [89–91, 93].

To get into more details, let us start by discussing the setting of our optically levitated nanosphere system and how the experiment is conducted first. The content of this chapter is mainly based on our work in Ref. [100].

## 4.2. Experimental setup

In our setup, silica beads of diameters 105.1nm and 2.56$\mu$m are held, one at a time, in an optical trap created by two focused laser beams with a beam waist of about 1$\mu$m, the intensities of which are variable but equal. The two beams have wavelengths around 1064nm but are made to be slightly different to prevent standing wave interference. The gas we use in our experiment is the normal air in the lab which is initially under a controlled temperature of 294 K. To control the concentration of the surrounding gas, the optical trap is set in a vacuum chamber connected to a pump. The motion of the beads, both in the radial and the axial directions with respect to the trap, is monitored real-time by detecting the scattered fraction of the trapping laser, using a microscope and a quadrant photodetector (QPD) mounted outside the chamber. In addition, when the intensity of the trapping laser is too low, a low-power laser beam with frequency 532nm is added to aid the detection. A picture of the real setup and a diagram describing it are shown in Figure 4.1 and Figure 4.2 respectively.

Now that we see the details of the setup, let us discuss some theories that

[1]To be more precise, we show how $T_{\mathsf{sur}}$ can be estimated from the emerging gas temperature $T^{\mathsf{em}}$. However, since we can obtain $T^{\mathsf{em}}$ from $T_{\mathsf{CM}}$ and the impinging gas temperature $T^{\mathsf{imp}}$, which is equal to the room temperature, as is shown in Eq.(4.35), this claim is also valid. The detail of what these various temperatures actually are and how they are related is discussed in section 4.4 and section 4.5.

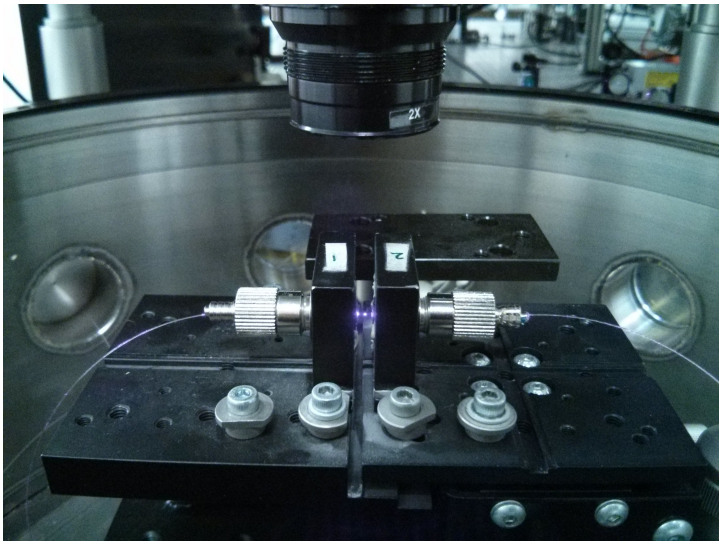


Figure 4.1.: **Picture of the actual setup.** The bright dot in the middle at the bottom of the picture is the light that is scattered by the levitating bead, trapped by an optical tweezer created from the laser beams coming out of two opposing fibres situated on the left and the right. At the top of the picture is the camera lens that is connected to a quadrant photodetector used for tracking the motion of the bead in two dimensions. The whole setup is put in a chamber that is connected to a pump (not shown in the picture) allowing pressure control. [Picture taken by Dr James Millen]

are the basis for our proposed "non-interacting baths model", in order to understand the non-equilibrium dynamics of this system. In particular, we will discuss how different degrees of freedom in the setup couple to each other and how that helps us to assess some relatively difficult-to-measure properties, such as the sphere surface temperature ($T_{\mathsf{sur}}$), from the easy-to-measure ones, such as the centre of mass temperature ($T_{\mathsf{CM}}$).

Before we start the theory discussion, let us briefly define some notations we will use in this chapter.

$\langle z \rangle$ : temporal average of an arbitrary variable $z$

$\tau$ : time period

T : temperature

$\alpha$ : accommodation coefficient

## 4.3. Theoretical background

### 4.3.1. Optically levitated nanosphere

The optically levitated nanosphere setup is composed of a nanoscale dielectric sphere being levitated against gravity in mid-air by optical tweezers. The dynamics of the sphere can be described as a Brownian particle being held in place by optical tweezers. To understand how this works in more detail, let us separately discuss optical tweezers and Brownian motion first.

#### Optical tweezers

Optical tweezers are an experimental tool which utilises an intense laser to trap a small dielectric material. The first successful demonstration of the technique was performed in 1971 by Ashkin and Dziedzic [101] on small transparent glass spheres levitated in air. This trapping technique is a basis for the development of more sophisticated trapping and cooling techniques for neutral atoms, the work that led to the award of Nobel Prize in Physics to Steven Chu, Claude Cohen-Tannoudji, and William D. Phillips in 1997.

The working principle of optical tweezers depends on the relative size between the trapped particle and the laser wavelength. Theoretically, in the limit where the size of the particle is much smaller than the wavelength of the laser (Rayleigh scattering), the particle (for example, a small silica bead) can be treated as an electric dipole which interacts with a non-homogeneous electric field created by the laser, giving rise to a force that pushes the particle along the gradient of the field. The relation between the force $\boldsymbol{F}$ and the laser intensity $I$ in this limit is $\boldsymbol{F} = \frac{2\eta}{c\epsilon_0}\boldsymbol{\nabla} I$, where $\eta$ is the polarisability of the particle, $c$ is the speed of light, and $\epsilon_0$ is the permittivity of free space[2]. The fact that the intensity of a laser beam is maximum at its centre and gradually dim along its radius indicates that the direction of the force acting on the dipole points towards the centre of the beam. Thus, by a careful tuning of the light, one can either hold or move the bead

[2]In our experiment, although the sizes of the beads are on a comparable scale with the wavelength and hence the relation between the force and the intensity gradient shown above does not exactly hold quantitatively, we find that it still holds qualitatively, i.e. the magnitude of the force is still roughly proportional to the magnitude of the intensity gradient and their directions are the same.

around. In fact, with the harmonic approximation, one can treat the trapped particle as a harmonic oscillator. This leads to the following equation of motion for the particle:

$$M\ddot{x}_d(t) = -M\omega_{d,0}^2 x_d(t), \tag{4.1}$$

where $x_d(t)$ is the position of the bead of mass $M$ relative to the centre of the trap in the $d$-direction and $\omega_{d,0}$ is the natural frequency of the trap, also in the $d$-direction. Note that the reason one also needs to add the subscript $d$ to the trap frequency is because it can become anisotropic (i.e. direction-dependent) due to the asymmetric geometry of the setup. Because of the highly controllable feature, the optical tweezers technique has been widely applied in many research areas, especially in biology and nanotechnology [90, 93, 102–106]. Recently, there is an interest in applying the technique to study quantum effects at the macroscopic scale [88, 89, 91, 92, 94–97].

**Brownian motion**

Brownian motion is the random motion of particles which are immersed in a body of fluid that is relatively static as a whole. Its first mathematical description was derived by Thiele in 1880 [107][3]. Later, Einstein [80] and Smoluchowski [109] independently showed theoretically how the phenomenon can be described in terms of the collisions between the Brownian particles and the fluid molecules. The merit of Einstein's and Smoluchowski's discoveries lies in the fact that they allow one to learn properties of the surrounding fluid at thermal equilibrium solely from the motion of the Brownian particles and, more astonishingly, to experimentally verify the existence of atoms and molecules, the notions which were only hypothesised at that time. In 1909, Perrin, following Einstein's theoretical result, performed experiments [110] which confirmed the existence of atoms and molecules for the first time and led to him receiving the Nobel Prize in Physics in 1926. Nowadays, Brownian motion is used in various studies ranging from dissipative processes [111, 112], soft matter physics [102–104],

[3]Thorvald Nicolai Thiele (1838-1910) was a Danish mathematician. Not only was he the first one who came up with the mathematical description of Brownian motion in 1880, he was also the first one who introduced the concept of cumulant in 1889 [108].

energy harvesting [113], and medical imaging [114].

The position $x_d(t)$ of a free Brownian particle in the $d$-direction is described by Langevin equation,

$$M\ddot{x}_d\left(t\right) = F_d^{\mathsf{fluc}}\left(t\right) - M\Gamma_d\dot{x}_d\left(t\right), \tag{4.2}$$

with an assumption that the force $F_d^{\mathsf{fluc}}(t)$ in the $d$-direction has a Gaussian white noise profile which satisfies two additional conditions,

$$\left\langle F_d^{\mathsf{fluc}}\left(t\right)\right\rangle = 0 \tag{4.3}$$

$$\left\langle F_d^{\mathsf{fluc}}\left(t\right) F_d^{\mathsf{fluc}}\left(t+t'\right)\right\rangle = 2k_B M T_d \Gamma_d\,\delta\left(t'\right). \tag{4.4}$$

Here, $\Gamma_d$ and $T_d$ are respectively the damping coefficient and the temperature of the fluid around the Brownian particle, both are in the $d$-direction. Note again that we need to distinguish between quantities that belong to different directions because their values may be different as a result of the asymmetric geometry of the setup or the system being in a certain non-equilibrium steady state. The angle brackets sign above denotes the temporal average, which can be computed by $\langle y\rangle = \lim_{\tau\to\infty}\frac{1}{\tau}\int_{-\tau/2}^{+\tau/2} y(t)\,dt$, for a time-dependent variable $y(t)$. Note that the variable $\tau$ in this context stands for a time period and the limit practically means the period must be long enough such that the obtained temporal averages converge reasonably to a single value.

Now that we learn about the optical tweezers and Brownian motion, we are ready to write the equation of motion of the optically levitated nanosphere, i.e.

$$M\ddot{x}_d\left(t\right) + M\Gamma_d\dot{x}_d\left(t\right) + M\omega_{d,0}^2 x\left(t\right) = F_d^{\mathsf{fluc}}\left(t\right), \tag{4.5}$$

which is basically the combination of the two situations discussed above. Before we continue, let us agree that we will omit the direction subscript $d$ from now on since it will be clear from the context which axis we are examining.

### 4.3.2. Power Spectrum

To be able to link the theory to the real experiment, one always needs to find the key quantities that are measurable in the experiment and link to all the other quantities that appear in the theory. In this part, we will discuss the power spectrum associated to the Langevin equation and show how it links the theory to a measurable quantity in the experiment. To start with, let us consider the Fourier transform of (4.5),

$$\begin{aligned}(-i\omega)^2\,\tilde{x}\,(\omega) - i\omega\Gamma\tilde{x}\,(\omega) + \omega_0^2\tilde{x}\,(\omega) &= \tilde{F}^{\mathsf{fluc}}\,(\omega)\,/M \\ \tilde{x}\,(\omega) &= \frac{\tilde{F}^{\mathsf{fluc}}\,(\omega)\,/M}{\omega_0^2 - \omega^2 - i\omega\Gamma},\end{aligned} \tag{4.6}$$

where $\tilde{x}\,(\omega) = \lim_{\tau\to\infty}\frac{1}{2\pi}\int_{-\tau/2}^{+\tau/2} e^{-i\omega t}x\,(t)dt$ is the Fourier transform of $x(t)$. We see that the relation between the position of the bead and the random force acting on it is linear in the Fourier space.

Next, define the power spectrum,

$$J\,(\omega) \equiv \lim_{\tau\to\infty}\frac{\langle|\tilde{x}\,(\omega)\,|^2\rangle}{\tau} = \lim_{\tau\to\infty}\frac{1}{\tau}\frac{\langle|\tilde{F}^{\mathsf{fluc}}\,(\omega)\,/M|^2\rangle}{|\omega_0^2 - \omega^2 - i\omega\Gamma|^2}. \tag{4.7}$$

Here, we assume that the damping coefficient is time-independent, which is the reason we can leave the denominator out of the temporal average. Let us now consider the force term in the numerator. One can rewrite it in terms of its Fourier transform as follows,

$$\langle|\tilde{F}^{\mathsf{fluc}}\,(\omega)\,|^2\rangle = \lim_{\tau'\to\infty}\lim_{\tau''\to\infty}\int_{-\tau'/2}^{+\tau'/2}\int_{-\tau''/2}^{+\tau''/2} dt''dt'\,e^{-i\omega(t'-t'')}\langle F^{\mathsf{fluc}}(t')F^{\mathsf{fluc}}(t'')\rangle \tag{4.8}$$

Then using the force correlation condition (4.4), one will get

$$\langle|\tilde{F}^{\mathsf{fluc}}\,(\omega)\,|^2\rangle = 2k_BMT\Gamma\lim_{\tau'\to\infty}\lim_{\tau''\to\infty}\int_{-\tau'/2}^{+\tau'/2}\int_{-\tau''/2}^{+\tau''/2} e^{-i\omega(t'-t'')}\delta(t''-t')\,dt''dt'. \tag{4.9}$$

Therefore, the power spectrum becomes

$$J(\omega) = \frac{2k_BT}{M} \frac{\Gamma}{\left(\omega_0^2 - \omega^2\right)^2 + (\omega\Gamma)^2}. \tag{4.10}$$

The power spectrum links together various parameters: position of the bead, trap frequency, damping coefficient, and temperature. The peak of the power spectrum is at the apparent peak frequency $\omega^* = \sqrt{\omega_0^2 - \frac{\Gamma^2}{2}}$, where the peak value is

$$J(\omega^*) = \frac{2k_BT}{M\Gamma\left(\omega^{*2} + \frac{\Gamma^2}{4}\right)} = \frac{2k_BT}{M\Gamma\tilde{\omega}^2}. \tag{4.11}$$

Here, the frequency $\tilde{\omega} = \sqrt{\omega_0^2 - \frac{\Gamma^2}{4}}$ is the apparent frequency in the presence of damping which is different from the bare frequency $\omega_0$. The power spectrum can be obtained experimentally by measuring the position of the bead over time according to its definition in (4.7). From (4.11), one can see that the available information encoded in the peak are the apparent trap frequency, the temperature, and the damping coefficient.

**Autocorrelation function**

An autocorrelation function is a two-point correlation function, or equivalently, a covariance function. It is a simple task to show that it is a Fourier transform of a power spectrum.

$$\begin{aligned}
\langle x(t)\, x\left(t+\tau'\right)\rangle &= \lim_{\tau\to\infty} \frac{1}{\tau} \int_{-\tau/2}^{+\tau/2} dt\, x(t)\, x\left(t+\tau'\right) \\
&= \lim_{\tau\to\infty} \lim_{\Omega\to\infty} \lim_{\Omega'\to\infty} \frac{1}{\tau} \int_{-\tau/2}^{+\tau/2} \int_{-\Omega}^{+\Omega} \int_{-\Omega'}^{+\Omega'} d\omega'\, d\omega\, dt\cdot \\
&\quad \tilde{x}(\omega) e^{-i\omega t} \tilde{x}^*(\omega') e^{+i\omega'(t+\tau')} \\
&= \lim_{\tau\to\infty} \frac{1}{\tau} \int_{-\infty}^{\infty} \frac{d\omega}{2\pi} \langle|\tilde{x}(\omega)|^2\rangle e^{i\omega\tau'} \\
&= \int_{-\infty}^{\infty} \frac{d\omega}{2\pi} J(\omega) e^{i\omega\tau'}.
\end{aligned} \tag{4.12}$$

This relationship implies that an autocorrelation function encodes the same information as its corresponding power spectrum. However, unlike the position profile, both objects do not completely capture all one can learn about

the dynamics of the system in general. The only exception is when the probability distribution of the position, derived from the position profile, is Gaussian, for example, in a Brownian motion. This can be seen by recalling that a Gaussian distribution is completely characterised by its arithmetic mean and covariances. However, the value of the arithmetic mean or the average position of the particle just depend on how the coordinates are set, which is simply a matter of the observer's choice. It therefore does not really contain any non-trivial information about the system. In contrast, the covariances do not vary with the coordinates. Thus, it is safe to consider that the autocorrelation function as well as the power spectrum completely capture the dynamics of a Brownian system.

To find an explicit form of the autocorrelation function, let us substitute $J(\omega)$ from (4.10) into (4.12) and solve. It is shown in Ref. [115] that, this is equal to

$$\langle x(t)\, x\left(t+\tau'\right)\rangle = \frac{2k_BT}{M\omega_0^2} e^{\frac{-\Gamma\tau'}{2}} \left(\cos\tilde{\omega}\tau' + \frac{\Gamma}{2\tilde{\omega}}\sin\tilde{\omega}\tau'\right). \tag{4.13}$$

Note that this relation is based on the assumption that the centre of the trap is always at the origin of the $x$-coordinate (i.e. at $x = 0$). If this is not true, one may need to keep reassigning the origin position to compensate the unwanted movement of the centre at all times. The function can be decomposed into two parts, the prefactor ($\frac{2k_BT}{m\omega_0^2}$) and the damped oscillation ($e^{\frac{-\Gamma\tau'}{2}}(\cos\tilde{\omega}\tau' + \frac{\Gamma}{2\tilde{\omega}}\sin\tilde{\omega}\tau')$). The prefactor can be read out from the $y$-intercept of the function. This part provides the information about temperature and bare trap frequency. Together with the oscillation part, which provides the damping coefficient and the damped frequency ($\tilde{\omega}$), one can also extract the information of all the other relevant parameters from the autocorrelation function.

## 4.4. The heating effect

The theoretical analysis of the setup we discussed so far concerns the nanosphere that is not too far from thermal equilibrium with the surrounding fluid (which could either be a liquid or a gas) that has a single well-defined temperature. The role of the optical trap is only to create a harmonic potential while the drag and fluctuating forces arise due to the surrounding fluid. In

other words, there is no coupling between the two sources that generate the forces. However, this model is too simplified as it does not capture what actually happens in the real setup.

In this section, we will discuss the dynamics of our optically levitated nanosphere setup in the presence of the heating effect, a phenomenon where the body of the nanosphere heats up because the energy it absorbs from the trapping laser is greater than the energy it loses via collisions with the surrounding fluid molecules. In other words, we take into account the fact that the laser does not only generate a harmonic trap but also supplies heat to the nanosphere via laser absorption. This consequently generates a heat transfer between the nanosphere and the surrounding fluid, which is dilute air in our setup. The heat then affects the dynamics of the air and how it interacts with the sphere, and in turn changes the dynamics of the sphere itself. One of the reasons why it is important to include this effect into our analysis is because, in reality, the nanosphere always absorbs some energy from the laser, thus the heating effect always takes place and affects the dynamics of the system to some degree. In our optically levitated nanosphere setting, the laser absorption is caused by the impurity present in the silica sphere. The fact that the whole sphere-air system of this setting is in Knudsen regime (large Knudsen number)[4] means the heat dissipation from the sphere to the surrounding in our setting occurs at a very slow rate, allowing the sphere to reach very high final bulk temperature. Moreover, the gas being very dilute also means the collision between its molecules happens at a much slower rate than the collision with the sphere that one may treat as if there is no heat transfer between the molecules in a close vicinity of the sphere, leading to a non-equilibrium thermodynamic situation where it is not possible to assign a single well-defined temperature to the gas. This final point is the basis of our "non-interacting baths model".

### 4.4.1. The non-interacting baths model

To accommodate the heating effect in the theoretical description of our experiment, we propose an *assumption* that the gas molecules in the vicinity

[4]Knudsen number: $K_n = \frac{\lambda}{L}$, where $\lambda$ is the mean free path and $L$ is the characteristic dimension which depends on the nature of the setup, is a dimensionless number that roughly determines whether one should treat the fluid in question as a continuous body (low $K_n$) or discrete spheres (high $K_n$).

of the sphere can be categorised into the impinging and emerging molecules (relative to the surface of the sphere), each of which forms a thermal bath with its own temperature. Since the molecules do not interact, the two baths are independent from each other and their temperatures are fixed. This additional assumption leads to a non-equilibrium setting for the sphere, since the sphere is now placed in an environment composed of two different temperatures. We will show that it is still possible to describe the dynamics of the sphere as a Brownian motion, with an effective damping coefficient and an effective temperature. This suggests that many nice properties of a Brownian system, for example, that the motion of a Brownian particle can be used to extract some information about its surrounding fluid, are still retained in the optically levitated nanosphere system, even though the heating effect actually drives it far away from equilibrium. We will see later that this fact allows us to determine several local properties of the non-equilibrium gas around our nanosphere as well as the surface temperature of the nanosphere itself from its position profile.

To describe our model more systematically, let us suppose that, initially, the temperature of the whole gas is $T^{\mathsf{imp}}$ while the surface temperature of the sphere is $T'_{\mathsf{sur}}$, where $T'_{\mathsf{sur}} > T^{\mathsf{imp}}$, due to the heating effect. Shortly after, some of the gas molecules will start to impinge on the surface of the sphere and stick to it temporarily. During this time, heat will transfer from the surface to the molecules, raising their energy before the molecules start to emerge from the sphere back to the chamber. We assume here that the energy distribution of the emerging gas is thermal with temperature $T^{\mathsf{em}}$. As this goes on, the surface temperature of the sphere will reach a steady value $T_{\mathsf{sur}}$ and the vicinity of the sphere will be filled with gas of two different temperatures $T^{\mathsf{imp}}$ and $T^{\mathsf{em}}$, forming two thermal baths. One expects that $T_{\mathsf{sur}} \geq T^{\mathsf{em}} \geq T^{\mathsf{imp}}$.

Let us now examine how the heating according to our model affects the dynamics of the sphere. The key assumption here is the independence of the two baths, which is justified by the fact that the gas as a whole is very dilute, so the molecules hardly interact with one another. Since they are independent, each one of them should individually act in the same way as what a single bath does i.e. exerting both a fluctuating force and a drag

force on the sphere. The equation of motion of the sphere is thus,

$$M\ddot{x}(t) + M\left(\Gamma^{\mathsf{imp}} + \Gamma^{\mathsf{em}}\right)\dot{x}(t) + M\omega_0^2 x(t) = F^{\mathsf{imp}}(t) + F^{\mathsf{em}}(t), \quad (4.14)$$

where the contribution from each bath is indicated by the superscripts. Furthermore, the independence assumption also implies that the statistics of the individual fluctuating force remains Gaussian with the mean

$$\langle F^{\mathsf{imp}}(t)\rangle = \langle F^{\mathsf{em}}(t)\rangle = 0 \quad (4.15)$$

and covariance

$$\langle F^{\mathsf{imp}}(t+\tau)F^{\mathsf{imp}}(t)\rangle = 2k_B T^{\mathsf{imp}}\Gamma^{\mathsf{imp}} M\delta(\tau) \quad (4.16)$$

$$\langle F^{\mathsf{em}}(t+\tau)F^{\mathsf{em}}(t)\rangle = 2k_B T^{\mathsf{em}}\Gamma^{\mathsf{em}} M\delta(\tau), \quad (4.17)$$

just like that of a single bath, while the cross-correlation between them is vanishing, i.e.

$$\langle F^{\mathsf{imp}}(t+\tau)F^{\mathsf{em}}(t)\rangle = 0. \quad (4.18)$$

In other words, the average and the autocorrelation of the total fluctuating force are

$$\langle F^{\mathsf{fluc}}(t)\rangle = 0 \quad (4.19)$$

$$\langle F^{\mathsf{fluc}}(t+\tau)F^{\mathsf{fluc}}(t)\rangle = 2k_B\left(T^{\mathsf{imp}}\Gamma^{\mathsf{imp}} + T^{\mathsf{em}}\Gamma^{\mathsf{em}}\right)M\delta(\tau), \quad (4.20)$$

where $F^{\mathsf{fluc}}(t) \equiv F^{\mathsf{imp}}(t) + F^{\mathsf{em}}(t)$. These conditions suggest the dynamics of the sphere can still be treated as a Brownian motion in a harmonic potential (cf. (4.3) and (4.4)), with the effective damping coefficient

$$\Gamma_{\mathsf{CM}} \equiv \Gamma^{\mathsf{imp}} + \Gamma^{\mathsf{em}} \quad (4.21)$$

and the effective temperature

$$T_{\mathsf{CM}} \equiv \frac{T^{\mathsf{imp}}\Gamma^{\mathsf{imp}} + T^{\mathsf{em}}\Gamma^{\mathsf{em}}}{\Gamma^{\mathsf{imp}} + \Gamma^{\mathsf{em}}}. \quad (4.22)$$

One can therefore rewrite the above force autocorrelation as

$$\langle F^{\mathsf{fluc}}(t+\tau)\, F^{\mathsf{fluc}}(t)\rangle = 2k_B T_{\mathsf{CM}} \Gamma_{\mathsf{CM}} M \delta(\tau)\,. \tag{4.23}$$

This gives the following power spectrum

$$J(\omega) = \frac{2k_B}{M} \frac{\Gamma_{\mathsf{CM}} T_{\mathsf{CM}}}{\left(\omega_0^2 - \omega^2\right)^2 + \omega^2 \left(\Gamma_{\mathsf{CM}}\right)^2}. \tag{4.24}$$

It should be emphasised that $T_{\mathsf{CM}}$ is not a temperature corresponding to any bath in the setting, but it is instead an effective temperature that characterises the random movement of the sphere. The sphere is put between the two baths with different temperatures, so it is in a non-equilibrium situation where the concept of temperature of its environment is ill-defined. Like ordinary Brownian settings, however, one can see that this controlled non-equilibrium Brownian system can be used as a probe to determine various properties, both of the bath and the sphere, that are difficult to be measured directly otherwise. For example, the emerging gas temperature ($T^{\mathsf{em}}$) can be obtained from the power spectrum, given that the impinging temperature ($T^{\mathsf{imp}}$) and both the damping coefficients ($\Gamma^{\mathsf{imp}}$ and $\Gamma^{\mathsf{em}}$) are known. In practice, however, it is a difficult task to directly measure the damping coefficient $\Gamma^{\mathsf{em}}$ that is corresponding to the emerging gas. To overcome this difficulty, a comprehensive examination of the interaction between the sphere and the surrounding gas molecules is required. To this end, we chose to apply an existing theoretical model from Ref. [116] to our setting as we are going to show next and found that we can rewrite $\Gamma^{\mathsf{em}}$ in terms of the impinging coefficient $\Gamma^{\mathsf{imp}}$ and the emerging gas temperature $T^{\mathsf{em}}$. With this result, it turns out surprisingly that, to determine $T^{\mathsf{em}}$, one does not actually need to know the value of both $\Gamma^{\mathsf{imp}}$ and $\Gamma^{\mathsf{em}}$ in the first place.

### 4.4.2. Diffusive collision

To acquire the desired relation between the impinging and emerging damping coefficients, we apply the analysis of diffusive collision between a small sphere and its surrounding gas molecules by Epstein from Ref. [116] to our non-interacting baths model. The idea is to explicitly compute and compare the two contributions of the drag force, one is from the impinging gas while the other is from the emerging one, under two assumptions:

1. The number of the gas molecules attached to the surface of the sphere is constant when the system reaches a steady state.

2. The nanosphere is much more massive than the surrounding gas molecules.

This is an elaboration of what we present in Ref. [100]. To start with, it is known that the origin of the drag force acting on an object comes from the momentum exchange between the object and the fluid molecules. Note that, by definition, all the impinging molecules must stop right at the surface after the collision and all the emerging molecules must start off from the surface. Consider the impinging bath. Since it is thermal, the probability density of the *velocity* of the molecules follows the Maxwell–Boltzmann distribution. In spherical coordinates, this can be written as

$$p^{\mathsf{imp}}\left(v_r, v_\theta, v_\phi\right) = N^{\mathsf{imp}} \left(\frac{h_{\mathsf{imp}}}{\pi}\right)^{3/2} e^{-\left(v_r^2+v_\theta^2+v_\phi^2\right)h_{\mathsf{imp}}}, \tag{4.25}$$

where $p^{\mathsf{imp}}\left(v_r, v_\theta, v_\phi\right)$ is the impinging velocity distribution in spherical coordinates, $N^{\mathsf{imp}}$ is the number density of the impinging gas molecule, $v_i$ is the $i$-component of the velocity $\boldsymbol{v} = v_r\hat{\boldsymbol{r}} + v_\theta\hat{\boldsymbol{\theta}} + v_\phi\hat{\boldsymbol{\phi}}$ of the molecule relative to the lab frame, $m$ is the mass of a gas molecule, and $h_{\mathsf{imp}} \equiv \frac{m}{2k_B T^{\mathsf{imp}}}$. We see that this is a function of the velocity with respect to the lab frame. Since we are to analyse the collision between a large number of molecules with a single bead, it is convenient to instead work in a reference frame where the bead is motionless. Suppose $\boldsymbol{V} = V_r\hat{\boldsymbol{r}} + V_\theta\hat{\boldsymbol{\theta}} + V_\phi\hat{\boldsymbol{\phi}}$ is the velocity of the bead relative to the lab frame at a certain instant, where $V_i$ is the $i$-component of the velocity of the bead, one can rewrite (4.25) with respect to the *instantaneously* comoving frame of the bead at that instant as [116]

$$\begin{aligned} p'^{\mathsf{imp}}\left(v_r', v_\theta', v_\phi'\right) &= N^{\mathsf{imp}} \left(\frac{h_{\mathsf{imp}}}{\pi}\right)^{3/2} e^{-\left((v_r'+V_r)^2+\left(v_\theta'+V_\theta\right)^2+\left(v_\phi'+V_\phi\right)^2\right)h_{\mathsf{imp}}} \\ &= N^{\mathsf{imp}} \left(\frac{h_{\mathsf{imp}}}{\pi}\right)^{3/2} e^{-v'^2 h_{\mathsf{imp}}} e^{-\left(2\boldsymbol{v'}\cdot\boldsymbol{V}+V^2\right)h_{\mathsf{imp}}} \\ &\approx N^{\mathsf{imp}} \left(\frac{h_{\mathsf{imp}}}{\pi}\right)^{3/2} \left(1 - 2\left(\boldsymbol{v'}\cdot\boldsymbol{V}\right)h_{\mathsf{imp}}\right) e^{-v'^2 h_{\mathsf{imp}}}. \end{aligned} \tag{4.26}$$

Here, $v_i' = v_i - V_i$ is the $i$-component of the instantaneous velocity $\boldsymbol{v'} = v_r'\hat{\boldsymbol{r}} + v_\theta'\hat{\boldsymbol{\theta}} + v_\phi'\hat{\boldsymbol{\phi}}$ of the molecule relative to the comoving frame. Note that the fact that $\boldsymbol{v'}$ is an instantaneous velocity with respect to the comoving frame

allows one to employ the same set of unit vectors (in spherical coordinates, i.e. $\{\hat{\boldsymbol{r}}, \hat{\boldsymbol{\theta}}, \hat{\boldsymbol{\phi}}\}$) as the one previously used in the corresponding lab frame. Suppose $V = \sqrt{V_r^2 + V_\theta^2 + V_\phi^2}$ is the magnitude of the velocity of the bead, the approximation in the last line is valid in the slow bead limit where $\boldsymbol{V} \cdot \boldsymbol{V} = V^2$ is negligible. This is justified for our setup using the conservation of momentum and the fact that the mass of the bead is much larger than that of the gas. Note that, with respect to this frame, the velocity distribution is not thermal any more due to the presence of the extra factor $1 - 2\left(\boldsymbol{v'} \cdot \boldsymbol{V}\right) h_{\mathsf{imp}}$. It indicates that the distribution in the comoving frame does depend on the relative direction between the velocities of the bead and the molecule. Now, consider a small surface element of the bead $d\boldsymbol{S} = dS\hat{\boldsymbol{r}}$. Without loss of generality, we assume that $\boldsymbol{V}$ points in the direction of $\theta = 0$, hence the angle between the surface element and the velocity of the bead is $\theta$. The number of the impinging particles colliding to this surface element per unit area per time i.e. the impinging flux is then

$$\begin{aligned} n^{S,\mathsf{imp}} &= \int_{-\infty}^{0} \int_{\mathbb{R}} \int_{\mathbb{R}} p'^{\mathsf{imp}}\left(v'_r, v'_\theta, v'_\phi\right)\left(-v'_r\right) dv'_\phi dv'_\theta dv'_r \\ &= \frac{N^{\mathsf{imp}}}{2\sqrt{\pi h_{\mathsf{imp}}}}\left(1 + \sqrt{\pi h_{\mathsf{imp}}}\cos\theta\, V\right). \end{aligned} \tag{4.27}$$

Note that the limit of integration in the variable $v'_r$ only covers half of the real line since the only relevant molecules are the impinging ones (i.e. the negative values). The contribution to the total drag force from the impinging molecules arises from the collision between these molecules and the bead. After the collision, because all the impinging molecules stop, they transfer all of their momenta to the sphere. By computing the net momentum transfer from the impinging flux all over the whole surface, it is shown in Ref. [116] that the corresponding drag force is equal to

$$\boldsymbol{f}_{\mathsf{drag}}^{\mathsf{imp}} = -\frac{4\pi}{3} m N^{\mathsf{imp}} R^2 \overline{v}_{T^{\mathsf{imp}}} \boldsymbol{V} = -M\Gamma^{\mathsf{imp}} \boldsymbol{V}, \tag{4.28}$$

where $M$ is the mass of the sphere[5], $\overline{v}_{T^{\mathsf{imp}}} = \sqrt{\frac{8k_B T^{\mathsf{imp}}}{\pi m}}$ is the *mean speed* of the impinging gas with respect to the lab frame at temparature $T^{\mathsf{imp}}$, $R$ is

[5]Precisely, $M$ is the mass of the sphere plus the mass of the gas molecules sticking on its surface at an instant, which generally varies with time. However, since the former is much larger, one may ignore the contribution from the latter.

the radius of the bead, and $\Gamma^{\mathsf{imp}} = \frac{4\pi}{3}\frac{mN^{\mathsf{imp}}R^2\overline{v}_{T^{\mathsf{imp}}}}{M}$. We choose to use the lower case $\boldsymbol{f}$ here to distinguish the force from the fluctuating force which is denoted by the upper case $\boldsymbol{F}$. The force points in the opposite direction to the velocity of the bead. Note that, even though this result arises from the analysis in the comoving frame, it also holds in the lab frame since a force is an absolute physical quantity, being invariant under transformations between inertial frames.

Let us now consider the emerging bath. According to the non-interacting baths model, the probability density of the emerging velocity, $p'^{\mathsf{em}}\left(v'_r, v'_\theta, v'_\phi\right)$, also follows the Maxwell–Boltzmann distribution, i.e.

$$p'^{\mathsf{em}}\left(v'_r, v'_\theta, v'_\phi\right) = N'^{\mathsf{em}}\left(\frac{h_{\mathsf{em}}}{\pi}\right)^{3/2} e^{-\left(v_r'^2+v_\theta'^2+v_\phi'^2\right)h_{\mathsf{em}}}, \tag{4.29}$$

where $N^{\mathsf{em}}$ is the number density of the emerging gas molecule and $h_{\mathsf{em}} \equiv \frac{m}{2k_B T^{\mathsf{em}}}$. However, note that this probability distribution is thermal with respect to the comoving frame, unlike the impinging one which is thermal with respect to the lab frame. In other words, the two distributions are *not* simultaneously thermal with respect to a single reference frame. The reason we use the primed notation for this probability density, in contrast to the unprimed notation of the impinging one, is to emphasise this fact. We will come back to this point later. Note also that, the values of both $N^{\mathsf{em}}$ and $T^{\mathsf{em}}$ cannot be directly measured and are still unknown at this point. To determine the number density, let us assume that the number of the gas molecules sticking on any given surface element of the bead at any given instant is constant[6]. In other words, the impinging and the emerging fluxes are assumed to always be equal i.e.

$$\begin{gathered} n^{S,\mathsf{imp}} = n^{S,\mathsf{em}} \\ \frac{N^{\mathsf{imp}}}{2\sqrt{\pi h_{\mathsf{imp}}}}\left(1+\sqrt{\pi h_{\mathsf{imp}}}\cos\theta\, V\right) = \int_0^\infty \int_{\mathbb{R}}\int_{\mathbb{R}} p'^{\mathsf{em}}\left(v'_r, v'_\theta, v'_\phi\right) v'_r dv'_\phi dv'_\theta dv'_r. \end{gathered} \tag{4.30}$$

[6]Another benefit of this zero net flux assumption is the following. Suppose the mass of the fluid molecules sticking on the sphere is significant that it needs to be taken into account, the assumption implies that the effective mass $M$ is time-independent.

By substituting (4.29) in (4.30), one can show that

$$N^{\mathsf{em}} = \left(\sqrt{\frac{h_{\mathsf{em}}}{h_{\mathsf{imp}}}}\right)\left(1+\sqrt{\pi h_{\mathsf{imp}}}\,\cos\theta\, V\right) N^{\mathsf{imp}}. \tag{4.31}$$

This shows the number density of the emerging gas depends on both position, i.e. angle $\theta$, and velocity $V$. To compute the drag force originating from the emerging molecules, we assume that the molecules initially stick on the surface. Therefore, the negative of the momentum of the emerging molecules is equal to the momentum transfer from the emerging molecules to the bead. On a surface element $d\boldsymbol{S} = dS\hat{\boldsymbol{r}}$, this is equal to

$$\begin{aligned}
\boldsymbol{\mathcal{P}}^{S,\mathsf{em}} &= \int_0^\infty \int_{\mathbb{R}}\int_{\mathbb{R}} \left(-m\boldsymbol{v'}\right) v'_r\, p'^{\mathsf{em}}\left(v'_r, v'_\theta, v'_\phi\right)\, dv'_\phi dv'_\theta dv'_r \\
&= -m\int_0^\infty \int_{\mathbb{R}}\int_{\mathbb{R}} v'^2_r\, p'^{\mathsf{em}}\left(v'_r, v'_\theta, v'_\phi\right)\, dv'_\phi dv'_\theta dv'_r \hat{\boldsymbol{r}} \\
&= -\frac{mN^{\mathsf{imp}}}{4\sqrt{h_{\mathsf{imp}}h_{\mathsf{em}}}}\left(1+\sqrt{\pi h_{\mathsf{imp}}}\,\cos\theta\, V\right)\hat{\boldsymbol{r}},
\end{aligned} \tag{4.32}$$

where $\boldsymbol{\mathcal{P}}^{S,\mathsf{em}} = \mathcal{P}^{S,\mathsf{em}}\hat{\boldsymbol{r}}$ is the momentum the surface element $d\boldsymbol{S}$ receives from the emerging molecule per unit area per time. It points parallel to the radial direction because the components in the other directions vanish after the integration. Similarly, we know that the contribution from the emerging molecules to the total drag force can be computed by integrating only the components of $\boldsymbol{\mathcal{P}}^{S,\mathsf{em}}$ in the direction of $\hat{\boldsymbol{V}}$ over the whole surface because the contributions from the other directions vanish. This amounts to

$$\begin{aligned}
\boldsymbol{f}^{\mathsf{em}}_{\mathsf{drag}} &= \left(\oint \left(\boldsymbol{\mathcal{P}}^{S,\mathsf{em}}\cdot\hat{\boldsymbol{V}}\right) dS\right)\hat{\boldsymbol{V}} \\
&= \left(\oint \mathcal{P}^{S,\mathsf{em}}\cos\theta dS\right)\hat{\boldsymbol{V}} \\
&= -\frac{mN^{\mathsf{imp}}R^2\pi^{3/2}V}{3\sqrt{h_{\mathsf{em}}}}\,\hat{\boldsymbol{V}}.
\end{aligned} \tag{4.33}$$

Again, due to the force being an absolute physical quantity, this result obtained from the comoving frame also holds in the lab frame. Finally,

since $\boldsymbol{f}_{\mathsf{drag}}^{\mathsf{em}} = -M\Gamma^{\mathsf{em}}\boldsymbol{V}$, we get

$$\Gamma^{\mathsf{em}} = \frac{mN^{\mathsf{imp}}R^2\pi^{3/2}}{3M\sqrt{h_{\mathsf{em}}}} = \frac{\pi}{8}\sqrt{\frac{T^{\mathsf{em}}}{T^{\mathsf{imp}}}}\Gamma^{\mathsf{imp}}, \tag{4.34}$$

where we use the fact that $h_{\mathsf{em}} \equiv \frac{m}{2k_BT^{\mathsf{em}}}$ and $\Gamma^{\mathsf{imp}} = \frac{8}{3}\frac{(\sqrt{2mk_BT^{\mathsf{imp}}\pi})N^{\mathsf{imp}}R^2}{M}$ to obtain the final expression. This is the desired relationship between the emerging and the impinging damping coefficients. Note however that, due to the presence of the still-unknown emerging gas temperature $T^{\mathsf{em}}$, one cannot use this relation to determine the value of $\Gamma^{\mathsf{em}}$ yet.

### 4.4.3. Slow bead approximation and the finding of the emerging gas temperature

Now, let us discuss the matter of having the two distributions that are not simultaneously thermal with respect to a single reference frame. We see that although the form of the Langevin equation (4.14) does not change due to the forces being absolute quantities as discussed earlier, the covariance relations do, to be strictly accurate. This is because they are properties of the thermal distribution which depend on which frame we are working in. Therefore, strictly speaking, Epstein's model of diffusive collision does not allow our non-interacting baths model. Nevertheless, we argue that the covariance relations should not change too significantly from the ones in the thermal case in the limit where the velocity of the bead is very small. This happens when the bead is much more massive than a single molecule of the gas, which it is in a typical optically levitated nanosphere setup. In such cases, the thermal covariance relations should still be usable as good approximations and our model should still hold. Thus (4.22) can be rewritten as

$$T_{\mathsf{CM}} = \frac{\left(T^{\mathsf{imp}}\right)^{3/2} + \frac{\pi}{8}\left(T^{\mathsf{em}}\right)^{3/2}}{\left(T^{\mathsf{imp}}\right)^{1/2} + \frac{\pi}{8}\left(T^{\mathsf{em}}\right)^{1/2}}. \tag{4.35}$$

We see that, by solving this equation, we can obtain $T^{\mathsf{em}}$ from $T^{\mathsf{imp}}$ and $T_{\mathsf{CM}}$ without the need to know the values of both damping coefficients[7]. With

[7]Note that $T_{\mathsf{CM}}$ can be obtained from the corresponding power spectrum or the position profile.

this knowledge of $T^{\mathsf{em}}$, it is clear that we can now determine the value of $\Gamma^{\mathsf{em}}$ as well, using Eq.(4.34). These results demonstrate theoretically that the optically levitated nanosphere can really be utilised to study properties of the non-equilibrium dilute gas in Knudsen regime around the nanosphere in a similar way to a Brownian particle in thermal equilibrium case. In fact, due to the coupling between the gas and the sphere, one can also determine some non-equilibrium properties of the nanosphere itself, for example, its surface temperature, from the properties of the gas as we will show next.

## 4.5. Accommodation coefficient and the surface temperature estimation

One can approximate the surface temperature of the nanosphere from the emerging gas temperature. Let us discuss the concept of the accommodation coefficient. The accommodation coefficient $\alpha \equiv \frac{\langle \Delta E \rangle}{\langle \Delta E_{max} \rangle}$ is the ratio between the average of the actual energy transfer via collision between a molecular gas and a thermal solid or liquid surface $\langle \Delta E \rangle$ and the average of the energy that would be transferred if the molecule is in contact with the surface until it reaches thermal equilibrium $\langle \Delta E_{max} \rangle$, assuming that the surface is big enough such that its temperature does not change throughout the process. In a special case where the initial temperature of the gas is well-defined and its energy is a linear function of its temperature, the accommodation coefficient is equal to the following [117]

$$\alpha = \frac{T^{\mathsf{em}} - T^{\mathsf{imp}}}{T_{\mathsf{sur}} - T^{\mathsf{imp}}}, \tag{4.36}$$

It is clear that, in principle, one can determine the surface temperature of the bead from the emerging gas temperature if the relevant accommodation coefficient is known[8]. In practice, however, the required value of the coefficient is not always available. As a first approximation, what one can do then is to rely on the fact that the emerging temperature must not be bigger than the surface temperature and treats the former as a lower bound of the latter. Still, by turning things around, one can estimate an unknown

[8] For example, the accommodation coefficient of air on silica is about 0.777 in a moderate range of surface temperature of around 300K according to Ref. [118], therefore the relationship between the two temperatures would be $T_{\mathsf{sur}} = T^{\mathsf{imp}} + \frac{T^{\mathsf{em}} - T^{\mathsf{imp}}}{0.777}$

accommodation coefficient using our method, given that the surface temperature can be measured by other techniques, for example, luminescent probes or blackbody radiation [119, 120].

## 4.6. Results and analysis

Let us now examine the experimental results and justify our assumptions and theoretical model.

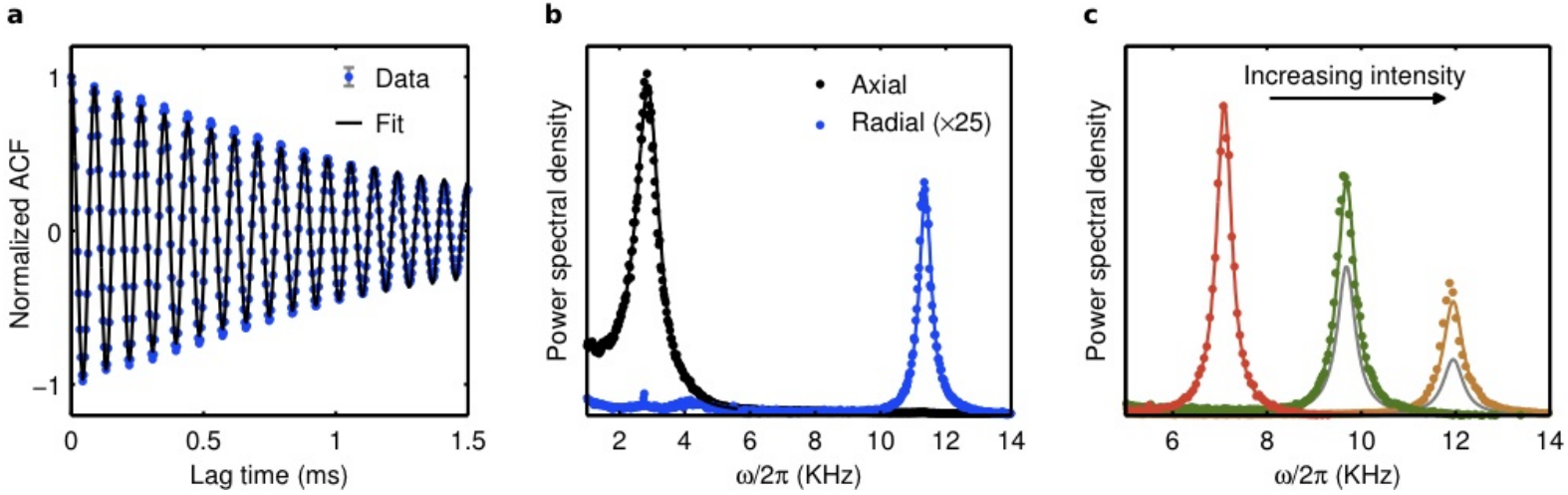



Figure 4.3.: **Two-dimensional Brownian motion and its variation with trap laser intensity [100].** All displayed data are for 105.1 nm spheres at 1 mbar. **a,** Autocorrelation function (ACF) of experimentally measured radial position (blue points with grey error bars) and fit with theory (black solid line). **b,** Measured axial (black points) and radial position (blue points) power spectra with fits to $J(\omega)$ (solid lines) over trap frequency $\frac{\omega}{2\pi}$. Because of the low damping at mbar pressures, the axial ($z$) and radial ($x$) peak frequencies, $\omega^*_{x,z} = \sqrt{\omega^2_{x,z} - \Gamma^2_{\mathsf{CM}}/2}$, approximate the trap frequencies $\omega_{x,z}$ and the damped frequency $\tilde{\omega}_{x,z}$. **c,** Measured radial power spectra (points) with fits (solid lines) for three values of trapping laser intensity. From left to right the intensity of the trapping laser beams is increased by a factor of 2.1 and the peak frequency $\omega^*_x/2\pi$ increases with intensity, as expected. If there were no temperature increase from the initial intensity (red) the peak height would behave as indicated by the grey solid lines. However, it can be seen that the height of the peak, $\frac{A}{\Gamma_{\mathsf{CM}}\tilde{\omega}^2_x} = \frac{2k_B T_{\mathsf{CM}}}{M\Gamma_{\mathsf{CM}}\tilde{\omega}^2_x}$, increases with intensity in comparison to the grey lines, indicating the increase of the centre-of-mass temperature, $T_{\mathsf{CM},\mathsf{x}}$, of the sphere.
This figure and the caption is taken directly from Ref. [100].

- *Brownian motion in harmonic potential*: First of all, we need to verify that the dynamics of the sphere is well-described by a Brownian particle in a harmonic potential. This is confirmed by the fact that the data results in a position autocorrelation, Figure 4.3a, and a power spectrum, Figure 4.3b, that fit well to (4.13) and (4.10) respectively.

- *The nature of the optical trap*: The second point to be verified is the nature of the optical trap. It is obvious from Figure 4.3b that the trapping frequency is significantly higher along the radial axis than the axial axis of the trap. This is due to the larger gradient of the electric field in the radial direction. Furthermore, the trapping frequency increases with the laser intensity as expected. This can be seen clearly from Figure 4.3c, where three power spectra, each is corresponding to a laser intensity which increases by a factor of 2.1 from the left to the right, are plotted and fitted.

- *The heating effect*: Next, let us verify whether the heating effect really occurs, and if so, how significant it is. In Figure 4.3c, by assuming that the change in the laser intensity only affects the trapping frequency $\omega_0$ (and hence also the damped frequency $\tilde{\omega}$) but not the centre of mass temperature $T_{\mathsf{CM}}$ or the damping coefficient $\Gamma_{\mathsf{CM}}$, we plot two power spectra numerically, showing as the grey curves in the figure, and compare them with the green and the yellow fitting curves from the actual data. All the parameters of the grey curves, apart from the trapping frequencies, are chosen to be the same as the red fitting curve, i.e. the fit corresponding to the lowest laser intensity out of the three. If the intensity really does affect only the trapping frequency, the two grey curves should superpose with the green and the yellow ones reasonably well. However, they do not. The differences in the fitting parameters between them clearly confirm the heating effect.

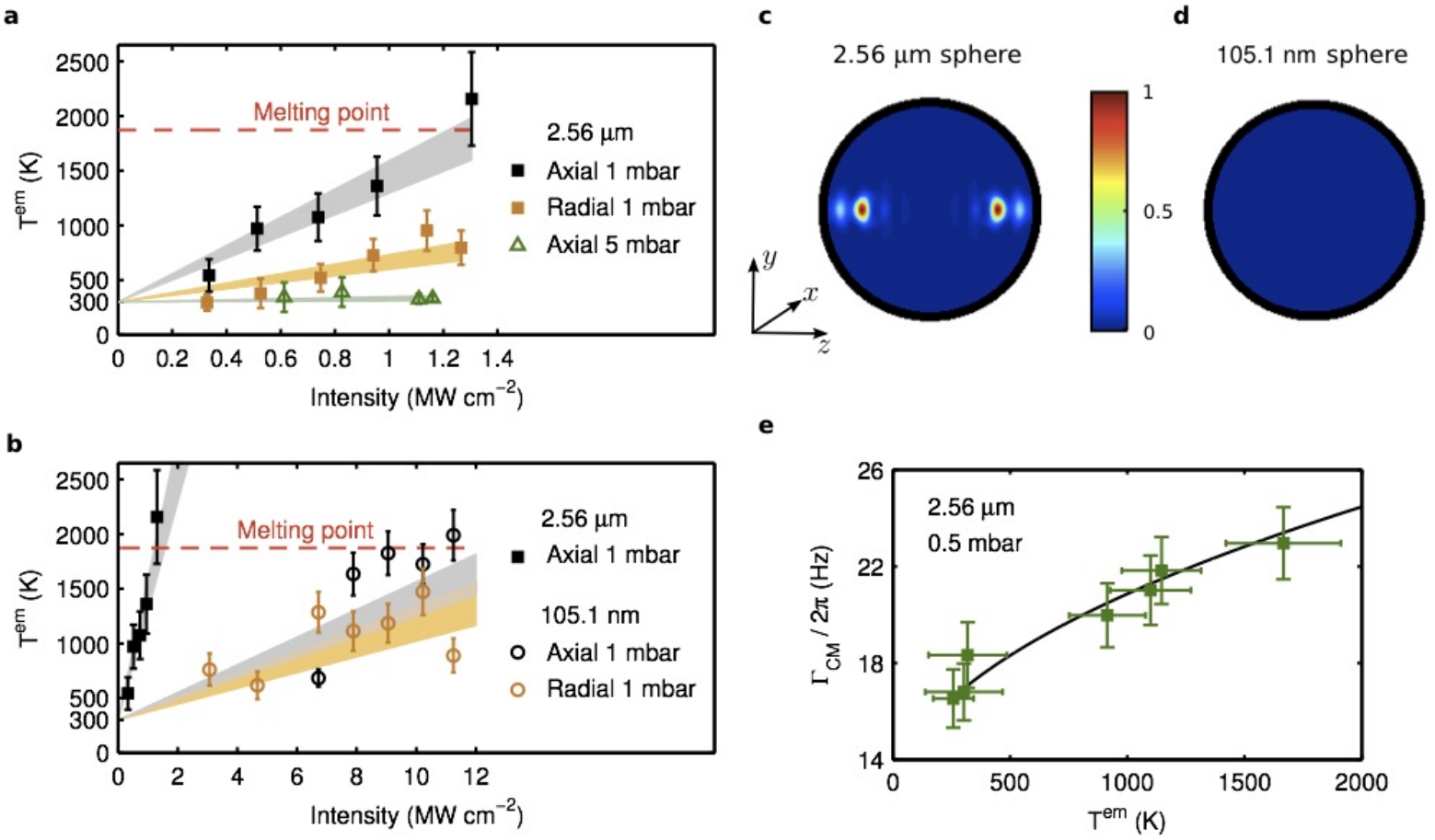



Figure 4.4.: **Analysis of heating as a function of pressure, spatial direction and sphere size [100].** **a,** Temperature of emerging gas particles with trapping laser intensity for the large spheres in the axial (black squares) and radial directions (orange squares) at 1 mbar, and in the axial direction at 5 mbar (green triangles). Asymmetric heating is observed at 1 mbar while no heating occurs at 5 mbar. The shaded areas show linear fits with one standard deviation of uncertainty indicating that a linear relationship $T^{\mathrm{em}} \propto T_{\mathrm{sur}} \propto I$ holds, as expected [121]. **b,** Temperature of emerging gas particles $T^{\mathrm{em}}$ with trapping laser intensity, for 105.1 nm diameter (open circles) and 2.56 $\mu$m diameter spheres (filled squares) at 1 mbar in the axial (black) and radial (orange) direction. Heating of the gas is clearly observed for both large and small spheres. The shaded areas show linear fits with one standard deviation of uncertainty as a guide to the eye. The red dashed lines in **a,b** indicate the melting temperature of silica (1873K, according to Ref. [122]). At intensities beyond the shown data points the spheres leave the trap. **c,** Field intensity inside the 2.56 $\mu$m spheres for two incident counter-propagating Gaussian beams clearly showing lensing of the light. **d,** Field intensity inside the 105.1 nm spheres for two incident counter-propagating Gaussian beams, showing a homogenous intensity throughout the spheres. **e,** Measured (green squares) variation of the damping coefficient $\Gamma_{\mathrm{CM}}$ for a 2.56 $\mu$m diameter sphere at 0.5 mbar over temperature of the emerging gas particles, $T^{\mathrm{em}}$. Also shown is the theoretical $\Gamma_{\mathrm{CM}}$ (black solid line) with no free parameters, using the experimentally given parameters $T^{\mathrm{imp}} = 294$ K and $\Gamma^{\mathrm{imp}} = 76.3$ Hz for 2.56 $\mu$m spheres.
This figure and the caption is taken directly from Ref. [100].

Now that we verified that the heating effect plays a significant role in the dynamics of the sphere, let us investigate how several parameters of our setup affect the heating. These parameters are the intensity of the laser, the pressure of the gas, and the size of the bead. To this end, we analyse the graphs in Figure 4.4a and 4.4b which display the relationships between the laser intensity and the emerging gas temperature of the beads of both sizes (2.56$\mu$m and 105.1nm) at two different pressures (1mbar and 5mbar), both in the radial and axial directions. We choose to plot with $T^{\mathsf{em}}$ instead of $T_{\mathsf{CM}}$ because of its significance as an estimate of $T_{\mathsf{sur}}$ which allows us to analyse the heating effect more conveniently. The emerging temperature $T^{\mathsf{em}}$ is calculated from the impinging gas temperature $T^{\mathsf{imp}}$ and the centre of mass temperature $T_{\mathsf{CM}}$ using (4.35). Here, we assume that the impinging gas temperature is equal to the room temperature which was fix to be at 294K, whereas the centre of mass temperature is obtained from the fitting parameter of the corresponding power spectrum.

- *The intensity of the laser*: Since the impinging temperature is constant, the positive slopes of the graphs in Figure 4.4a and 4.4b mean $T_{\mathsf{CM}}$ increases with the intensity, which re-confirm the heating effect.
- *The pressure of the gas*: We know that higher pressure implies that more energy is transferred between the gas and the sphere per unit time. To put it simply, one may consider the laser to be the cause of the "heating up" whereas the gas causes the "cooling down". Thus, with all the other parameters being identical, we expect that the surface of the sphere surrounded by higher gas pressure should be colder than its counterpart. This indeed is the case in our experiment, which can be seen in Figure 4.4a by comparing the graphs of the 2.56$\mu$m sphere in the axial direction between 1mbar and 5mbar. It is clear that while the emerging temperature at 1mbar increases with the laser intensity, the one at 5mbar does not change noticably at all.
- *The size of the bead*: The size of the bead affects the heating in two different aspects. First, recall the "heating up" mechanism in the bead occurs due to laser absorption by the impurities that

are distributed in its bulk. Therefore, the amount of laser energy absorbed is proportional to the volume of the sphere. This is in contrast to the "cooling down" mechanism by the gas which only takes energy away from the surface of the sphere, hence the amount of energy taken away is proportional to the surface area. Given a fixed laser intensity and gas pressure, it is expected then that the net energy absorbed by the bead should be proportional to its radius. This behaviour is reflected in Figure 4.4b where the emerging temperature of the 2.56$\mu$m-nanosphere rises at a much faster rate than that of the 105.1nm-nanosphere, at the same intensity, pressure (which is 1mbar in the figure), and direction (which is axial in the figure). The second aspect of the size effect follows from the fact the silica refracts light. In other words, it also acts as a lens which changes the energy distribution in the laser. Figure 4.4c and 4.4d show our simulation of this lensing effect using generalized Lorentz-Mie theory and the Optical Tweezers Toolbox [123]. From the simulation, we can see the difference in the bulk temperature profiles between the 2.56$\mu$m and the 105.1nm beads. It is clear that the anisotropy due to the lensing effect only arises in the case of the large sphere. Again, we can also observe this effect from the real data in Figure 4.4a and 4.4b. In Figure 4.4a, the two plots of the 2.56$\mu$m at 1mbar in Figure 4.4a suggest a significant anisotropy in the heating rate for the large sphere. This is not the case for the small sphere, however, as the two plots of the 105.1nm at 1mbar in Figure 4.4b are not significantly different.

- *The non-interacting baths model*: Ultimately, we need to verify whether the heating effect actually behaves as is described by our non-interacting baths model, which is the key result that allows us to estimate the surface temperature of the bead from its position profile. Here, we present two experimental results which strongly support its validity. Firstly, Figure 4.4e shows the relationship between the emerging gas temperature and the effective damping coefficient corresponding to the centre of mass degree of freedom of the 2.56$\mu$m at 0.5mbar. The actual data is displayed as the green dots with error bars while the

theoretical result without any fitting parameter is shown as the black curve. The fact that the theoretical result derived from our model fits very well with the actual data without the need for any free parameter adjustment (i.e. data fitting) serves as the first strong evidence in support of our model. Secondly, let us consider the heating effect again. If the calculated emerging temperature truly is a lower bound of the surface temperature as our model suggests, it should be impossible to keep trapping the sphere when the laser intensity is high enough such that the emerging temperature reaches the melting point of silica ($\approx$ 1873K, according to [122]), because the bead should start to melt down and lose from the trap in such a situation. To verify this point, we added a horizontal line indicating the melting temperature of silica in Figure 4.4a and 4.4b. It can be seen that the highest emerging temperature that each individual setting in Figure 4.4b can reach is just about the melting point. Since these points are the final data we can obtain when the intensity is increasing before the bead is undetectable, it serves as an evidence that the bead does melt and the emerging gas temperature can be used to estimate its surface temperature.

- *Trap loss mechanisms*: The problem of trap loss at low pressure has been encountered in optically levitated sphere experiments since their early days [94, 98, 99]. Here, as an additional analysis, we discuss the underlying mechanisms causing trap loss in optically levitated system. By separately analysing the behaviour of the larger and smaller spheres, we discover that melting is the major cause of the larger sphere leakage, while it plays a smaller role in the case of the smaller sphere. Let us discuss the larger sphere first. In Figure 4.5a, we see that the lowest attainable pressure of the larger bead increases with the intensity. This is in accordance with the melting hypothesis, i.e. at a given laser intensity, the bead should start to melt down and lose from the trap when the pressure is below a certain value that the energy dissipating rate is too slow. Furthermore, the plot in Figure 4.5b shows that the intensity of the scattered light[9] from the big sphere

[9]Note the difference between the intensity of the laser which creates the trap and the intensity of the laser scattered from the bead. The latter is what we are considering here.

that is detected by QPD decreases when we reduce the pressure in the trap, keeping the intensity of the laser that makes the trap fixed. This suggests that the sphere melts down and becomes smaller, hence scatters less light to the QPD. Now, let us move onto the smaller bead. In a stark contrast to the larger sphere, the minimum attenable pressure of the smaller sphere appears not to change significantly with the intensity, but being a constant of about 0.95mbar. This implies that, for the smaller sphere, the trap loss is not mainly caused by melting but other temperature-independent processes, for example, parametric heating, which results from any noise presented in the setup such as laser noise and vibrations. This is especially the case when the pressure and the intensity are low. The approximately constant intensity of the scattered laser and the pressure of the smaller sphere in Figure 4.5b shows more support on this point.

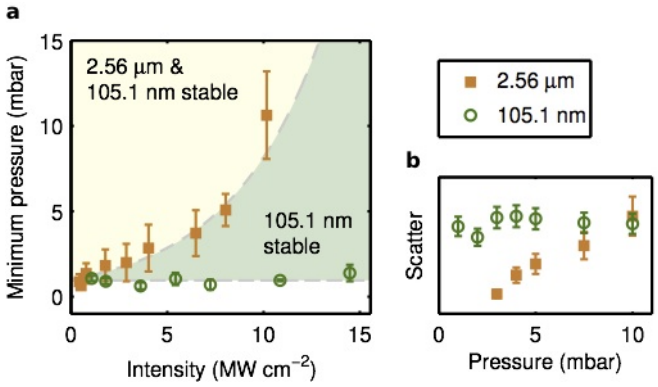



Figure 4.5.: **Minimum attainable pressure [100]. a,** Minimum pressure for which 2.56 $\mu$m spheres (orange squares) and 105.1 nm spheres (green circles) were stably trapped, versus intensity. This data is averaged over different spheres of each size (>5) at each intensity. Due to their strong heating the 2.56 $\mu$m spheres evaporate at high intensities, leading to an intensity dependent attainable pressure. In contrast, the smaller spheres are lost below an average pressure of 0.95 mbar regardless of the laser intensity. **b,** Scatter plot over pressure at fixed intensity 1.3 MW cm$^{-2}$ showing the total scattered light intensity from the 2.56 $\mu$m spheres (orange squares) and 105.1 nm spheres (green circles). At lower pressure, the scatter drops strongly for the 2.56 $\mu$m spheres indicating that they have evaporated to a smaller size, while the 105.1 nm spheres show an approximately constant scatter.
This figure and the caption is taken directly from Ref. [100].

## 4.7. Chapter summary

To summarise, we propose a theoretical model called "the non-interacting baths model" in order to describe the dynamics of a nanosphere that is optically trap in a chamber filled with a very dilute gas in Knudsen regime. We take into account the fact that there are always some impurities in the body of the sphere which absorb the laser, causing the sphere as well as part of the gas that it interacts with to heat up. The key idea of this model is the categorisation of the surrounding gas into 2 separate groups, the one that is impinging on the sphere and the one that is heated up by heat transfer from the surface of the sphere before emerging from it. We treat these two groups of gas as if they form two separate thermal baths of different temperatures which individually interact with the sphere. The justification

for this separation is the fact that the gas is very dilute that the collision rate among the molecules is much smaller than that between the molecules and the sphere. This leads to a non-equilibrium dynamics of the whole system where there arises 4 distinct temperatures: the impinging and the emerging gas temperatures, the sphere centre of mass temperature, and the sphere surface temperature. It is shown that, even though, the system is in a non-equilibrium state due to the presence of several local temperatures instead of one single temperature, it is still possible to treat the dynamics of the sphere as a Brownian one with an effective temperature and an effective damping coefficient. This implies that one can still learn all about its dynamics from its corresponding power spectrum or autocorrelation function. Together with the diffusive collision model proposed by Epstein [116], we show how one can obtain the emerging gas temperature and the emerging damping coefficient, which are non-equilibrium properties of the gas that are difficult to be measured directly, from analysing the power spectrum of the sphere. These results further allow us to estimate either the surface temperature of the sphere or the accommodation coefficient, depending on which of the two is known beforehand. We see that the experimental results agree with our theoretical analysis to a good degree. The data show how the axes of the trap, the size of the bead, the pressure of the gas, and the intensity of the laser affect the dynamics of the system. The relationship among the four temperatures according to the model as well as the heating effect is strongly confirmed by the observation that the bead melts.

The results of our study provides a deeper understanding of the non-equilibrium dynamics of the optically levitated nanosphere and opens a new way to experimentally study non-equilibrium dynamics of gases in Knudsen regime. In particular, we see that our optically levitated nanosphere setup can be applied for thermometry purposes. The fact that the sphere melts down in the low pressure regime is also interesting because it confirms a hypothesis that has been widely discussed in the community that the melting is one of the mechanisms that causes optical trap leak in such a setting and prevents one to bring the centre of mass degree of freedom of the sphere down to the ground state.

## 4.8. Remark on Jarzynski equality verification

The results we learn about the dynamics of the levitated nanosphere discussed above imply that it is *impossible* to use the optically levitated nanosphere setup as it is, without an appropriate modification, to verify Jarzynski equality as we expected initially. To see this clearly, let us examine the situation carefully as follows. To begin with, the optically levitated nanosphere setup is composed of many degrees of freedom, thus one first needs to choose which one to work with. The centre of mass motion is the sensible choice since the random variable we can directly measure from this setup is the position of the bead. Following this choice, the corresponding energy can be computed from the position profile while the centre of mass temperature can be read from the power spectrum as is discussed earlier. Next, we need to devise an appropriate protocol. It is clear that the only two parameters one can manipulate in this setup is the gas pressure and the laser intensity, thus any possible protocol can always be decomposed into a combination of variations of these two parameters. This is where the problem lies. Recall that the kind of protocol which satisfies Jarzynski equality is the one where the manipulable parameters of the system change in such a way that do *not* affect the temperature of the corresponding bath. This is absolutely sensible in a normal circumstance where the system and the bath are independent. However, in the levitated nanosphere system, the centre of mass temperature is not corresponding to any actual bath. In fact, it is determined by the random motion of the bead itself. Thus, the fact that the variation of pressure and intensity affects the centre of mass temperature as is discussed earlier signifies that it is impossible to implement such a protocol in this kind of setup. This leads to the conclusion that the optically levitated nanosphere setup in the regime considered here *cannot* be used for verifying the original Jarzynski equality and its variations as long as the corresponding protocols require the same condition of temperatures as mentioned above.

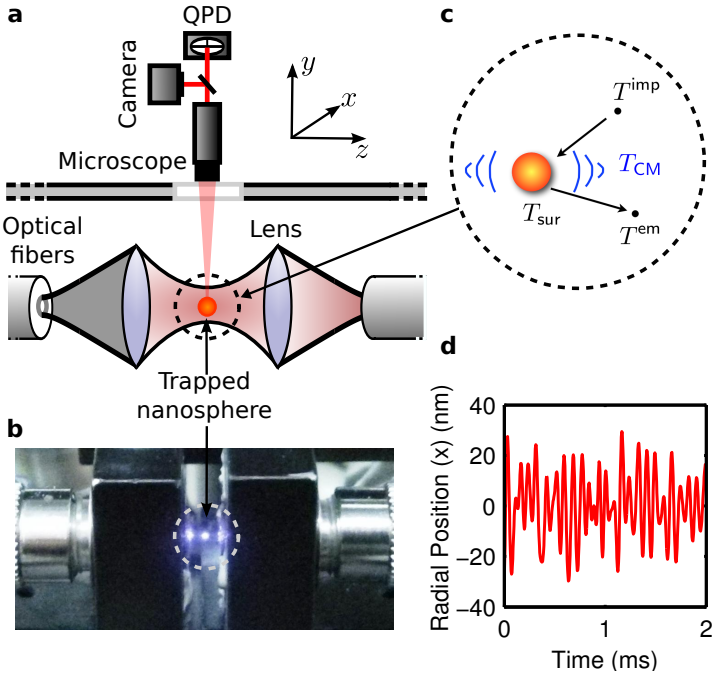



Figure 4.2.: **Experimental schematic and photograph of levitation experiment. a,** Silica spheres are levitated in a dual-beam optical tweezer inside a vacuum chamber. Light of wavelength 1064 nm is coupled into lenses from single-mode optical fibers, creating an optical trap. The motion of the levitated sphere is monitored with a camera and a quadrant photodetector (QPD). **b,** Photograph of the trapping region with trapped sphere visibly scattering trap light. **c,** Schematic showing the temperatures involved in a collision with a heated sphere: the sphere's centre-of-mass temperature ($T_{CM}$) and surface temperature ($T_{sur}$), and the temperatures of the impinging gas particles ($T^{imp}$) and emerging gas particles ($T^{em}$) with $T^{imp} < T_{CM} < T^{em} < T_{sur}$. **d,** Typical Brownian motion position trace for a 105.1 nm sphere at 1 mbar.
This figure and the caption is taken directly from Ref. [100].

# 5. Summary and outlook

All of our studies presented in this thesis revolve around a single idea, i.e. all the information associated to a random variable lies in its statistics, which is completely encoded in its probability distribution or other equivalent representations. In the first part, we have theoretically investigated various existing concepts in statistical mechanics and related fields in physics, namely, partition function, Rényi entropies, relative Rényi entropies, Tsallis entropies, and relative Tsallis entropies, in order to identify them with several mathematical concepts that equivalently represent a probability distribution. This provides a better understanding of how to completely quantify what one can learn from a stochastic system. It shows that fluctuation is not necessarily equivalent to unwanted noise, as meaningful information can be extracted if one analyses it in the right way. In particular, we demonstrate that Rényi entropies naturally arise as the parameterised exponential means of the surprisals. Therefore, they form a complete measure of the uncertainty or information associated to a system, even in the situations where the asymptotic equipartition property does not hold and hence Shannon entropy fails to capture the uncertainty properly. In a similar way, we also show that relative Rényi entropies form a complete measure of the relative uncertainty of a given distribution with respect to a reference one. Furthermore, we derive the $\alpha$-Jarzynski equality, a family of Jarzynski-like equalities written in terms of relative Rényi entropies where the reference state is a thermal state. They completely capture the distribution of work done on a system that is connected to a single large heat bath and give rise to a family of second-law-like inequalities, which boils down to the conventional second law in the small fluctuation limit. We show that these second law relations are equivalent to the monotonicity in $\alpha$ of relative Rényi entropies. As a generalisation of the standard Jarzynski equality, our $\alpha$-Jarzynski equality also allows one to determine all the unknown $\alpha$-free energy landscape of the system of interest from the work

distribution. We also study the often-overlooked initial full-rank condition which is required for the standard Jarzynski equality to hold. This gives rise to an operational interpretation of Tsallis entropy of order 0 as a measure of the absolute irreversibility of the corresponding process.

As a real-world example of how an equivalent representation helps in understanding the properties of a non-equilibrium system, we utilise it in the analysis of our experimental study of the non-equilibrium dynamics of an optically levitated nanosphere. The highly non-thermal-equilibrium situations in this setup are due to the heating induced by laser absorption of the nanosphere. We find that the dynamics of the sphere can be described effectively by Brownian motion, which implies that the power spectrum obtained from the experiment fully encodes all one can learn from its dynamics. These include the local temperatures and several other properties of the non-equilibrium gas surrounding the sphere. Moreover, one can obtain the lower bound estimation of the surface temperature of the sphere from it as well. We test the accuracy of the temperatures obtained from the analysis by comparing them against the melting point of the nanosphere and find that they are in a good agreement. These results are significant as they serve as a quantitative support for a relevant trap loss mechanism and suggest that the setup may be used as a promising new thermometry technique in a nanoscale experiment.

Non-equilibrium thermodynamics is an active field of research where a lot of new results are still to be investigated. It is important both fundamentally, as it describes most of the real-world processes happening around, and also practically, as modern technology is rapidly developing towards the nano and quantum scales where the degree of fluctuation becomes relatively much higher and cannot be ignored. Our results, both theoretical and experimental, provide new insight into the subject. However, all of our results and analysis may still be considered classical. This is because we have not yet fully taken quantum coherence and correlation into account on the theory side, and we also have not been able to reach the quantum regime on the experimental side. We believe that a promising direction to include the true quantumness in the theoretical part is to consider the Jarzynski relation with quantum feedback protocol (as in Ref. [124], for example) and generalise it in terms of a moment-generating function, similar to how we did to the normal Jarzynski relation without feedback control.

This may lead to a discovery of more quantum second laws, the searching of which is currently one of the active research topics in the field of quantum thermodynamics. On the experimental side, the heating effect is the main obstruction that prevents the optically levitated nanosphere setup from reaching the quantum regime as well as from being used to verify the classical Jarzynski equality and its variations. To overcome this problem, a proposal of using a hybrid electro-optical trap instead of just the optical trap is recently proposed in Ref. [97] by the optomechanics group at University College London who are also the authors of Ref. [100]. We believe that, with a successful implementation of this new kind of trap, they should be able apply it to verify Jarzynski equality and its variations as well as to determine the $\alpha$-free energy landscapes of a certain complicated nanoscale system experimentally in the near future, both in the classical and in the quantum regimes.

# A. Appendix

## A.1. Multivariate Laplace transform

For a multivariate function $b(\boldsymbol{y})$, the Laplace transform $\mathcal{L}\{b(\boldsymbol{y})\}(\boldsymbol{\xi})$ is defined as

$$\mathcal{L}\{b(\boldsymbol{y})\}(\boldsymbol{\xi}) = \int_0^\infty \dots \int_0^\infty b(\boldsymbol{y})\, e^{-\boldsymbol{\xi}\cdot\boldsymbol{y}} dy_1 \dots dy_n, \tag{A.1}$$

where $\boldsymbol{y} = (y_1, y_2, \dots, y_n)$ and $\boldsymbol{\xi} = (\xi_1, \xi_2, \dots, \xi_n)$ are ordered sets (i.e. vectors) of the variables $y_i$ and $\xi_i$ respectively. The notation $\boldsymbol{\xi} \cdot \boldsymbol{y}$ means the inner product between $\boldsymbol{\xi}$ and $\boldsymbol{y}$. Again, each complex number $\xi_i$ is the corresponding Laplace conjugate of the real variable $y_i$. Note that the transform does not change the number of variables.

## A.2. Multivariate moment-generating function

Suppose $\boldsymbol{X} = (x_1, x_2, \dots, x_n)$ is a random vector, i.e. an ordered set of multiple random variables, the moment-generating function $\boldsymbol{X}$ is

$$M_{\boldsymbol{X}}(\boldsymbol{\alpha}) \equiv \overline{\mathcal{L}}\{P(\boldsymbol{X})\}(-\boldsymbol{\alpha}) = \langle e^{\boldsymbol{\alpha}\cdot\boldsymbol{X}} \rangle, \tag{A.2}$$

where $\boldsymbol{\alpha} = (\alpha_1, \alpha_2, \dots, \alpha_n)$ is the vector which contains the Laplace conjugate variables to the random vector $\boldsymbol{X}$.

## A.3. Characteristic function

The bilateral Laplace transform of a probability distribution $P(X)$ of a random variable $X$ when the Laplace conjugate variable is imaginary is equivalent to the *characteristic function* in statistics. This is a complex-valued function of the real variable $\eta$, denoted by $\phi_X(\eta)$. From Eq.(2.3),

and Eq.(2.9), we have

$$\phi_X(\eta) \equiv \overline{\mathcal{L}}\{P(X)\}(-i\eta) = \mathcal{F}\{P(X)\}(-\eta) = \langle e^{i\eta X}\rangle. \tag{A.3}$$

Moreover, following from Eq.(A.1), the characteristic function corresponding to multiple random variables is

$$\phi_{\boldsymbol{X}}(\boldsymbol{\eta}) \equiv \overline{\mathcal{L}}\{P(\boldsymbol{X})\}(-\boldsymbol{\eta}) = \langle e^{i\boldsymbol{\eta}\cdot\boldsymbol{X}}\rangle. \tag{A.4}$$

The characteristic function plays an important role in statistics as it is the Fourier transform of the probability distribution (the Laplace transform with imaginary conjugate variables), hence can be used as its alternative that sometimes makes an analysis easier.

## A.4. Computing moments

Just like its name suggests, the moment-generating function generates moments. To be more precise, one can obtain the $n^{th}$ moment of the observable $X$, i.e. $\langle X^n\rangle$, with respect to the probability distribution $P(X)$ from the $n^{th}$ derivative of the corresponding moment-generating function $M_X(\alpha)$, evaluated at $\alpha = 0$. This can be clearly seen if one first expands the exponential function using Taylor series,

$$M_X(\alpha) \equiv \langle e^{\alpha X}\rangle = \sum_{m=0}^{\infty} \frac{\alpha^m \langle X^m\rangle}{m!}. \tag{A.5}$$

Then take the $n^{th}$ derivative and evaluate the result at $\alpha = 0$.

$$\frac{d^n}{d\alpha^n} M_X(\alpha)\bigg|_{\alpha=0} = \langle X^n\rangle. \tag{A.6}$$

Note that one can also obtain the $n^{th}$ moments from a characteristic function in a similar fashion,

$$(-i)^n \frac{d^n}{d\eta^n}\phi_X(\eta)\bigg|_{\eta=0} = \langle X^n\rangle. \tag{A.7}$$

Moreover, in multivariate cases, a cross-moment $\langle X_1^\mu X_2^\nu \dots X_n^\sigma \rangle$ can be computed by

$$\langle X_1^\mu X_2^\nu \dots X_n^\sigma \rangle = \frac{d^\mu}{d\alpha_1^\mu} \frac{d^\nu}{d\alpha_2^\nu} \dots \frac{d^\sigma}{d\alpha_n^\sigma} M_{\boldsymbol{X}}(\boldsymbol{\alpha}) \Big|_{\boldsymbol{\alpha}=\mathbf{0}} \tag{A.8}$$

$$= (-i)^{\mu+\nu+\dots+\sigma} \frac{d^\mu}{d\eta_1^\mu} \frac{d^\nu}{d\eta_2^\nu} \dots \frac{d^\sigma}{d\eta_n^\sigma} \phi_{\boldsymbol{X}}(\boldsymbol{\eta}) \Big|_{\boldsymbol{\eta}=\mathbf{0}} \tag{A.9}$$

where $\mathbf{0}$ denotes the zero vector, the dimension of which is the same as $\boldsymbol{X}$ with all the elements being 0.

## A.5. Some properties of characteristic function and moment-generating function

Most properties of the two functions follow directly from the properties of a Laplace transform. Here, we will only discuss several ones that are related to our analysis. Other properties can be found in statistics books, for example [3, 125].

### A.5.1. Existence

The characteristic function always exists since the sum in Eq.(A.4) never diverges. In contrast, the moment-generating function does not always exist, i.e. the sum in Eq.(A.5) is not always convergent. The range of the parameter $\alpha$ which gives a convergent moment-generating function is called its radius of convergence. We will mainly deal with parameters within the radius of convergence in the subsequent discussion.

It should be noted that the non-existence of a moment-generating function does not imply the non-existence of some of its corresponding moments. To compute the moments in such cases, one can rely on the fact that the characteristic function always exists and use Eq.(A.7) instead.

### A.5.2. Sum of independent random variables

The moment-generating function of a *sum* of *independent* variables is equal to the *product* of the moment-generating functions of the individual variables. Suppose $\boldsymbol{Y} = \sum_{i=1}^{N} a_i \boldsymbol{X_i}$, where each $\boldsymbol{X_m}$ is a random vector (an ordered set of random variables) that is independent from $\boldsymbol{X_n}$ for $m \neq n$,

and $a_m$ is its corresponding real coefficient. Their moment-generating functions are related as

$$M_{\boldsymbol{Y}}(\boldsymbol{\alpha}) = \prod_{i=1}^{N} M_{\boldsymbol{X_i}}(a_i \boldsymbol{\alpha_i}). \tag{A.10}$$

The relation can be proven straightforwardly from the definition of the moment-generating function Eq.(A.2). Similarly, for the characteristic function, we also have

$$\phi_{\boldsymbol{Y}}(\boldsymbol{\eta}) = \prod_{i=1}^{N} \phi_{\boldsymbol{X_i}}(a_i \boldsymbol{\eta_i}). \tag{A.11}$$

### A.5.3. Monotonicity

It is a fact that a continuous function is monotonic if and only if it is injective. Therefore,

- *Characteristic function*: No monotonicity due to the periodic nature of sinusoidal functions.
- *Moment-generating function*: Depending on the signs of the random variable
  - *All have the same signs*: The monotonicity property holds.
    - *all signs are positive*: monotonic increasing
    - *all signs are negative*: monotonic decreasing
  - *Mixed signs*: No monotonicity.

## A.6. Some properties of the cumulant-generating function and cumulant

### A.6.1. Existence

Since a cumulant-generating function is the logarithm of a moment-generating function, it does not always exist. However, the non-existence of a cumulant-generating function does not imply the non-existence of some of its cumulants. Similar to the moments, in such cases, one may still be able to com-

pute the cumulants from the logarithm of the corresponding characteristic function.

### A.6.2. Sum of independent random variables

The cumulant-generating function of a *sum* of *independent* variables is equal to the *sum* of the cumulant-generating functions of the individual random variables. Again, suppose $\boldsymbol{Y} = \sum_{i=1}^{N} a_i \boldsymbol{X_i}$, where each $\boldsymbol{X_m}$ is a random vector that is independent from $\boldsymbol{X_n}$ for $m \neq n$, and $a_m$ is its corresponding real coefficient. Their cumulant-generating functions are related as follows,

$$C_{\boldsymbol{Y}}(\boldsymbol{\alpha}) = \sum_{i=1}^{N} C_{\boldsymbol{X_i}}(a_i \boldsymbol{\alpha_i}). \tag{A.12}$$

## A.7. Non-addivitity property of Tsallis entropy and relative Tsallis entropy

It is well-known that Tsallis entropy has a unique non-additivity property. Suppose that $\rho'$ is a state being independent from $\rho$, one may prove this property starting from the additivity of Rényi entropy as follows,

$$S_\alpha(\rho \otimes \rho') = S_\alpha(\rho) + S_\alpha(\rho').$$

Then, from (2.75), we can rewrite Rényi entropy in terms of Tsallis entropy. Together with the identity that the logarithm of a product is equal to the sum between the individual logarithms, we will have

$$\begin{aligned} \ln\left[1-(\alpha-1)\,\mathcal{T}_\alpha(\rho\otimes\rho')\right] &= \ln\left\{\left[1-(\alpha-1)\,\mathcal{T}_\alpha(\rho)\right]\left[1-(\alpha-1)\,\mathcal{T}_\alpha(\rho')\right]\right\} \\ 1-(\alpha-1)\,\mathcal{T}_\alpha(\rho\otimes\rho') &= 1-(\alpha-1)\left[\mathcal{T}_\alpha(\rho)+\mathcal{T}_\alpha(\rho')-(\alpha-1)\,\mathcal{T}_\alpha(\rho)\,\mathcal{T}_\alpha(\rho')\right]. \end{aligned} \tag{A.13}$$

Therefore,

$$\mathcal{T}_\alpha(\rho\otimes\rho') = \mathcal{T}_\alpha(\rho)+\mathcal{T}_\alpha(\rho')-(\alpha-1)\,\mathcal{T}_\alpha(\rho)\,\mathcal{T}_\alpha(\rho'). \tag{A.14}$$

This shows that, in contrast to joint Rényi entropy, the joint Tsallis entropy of independent states is not simply equal to the sum between the individual ones.

The non-additivity property does not only hold for Tsallis entropy, but also for relative Tsallis entropy. Suppose $\sigma$ and $\sigma'$ are another two independent states, one can prove that [44]

$$\mathcal{T}_\alpha\left(\rho\otimes\rho'||\sigma\otimes\sigma'\right)=\mathcal{T}_\alpha\left(\rho||\sigma\right)+\mathcal{T}_\alpha\left(\rho'||\sigma'\right)-\left(\alpha-1\right)\mathcal{T}_\alpha\left(\rho||\sigma\right)\mathcal{T}_\alpha\left(\rho'||\sigma'\right). \tag{A.15}$$

# Bibliography


[1] J. J. Kelly, *Graduate Mathematical Physics* (John Wiley & Sons, 2008).

[2] M. D. Adams, *Continuous-Time Signals and Systems (Version 2013-09-11)* (Michael Adams, 2013).

[3] T. A. Severini, *Elements of Distribution Theory* (Cambridge University Press, 2005).

[4] J. Marcinkiewicz, Mathematische Zeitschrift **44**, 612 (1939).

[5] B. Holmquist, Stochastic Analysis and Applications **6**, 273 (1988).

[6] A. Kolmogorov, Atti Accad. Naz. Lincei Rend. **12**, 388 (1930).

[7] M. Nagumo, Japanese journal of mathematics :transactions and abstracts **7**, 71 (1930).

[8] A. Rényi, Proceedings of the fourth Berkeley Symposium on Mathematics, Statistics and Probability 1960 **547** (1961).

[9] G. H. Hardy, J. E. Littlewood, and G. Pólya, *Inequalities* (Cambridge University Press, 1952).

[10] R. Renner and S. Wolf, in Proc. IEEE Int. Symposium on Inf. Theory, Chicago, Illinois, USA, June 27 - July 2 (2004).

[11] J. C. Principe, *Information Theoretic Learning: Renyi's Entropy and Kernel Perspectives* (Springer Science & Business Media, 2010).

[12] T. van Erven and P. Harremoes, Rényi divergence and majorization, in *2010 IEEE International Symposium on Information Theory*, pp. 1335–1339, IEEE, 2010.

[13] M. M. Wilde, A. Winter, and D. Yang, Communications in Mathematical Physics **331**, 593 (2014).

[14] J. C. Baez, (2011), arXiv:1102.2098.

[15] O. C. O. Dahlsten, R. Renner, E. Rieper, and V. Vedral, New Journal of Physics **13**, 053015 (2011).

[16] J. Åberg, Nature Communications **4**, 1925 (2013).

[17] M. Horodecki and J. Oppenheim, Nature Communications **4**, 2059 (2013).

[18] F. Brandão, M. Horodecki, N. Ng, J. Oppenheim, and S. Wehner, Proceedings of the National Academy of Sciences **112**, 201411728 (2015).

[19] N. Y. Halpern, A. J. P. Garner, O. C. O. Dahlsten, and V. Vedral, (2014), arXiv:1409.3878.

[20] M. O. Hill, Ecology **54**, 427 (1973).

[21] M. Pietrzak, G. A. Rempała, M. Seweryn, and J. Wesołowski, (2015), arXiv:1505.03220.

[22] G. Adesso, D. Girolami, and A. Serafini, Physical Review Letters **109**, 190502 (2012).

[23] M. Tribus, *Thermostatics and thermodynamics: an introduction to energy, information and states of matter, with engineering applications* (Van Nostrand, 1961).

[24] M. Tomamichel, R. Colbeck, and R. Renner, IEEE Transactions on Information Theory **55**, 5840 (2009).

[25] C. E. Shannon, Bell System Technical Journal **27**, 379 (1948).

[26] M. Muller-Lennert, F. Dupuis, O. Szehr, S. Fehr, and M. Tomamichel, Journal of Mathematical Physics **54**, 122203 (2013).

[27] D. Petz, Reports on Mathematical Physics **23**, 57 (1986).

[28] K. M. R. Audenaert and N. Datta, Journal of Mathematical Physics **56**, 022202 (2015).

[29] T. Ando, Linear Algebra and its Applications **26**, 203 (1979).

[30] F. Hiai, Linear Algebra and its Applications **439**, 1568 (2013).

[31] S. Beigi, Journal of Mathematical Physics **54**, 122202 (2013).

[32] R. L. Frank and E. H. Lieb, Journal of Mathematical Physics **54**, 122201 (2013).

[33] C. Tsallis, Journal of Statistical Physics **52**, 479 (1988).

[34] J. Cartwright, Physics World (2014).

[35] L. Burlaga and A. Viñas, Physica A: Statistical Mechanics and its Applications **356**, 375 (2005).

[36] S. Chatrchyan *et al.*, Journal of High Energy Physics **2011**, 86 (2011).

[37] B. Liu and J. Goree, Physical Review Letters **100**, 055003 (2008).

[38] E. Lutz, Physical Review A **67**, 051402 (2003).

[39] P. Douglas, S. Bergamini, and F. Renzoni, Physical Review Letters **96**, 110601 (2006).

[40] F. Caruso and C. Tsallis, Physical Review E **78**, 021102 (2008).

[41] S. Abe, Physics Letters A **312**, 336 (2003).

[42] S. Abe, Physics Letters A **324**, 507 (2004).

[43] L. Borland, A. R. Plastino, and C. Tsallis, Journal of Mathematical Physics **39**, 6490 (1998).

[44] S. Furuichi, (2004), arXiv:0406178v5.

[45] C. Jarzynski, Physical Review Letters **78**, 2690 (1997).

[46] J. Hermans, The Journal of Physical Chemistry **95**, 9029 (1991).

[47] G. Hummer and A. Szabo, Proc. Natl. Acad. Sci. U. S. A. **98**, 3658 (2001).

[48] T. Sagawa, Second law-like inequalities with quantum relative entropy: an introduction, in *Lectures on Quantum Computing, Thermodynamics and Statistical Physics*, edited by M. Nagahara and T. Shuu, chap. Second law, p. 127, World Scientific Publishing Company, Singapore, 2012.

[49] G. Crooks, Journal of Statistical Physics **90**, 1481 (1998).

[50] G. E. Crooks, Physical Review E **60**, 2721 (1999).

[51] H. Tasaki, (2000), arXiv:0009244.

[52] P. Talkner and P. Hänggi, Journal of Physics A: Mathematical and Theoretical **40**, F569 (2007).

[53] P. Talkner, M. Campisi, and P. Hänggi, Journal of Statistical Mechanics: Theory and Experiment **2009**, P02025 (2009).

[54] D. Cohen and Y. Imry, Physical Review E **86**, 011111 (2012).

[55] M. Campisi, P. Talkner, and P. Hänggi, Physical Review Letters **102**, 210401 (2009).

[56] D. M. Carberry *et al.*, Physical Review Letters **92**, 140601 (2004).

[57] F. Douarche, S. Ciliberto, A. Petrosyan, and I. Rabbiosi, Europhysics Letters **70**, 593 (2005).

[58] D. Collin *et al.*, Nature **437**, 231 (2005).

[59] S. Schuler, T. Speck, C. Tietz, J. Wrachtrup, and U. Seifert, Physical Review Letters **94**, 1 (2005).

[60] V. Blickle, T. Speck, L. Helden, U. Seifert, and C. Bechinger, Physical Review Letters **96**, 070603 (2006).

[61] T. B. Batalhão *et al.*, Physical Review Letters **113**, 140601 (2014).

[62] F. G. S. L. Brandão, M. Horodecki, J. Oppenheim, J. M. Renes, and R. W. Spekkens, Physical Review Letters **111**, 250404 (2013).

[63] M. Lostaglio, D. Jennings, and T. Rudolph, Nature Communications **6**, 6383 (2015).

[64] D. Egloff, O. C. O. Dahlsten, R. Renner, and V. Vedral, New Journal of Physics **17**, 073001 (2015).

[65] P. Ćwikliński, M. Studziński, M. Horodecki, and J. Oppenheim, Physical Review Letters **115**, 210403 (2015).

[66] C. Jarzynski, Journal of Statistical Physics **98**, 77 (2000).

[67] S. Yukawa, Journal of the Physical Society of Japan **69**, 2367 (2000).

[68] P. Talkner, E. Lutz, and P. Hänggi, Physical Review E **75**, 7 (2007).

[69] H. T. Quan and H. Dong, (2008), arXiv:0812.4955.

[70] J. Liphardt, S. Dumont, S. B. Smith, I. Tinoco, and C. Bustamante, Science **296**, 1832 (2002).

[71] N. C. Harris, Y. Song, and C.-H. Kiang, Physical Review Letters **99**, 068101 (2007).

[72] W. J. Greenleaf, K. L. Frieda, D. A. N. Foster, M. T. Woodside, and S. M. Block, Science **319**, 630 (2008).

[73] A. Imparato, F. Sbrana, and M. Vassalli, Europhysics Letters **82**, 58006 (2008).

[74] M. Janke *et al.*, Nature nanotechnology **4**, 225 (2009).

[75] A. N. Gupta *et al.*, Nature Physics **7**, 631 (2011).

[76] O.-P. Saira *et al.*, Physical Review Letters **109**, 180601 (2012).

[77] G. Huber, F. Schmidt-Kaler, S. Deffner, and E. Lutz, Physical Review Letters **101**, 70403 (2008).

[78] S. An *et al.*, Nature Physics **11**, 193 (2014).

[79] C. Jarzynski, Nature Physics **7**, 591 (2011).

[80] A. Einstein, Annalen der Physik **322**, 549 (1905).

[81] H. Nyquist, Physical Review **32**, 110 (1928).

[82] J. Sung, (2005), arXiv:0506214.

[83] D. H. E. Gross, (2005), arXiv:0508721.

[84] C. Jarzynski, (2005), arXiv:0509344.

[85] D. H. E. Gross, (2005), arXiv:0509648.

[86] Y. Murashita, K. Funo, and M. Ueda, Physical Review E **90**, 042110 (2014).

[87] K. Funo, Y. Murashita, and M. Ueda, New Journal of Physics **17**, 075005 (2015).

[88] A. Cleland, Nature Physics **5**, 458 (2009).

[89] D. E. Chang *et al.*, Proceedings of the National Academy of Sciences of the United States of America **107**, 1005 (2010).

[90] O. Romero-Isart, M. L. Juan, R. Quidant, and J. I. Cirac, New Journal of Physics **12** (2010).

[91] T. Li, S. Kheifets, and M. Raizen, Nature Physics **7**, 527 (2011).

[92] G. A. T. Pender, P. F. Barker, F. Marquardt, J. Millen, and T. S. Monteiro, Physical Review A **85**, 021802 (2012).

[93] J. Gieseler, B. Deutsch, R. Quidant, and L. Novotny, Physical Review Letters **109**, 1 (2012).

[94] T. S. Monteiro *et al.*, New Journal of Physics **15**, 015001 (2013).

[95] N. Kiesel *et al.*, Proceedings of the National Academy of Sciences of the United States of America **110**, 14180 (2013).

[96] M. Arndt and K. Hornberger, Nature Physics **10**, 271 (2014).

[97] J. Millen, P. Fonseca, T. Mavrogordatos, T. Monteiro, and P. Barker, Physical Review Letters **114**, 123602 (2015).

[98] A. Ashkin and J. M. Dziedzic, Applied Physics Letters **28** (1976).

[99] D. R. Burnham, P. J. Reece, and D. McGloin, Physical Review E **82**, 051123 (2010).

[100] J. Millen, T. Deesuwan, P. Barker, and J. Anders, Nature Nanotechnology **9**, 425 (2014).

[101] A. Ashkin and J. Dziedzic, Applied Physics Letters **19**, 283 (1971).

[102] A. Ashkin, J. M. Dziedzic, and T. Yamane, Nature **330**, 769 (1987).

[103] C. Tischer *et al.*, Applied Physics Letters **79**, 3878 (2001).

[104] N. R. Guydosh and S. M. Block, Nature **461**, 125 (2009).

[105] A. A. Geraci, S. B. Papp, and J. Kitching, Physical Review Letters **105**, 101101 (2010).

[106] Z.-q. Yin, T. Li, and M. Feng, Phys. Rev. A **83**, 013816 (2011).

[107] T. N. Thiele, *Sur la compensation de quelques erreurs quasi-systematiques par la methode des moindres carres* (C. A. Reitzel, Copenhagen, 1880).

[108] T. N. Thiele, *Almindelig Iagttagelseslaere: Sandsynlighedsregning og mindste Kvadraters Methode* (C. A. Reitzel, Copenhagen, 1889).

[109] M. von Smoluchowski, Annalen der Physik **326**, 756 (1906).

[110] J. B. Perrin, Annales de chimie et de physique **18**, 5 (1909).

[111] T. Franosch *et al.*, Nature **478**, 85 (2011).

[112] A. Bérut *et al.*, Nature **483**, 187 (2012).

[113] P. Hänggi and F. Marchesoni, Reviews of Modern Physics **81**, 387 (2009).

[114] D. Le Bihan *et al.*, Radiology **161**, 401 (1986).

[115] M. Wang and G. Uhlenbeck, Reviews of Modern Physics **17**, 323 (1945).

[116] P. S. Epstein, Physical Review **23**, 710 (1924).

[117] F. O. Goodman, The Journal of Physical Chemistry **84**, 1431 (1980).

[118] D. Ganta, E. B. Dale, J. P. Rezac, and A. T. Rosenberger, The Journal of Chemical Physics **135**, 084313 (2011).

[119] L. Landström and P. Heszler, The Journal of Physical Chemistry B **108**, 6216 (2004).

[120] C. D. S. Brites *et al.*, Nanoscale **4**, 4799 (2012).

[121] E. J. G. Peterman, F. Gittes, and C. F. Schmidt, Biophysical Journal **84**, 1308 (2003).

[122] Azonano.com, Silicon Dioxide, Silica (SiO2) Nanoparticles Properties, Applications, 2013.

[123] T. A. Nieminen *et al.*, Journal of Optics A: Pure and Applied Optics **9**, S196 (2007).

[124] K. Funo, Y. Watanabe, and M. Ueda, Physical Review E **88**, 052121 (2013).

[125] E. Lukacs, *Characteristic Functions* (Hafner Publishing Company, 1970).